UNIVERSIDADE FEDERAL DO CEARÁ
CENTRO DE CIÊNCIAS AGRÁRIAS
DEPARTAMENTO DE ENGENHARIA AGRÍCOLA
PROGRAMA DE PÓS-GRADUAÇÃO EM ENGENHARIA AGRÍCOLA

GLÁUBER PONTES RODRIGUES

EVAPORATIVE LOSSES IN A DRY TROPICAL REGION: DIRECT MEASUREMENTS, REMOTE SENSING ASSESSMENT AND IMPACT OF CLIMATE CHANGE ON WATER AVAILABILITY IN CEARÁ, BRAZIL

FORTALEZA
2023

GLÁUBER PONTES RODRIGUES

EVAPORATIVE LOSSES IN A DRY TROPICAL REGION: DIRECT MEASUREMENTS, REMOTE SENSING ASSESSMENT AND IMPACT OF CLIMATE CHANGE ON WATER AVAILABILITY IN CEARÁ, BRAZIL

Tese apresentada ao Programa de Pós-Graduação em Engenharia Agrícola da Universidade Federal do Ceará, como requisito parcial à obtenção do título de Doutor em Engenharia Agrícola. Área de concentração: Manejo e Conservação de Bacias Hidrográficas no Semiárido.

Orientador: Prof. Dr. José Carlos de Araújo.
Coorientador: Prof. Dr. George Leite Mamede.
Coorientadora: Profª. Drª. Arlena Brosinsky.

FORTALEZA

2023

Dados Internacionais de Catalogação na Publicação
Universidade Federal do Ceará
Sistema de Bibliotecas
Gerada automaticamente pelo módulo Catalog, mediante os dados fornecidos pelo(a) autor(a)

R613e Rodrigues, Gláuber Pontes.
Evaporative losses in a dry tropical region : direct measurements, remote sensing assessment and impact of climate change on water availability in Ceará, Brazil / Gláuber Pontes Rodrigues. – 2023.
117 f. : il. color.

Tese (doutorado) – Universidade Federal do Ceará, Centro de Ciências Agrárias, Programa de Pós-Graduação em Engenharia Agrícola, Fortaleza, 2023.
Orientação: Prof. Dr. José Carlos de Araújo.
Coorientação: Prof. Dr. George Leite Mamede.

1. Evaporação. 2. Instrumentação meteorológica. 3. Sensoriamento remoto. 4. Modelos regionais. 5. Disponibilidade hídrica. I. Título.

CDD 630

GLÁUBER PONTES RODRIGUES

EVAPORATIVE LOSSES IN A DRY TROPICAL REGION: DIRECT MEASUREMENTS, REMOTE SENSING ASSESSMENT AND IMPACT OF CLIMATE CHANGE ON WATER AVAILABILITY IN CEARÁ, BRAZIL

Tese apresentada ao Programa de Pós-Graduação em Engenharia Agrícola da Universidade Federal do Ceará, como requisito parcial à obtenção do título de Doutor em Engenharia Agrícola. Área de concentração: Manejo e Conservação de Bacias Hidrográficas no Semiárido.

Aprovada em: 31/03/2023.

BANCA EXAMINADORA

_____
Prof. Dr. José Carlos de Araújo (Orientador)
Universidade Federal do Ceará (UFC)

_____
Prof. Dr. George Leite Mamede (Coorientador)
Universidade da Integração Internacional da Lusofonia Afro-Brasileira (UNILAB)

_____
Drª. Arlena Brosinsky (Coorientadora)
Centro Alemão de Geociências de Potsdam (GFZ)

_____
Profª. Drª. Adelena Gonçalves Maia (Avaliadora)
Universidade Federal do Rio Grande do Norte (UFRN)

_____
Prof. Dr. Lucas Melo Vellame (Avaliador)
Universidade Federal do Recôncavo da Bahia (UFRB)

_____
Prof. Dr. Everton Alves Rodrigues Pinheiro (Avaliador)
Universidade Federal do Tocantins (UFT)

_____
Profª. Drª. Isabel Cristina da Silva Araújo (Avaliadora)
Universidade Federal do Ceará (UFC)

À Tereza e Bárbara.

À minha avó Conceição e ao meu tio Luís Carlos.

AGRADECIMENTOS

A Deus, pela proteção em todos os caminhos.

À Tereza, Bárbara e Lícia, por depositarem fé e amor imenso em mim, sobretudo nos momentos (não raros) em que falhei ou me fiz ausente; que vibraram com cada conquista minha e não me deixaram esmorecer com os tropeços.

À minha avó Conceição, uma das mulheres mais fortes que já conheci; que lutou a vida inteira para que seus filhos tivessem acesso à educação e dignidade.

Aos tios e às tias pelo fundamental apoio desde o momento em que ingressei na Universidade em 2011, contribuindo para que nela eu permanecesse.

Ao professor José Carlos de Araújo pela paciência e sabedoria compartilhadas; por sempre me atender com atenção, enriquecendo meus conhecimentos a cada conversa e inspirando-me a ser um profissional e um ser humano melhor.

À Arlena Brosinsky, pela gentileza e paciência inesgotáveis; por sempre me atender com amabilidade sem fim, mesmo com diferenças de fuso-horário; porém, sobretudo, por sempre fazer jus à objetividade e franqueza características dos alemães sem perder a cordialidade.

A Armin Raabe e Peter Holstein por gentilmente disponibilizarem os sensores utilizados no primeiro capítulo desta tese e por terem se tornado mentores e amigos.

À Saskia Förster e Birgit Heim pelas discussões iniciais relacionadas a sensoriamento remoto, nos primeiros meses da minha estadia em Potsdam.

Aos membros da banca: o co-orientador George Mamede, a co-orientadora Arlena Brosinsky, Adelena Maia, Isabel Araújo, Everton Pinheiro e Lucas Vellame, por aceitarem prontamente o convite e pelas importantíssimas contribuições a esta tese e aos trabalhos dela derivados.

Aos amigos e amigas do Hidrosed: Suziane, por toda a paciência e confiança em mim; a Álisson Simplício, Arianna Sotomayor, Bruno Pereira, Cicero Almeida, Christine Coelho, Eduardo Lima, Jairo Soares, Pedro Alencar, Thales Lima, Ítalo Sampaio e Arnaldo Sales, pelo companheirismo e pelos essenciais momentos de descontração, sendo estes dois últimos meus companheiros fraternos e de idas à campo; a Márcio Régys, por ser um raro exemplo de bondade; à Gabi "*Sundays*", Brenno Carneiro, Érika Roanna e Eveline Silva pela frequente disposição em ajudar e me tranquilizar, e por se envolverem em discussões fundamentais da pesquisa. À Sharon pela disposição em ajudar com a "infraestrutura" da defesa.

Aos professores e professoras do Departamento de Engenharia Agrícola, em

especial aos professores Carlos Alexandre e Pedro Medeiros, que não estiveram presentes na banca como avaliadores desta tese, mas contribuíram na qualificação e participaram de todos os momentos desde o mestrado, como avaliadores e amigos.

Aos funcionários e às funcionárias do Departamento de Engenharia Agrícola, por propiciarem um ambiente de trabalho e estudos digno, sobretudo “Aninha” Rodrigues.

Aos colegas da Universidade de Potsdam: Irene Hahn, Andreas “Andi” Bauer, Daniel Bazant, Till Francke, Gerd Bürger, Axel Bronstert, Sophia Dobkowitz, Kata Schmidt, sobretudo por mostrarem o lado amoroso e receptivo dos alemães durante as reuniões do AG-Spree, nos intervalos de almoço ou nos passeios de bicicleta.

Aos amigos e amigas que fiz em Potsdam: Alain Bapolisi, Lingxiao Gong, Elisa Pjerrza, Maria Rosa Scicchitano, Ceren Kocaman, Simon, Julien Amalberti, Vera Zolotareva, Claudia Traini, Iris Dupont-Nivet e Eva Dirix pela convivência fraterna e calorosa mesmo nos dias mais frios e “curtos” de inverno.

A Sullyandro Guimarães, do Instituto de Climatologia de Potsdam – PIK, pelos esclarecimentos relacionados à modelagem climática, desde a fundamentação teórica à aquisição de dados.

Aos funcionários da Companhia de Gestão dos Recursos Hídricos (COGERH) por facilitarem o acesso ao açude Gavião e à implementação do equipamento, em especial aos operadores Fernando, Jairo, Ivan e Singleuster.

A seu Luiz Rodrigues, por facilitar todas as idas a campo no Gavião e a instalação dos experimentos.

À Fundação Cearense de Apoio ao Desenvolvimento Científico e Tecnológico (Funcap) pelo apoio financeiro com a manutenção da bolsa de auxílio.

À Coordenação de Aperfeiçoamento de Pessoal de Nível Superior (CAPES) e ao DAAD (Serviço Alemão de Intercâmbio Acadêmico) pela bolsa de doutorado sanduíche (edital n° 23/2019 - Programa Conjunto de bolsas de Doutorado na República Federal da Alemanha) e pelo projeto PrInt (88881.311770/2018-01), que permitiu a ida dos pesquisadores alemães Armin Raabe e Peter Holstein à Fortaleza.

O presente trabalho foi realizado com apoio da Coordenação de Aperfeiçoamento de Pessoal de Nível Superior - Brasil (CAPES) - Código de Financiamento 001.

“Em nossa época, o cientista precisa tomar consciência da utilidade social e do destino prático reservado a suas descobertas.”
Florestan Fernandes (1920-1995)

“Fazer uma tese significa divertir-se, e a tese é como um porco: nada se desperdiça.”
Umberto Eco (1932-2016)

RESUMO

O estado do Ceará, no semiárido brasileiro, é abastecido por uma densa rede de reservatórios (mais de 30 mil) que são vulneráveis à seca e ao déficit hídrico. O preciso conhecimento do processo de evaporação é fundamental para gerenciamento dos recursos hídricos e avaliação de prováveis impactos de mudanças climáticas na disponibilidade de água. A presente tese foi desenvolvida em diferentes áreas de estudo no Ceará. Na primeira parte do estudo, desenvolvida no açude Gavião, estimou-se a evaporação do lago por quatro abordagens: duas equações (Penman e uma adaptação de Dalton) e dois sensores de medição direta (um que funciona por diferença de pressão e outro com ondas acústicas). Os sensores foram instalados em tanques flutuantes e as equações baseadas em variáveis coletadas em uma estação meteorológica embarcada em uma balsa. A segunda parte consta da análise do impacto de mudanças climáticas na evaporação dos reservatórios Gavião, Pacoti e Riachão; além da estimativa da futura disponibilidade hídrica (2070-2099) na Região Metropolitana de Fortaleza, abastecida pelos referidos açudes. Estimou-se a evaporação histórica (1961-2005) por meio da equação de Penman com dados de estação meteorológica do Instituto Nacional de Meteorologia – INMET localizada em Fortaleza, e o algoritmo de sensoriamento remoto AquaSEBS foi aplicado a imagens Landsat 5 e 8 para estimar a evaporação do lago. O impacto sobre a disponibilidade hídrica foi estimado usando modelagem estocástica. Utilizaram-se simulações dos modelos regionais climáticos Eta-CanESM2 e Eta-MIROC5, desenvolvidos pelo Instituto Nacional de Pesquisas Espaciais – INPE. Os modelos geraram quatro cenários de mudanças climáticas baseados nas taxas de evaporação simuladas. A terceira parte consta de quatro meses de medição direta da evaporação com um sensor de pressão instalado em dois tanques evaporimétricos. Objetivou-se estimar o efeito da presença da macrófita flutuante *Eichhornia crassipes* na evapotranspiração de tanques. Dos resultados desta tese, as principais conclusões são: (i) as abordagens para estimativa de evaporação apresentaram desempenho satisfatório, com destaque à adaptação de Dalton para passo horário, e do sensor acústico, que apresentou valores aceitáveis em passos de 4 horas ($r > 0,6$) ou mais; (ii) um dos cenários climáticos prevê aumento na taxa evaporativa (12% no fim do século 21 com relação ao período histórico) e os outros mostram estabilidade (variando de -2% a +2%), evidenciando a incerteza na modelagem climática mesmo feita para mesma região e mesmos dados; (iii) o algoritmo de sensoriamento remoto apresentou resultados aceitáveis para estimar evaporação nos corpos hídricos, diferindo em 27% das estimativas feitas com base nos dados de estação em terra; (iv) Notou-se que as taxas evaporativas são maiores (≈16%) na presença de plantas aquáticas. As descobertas deste

trabalho são contribuições importantes para um monitoramento preciso das perdas de água por evaporação e operação em reservatórios, particularmente em regiões secas.

Palavras-chave: evaporação; instrumentação meteorológica; sensoriamento remoto; modelos regionais; disponibilidade hídrica.

ABSTRACT

The state of Ceará, in the Brazilian semiarid region, is supplied by a dense network of reservoirs (over 30,000) that are vulnerable to drought and water deficit. Precise knowledge of the evaporation process, which corresponds to roughly 30% to 50% of the water balance, is fundamental for the management of water resources and the assessment of probable impacts of climate change on water availability. This dissertation was developed in different study areas in Ceará. Its first part examines the Gavião reservoir and estimates lake evaporation by using the following four approaches: two equations (Penman and one adaptation of Dalton) and two direct measurement sensors (one based on pressure difference and the other one on acoustic signals). The sensors were installed in floating tanks and the equations drew on variables collected from a meteorological station on board a raft. The second part analyses the impact of climate change on evaporation in the Gavião, Pacoti and Riachão reservoirs and also estimates future water availability (2070-2099) in the Metropolitan Region of Fortaleza, supplied by these reservoirs. Historical evaporation (1961-2005) was estimated using the Penman equation with data from a meteorological station of the National Institute of Meteorology - INMET located in Fortaleza, and the remote sensing algorithm AquaSEBS was applied to Landsat 5 and 8 images to estimate lake evaporation. The impact on water availability was determined by using stochastic modelling. We used simulations of the regional climate models Eta-CanESM2 and Eta-MIROC5, developed by the National Institute for Space Research – INPE. These models generated four climate-change scenarios based on the simulated evaporation rates. This study's third part is composed of four months of direct measurement of evaporation with a pressure sensor installed in two evaporation tanks. The aim was to gauge the effect of the presence of the floating macrophyte Eichhornia crassipes on free surface evapotranspiration. The main conclusions resulting from this dissertation are: (i) the approaches for evaporation estimation presented satisfactory performance, with emphasis on Dalton's adaptation for hourly steps, and on the acoustic sensor, which presented acceptable values for steps of 4 hours ($r > 0.6$) or more; (ii) one of the climate scenarios predicts an increase in the evaporative rate (12% by the end of the 21st century in relation to the historical period) and the others show stability (varying from -2% to +2%); this fact highlights the uncertainty in climate modelling even within the same region and data; (iii) the remote sensing algorithm presented acceptable results for estimating evaporation from water bodies, differing by 27% from the assessment made based on data from an on-land station; (iv) evaporation rates were found to be higher ($\approx$ 16%) in the presence of

aquatic plants. The findings of this work are important contributions for an accurate monitoring of water losses through evaporation and reservoir operations, particularly in dry regions.

Keywords: evaporation; meteorological instrumentation; remote sensing; regional models; water availability

LIST OF FIGURES

LIST OF TABLES

CONTENTS

1 INTRODUCTION

Open surface reservoirs for water storage are ancient infrastructures with oldest historical records dating back about 4000 years (TIAN *et al.*, 2022). It is estimated that millions of reservoirs with an area of more than 100 m² are in operation worldwide (ZARFL *et al.*, 2015). Reservoirs play a central role for storage, human supply and agricultural purposes, but are all impacted by evaporative losses (BURT *et al.*, 2005; CRAIG, 2006; MARTÍNEZ ALVAREZ *et al.*, 2008). In a recent global study on evaporation, Zhao *et al.* (2022) used satellite observations and modelling tools to quantify the evaporation volume of 1.42 million global lakes from 1985 to 2018. They found that long-term average lake evaporation is 1500 ± 150 km³ year^{-1} with an increase rate of 3.12 km³ year^{-1}. While only accounting for 5% of the global lake storage capacity, artificial lakes (i.e., reservoirs) contribute 16% to the evaporation volume.

Evaporation is an important component of a water budget (ASSOULINE, 1993; LENSKY; DVORKIN; LYAKHOVSKY, 2005). In many cases, there are other unknown components that affect it, such as water input from adjacent basins or water losses due to soil infiltration, and an accurate estimate of evaporation can improve the assessment of these unknown factors (ASSOULINE, 1993; TANNY *et al.*, 2008). Therefore, efforts have been invested over decades to develop the tools to estimate this variable (LENTERS; KRATZ; BOWSER, 2005; LINACRE, 1993; ROSENBERRY *et al.*, 2007), but accurate assessments of evaporation rates are still a challenge even after numerous approaches developed over the last 200 years (MCMAHON; FINLAYSON; PEEL, 2016).

In a regional perspective, Zhao and Gao (2019) showed that annual total reservoir evaporation from large reservoirs (storage capacity greater than 0.1 km³) in the United States is equivalent to 93% of the annual public water supply of that country in 2010. Craig *et al.* (2005) reported that annual total reservoir evaporation from farm reservoirs in Queensland and New South Wales in Australia is up to 40% of the storage capacity of these reservoirs. Zhang *et al.* (2017) found that annual total reservoir evaporation from 200 reservoirs in Texas in the United States is equivalent to 53% of annual local water use.

Evaporation from a water surface is driven by wind, water-air vapor pressure gradients and the internal heat stored in the water, which is supplied by external sources such as solar radiation and/or downward sensible heat flux (BRUTSAERT, 2005). Consequently, the main approaches generally applied to estimate evaporation rates are the energy budget method that remains by far the most common for estimating surface fluxes and that has been widely

applied to lakes; the flux-gradient approach for heat and mass transfer across the boundary-layer over the water surface; and a combination between the two (BRUTSAERT, 1982, 2005; MONTEITH; UNSWORTH, 1990). All these methods rely on the measurement of standard meteorological variables (solar radiation, air temperature and humidity, wind speed) and require evaluating the heat storage within the water body; that's why they provide indirect estimates of the evaporation rates. The development of fast-response sensors such as sonic anemometers or infrared and ultraviolet absorption hygrometers make it possible to apply the eddy-correlation method (SWINBANK, 1951) for direct measurement of latent and sensible heat fluxes from the water surface.

Evaporation estimations of water bodies can be made by using direct or indirect methods. The eddy-correlation technique is considered a direct method, that despite certain limitations is the most accurate and reliable technique for evaporation measurements (ITIER; BRUNET, 1996). Yet it requires expensive instruments and highly demanding data analysis. Indirect methods for evaporation estimation are more commonly used, although they could be associated with relatively large uncertainties (ASSOULINE, 1993). During past decades the eddy-correlation method was used for direct evaporation measurements of lakes, reservoirs and even the sea (ALLEN; TASUMI, 2005; ASSOULINE; MAHRER, 1993; LIU *et al.*, 2009; MCGOWAN *et al.*, 2010; SENE; GASH; MCNEIL, 1991; TANNY *et al.*, 2008, 2011). The eddy-correlation system allows determining the diurnal behaviour of evaporation at a high temporal resolution. Since evaporation is responding to both solar radiation (by heating the water body) and wind velocity, the method enables the partitioning between these two factors if they are distinct in time. While radiation has a characteristic diurnal cycle, typically peaking at noon, this is not the case for wind speed that has a more erratic pattern, which may or may not overlap the radiation diurnal pattern. Therefore, the distinction between the relative contributions of aerodynamic and radiative effects on evaporation is challenging.

Most previous studies on evaporation from water bodies reported an evaporation diurnal course with a single peak, associated with the diurnal wind speed and radiation peaks (MCGLOIN *et al.*, 2014; MCJANNET; COOK; BURN, 2013). To the best of our knowledge, only Sene *et al.* (1991) reported several peaks of diurnal evaporation which were associated with wind speed peaks. Only few papers describe the diurnal course of evaporation, which is critical to explore modulation due to radiation and wind.

Of course, not for all water resources management purposes there is the need for such precision in evaporation estimation. For reservoir water regulation, for instance, it is

enough to obtain information in daily steps or even less. However, there are reservoirs of various sizes. Only in the state of Ceará, northeast Brazil, there are tens of thousands of dams, built continuously during one hundred years (mostly from 1910 to 2010) and ranging from micro (0.10 hm^3) to very large (10,000 hm^3) (DE ARAÚJO *et al.*, 2022). It is known that the evaporative rate is not to be considered the same from every water surface (although it is often considered so for ease, depending on the case of study). Conventional techniques that employ point measurements to estimate the components of the energy balance are representative only of local scales and cannot be extended to large areas because of the heterogeneity of land surfaces and the dynamic nature of heat transfer processes. Remote sensing is probably the only technique which can provide representative measurements of several relevant physical parameters at scales from a point to a continent. Techniques using remote sensing information to estimate atmospheric turbulent fluxes are therefore essential when dealing with processes that cannot be represented by point measurements only.

This explains the importance of more accurate evaporation measurements and of techniques that can spatially represent the variation and seasonality of evaporative rates as a basis for studies of possible climate change impacts. Climate models invariably rely on data measured with precision and continuity. In hydrology and in studies relating to water availability, free-surface evaporation plays an important role. Climate change is critical for water resource planning: The water cycle is expected to be accelerated because of temperature increase, among others. In arid and semiarid climates, climate change is expected to worsen water shortage episodes. Investigations show the sensitivity of lakes to climate and demonstrate that physical, chemical and biological lake properties respond rapidly to climate-related changes (ADRIAN *et al.*, 2009; ROSENZWEIG *et al.,* 2007). Reservoirs are essential infrastructures for the economic and social development of the region, and their evaporation losses are significant for the water system and can severely impact water availability and allocation (MALVEIRA; ARAÚJO; GÜNTNER, 2012; MAMEDE *et al.*, 2012; PETER *et al.*, 2014).

The continuous increase of water demand has been subject of concern; it requires increasingly efficient management systems, particularly in water-scarce regions such as the Brazilian semiarid, a one-million km^2 area and home to 25 million inhabitants. Since it is an area with a long dry season (around 8 months), the population depends heavily on water supply from reservoirs. However, several driving forces lead to the consistent decline of network water availability, such as reservoir silting (DE ARAÚJO; GÜNTNER; BRONSTERT, 2006) and

pollution (ZUO *et al.*, 2015). The intensive growth of aquatic plants (macrophytes) is often related to the high load of nutrient pollutants in reservoirs, leading to a process named eutrophication. Macrophytes can considerably restrict water functions. The eutrophication process is the result of a sediment and nutrient transfer from the basin to the reservoirs, resulting in high nutrient concentrations, mainly phosphorus and nitrogen (LIRA *et al.*, 2020).

In the light of the above, this dissertation presents: a first chapter concerning a bibliometric analysis using the Web of Science (WoS) database to assess the historic evolution and future prospects (emerging fields of application) of reservoir evaporation; a second chapter concerning the direct measurement of evaporation in a reservoir located in a dry tropical region (Ceará, Brazil), presenting a novel sensor; a third chapter covering the assessment of evaporation in the same region using remote sensing and, afterwards, the evaluation of the impacts of climate change scenarios on the water availability in the State Capital Metropolitan Region (with a population of 4 million inhabitants invariably depending on reservoir water); and a fourth chapter which addresses the issue of macrophytes and their impact on open-water evaporation. The general objective of this thesis was to estimate evaporation in water bodies in the state of Ceará using different methods in order to produce more precise information on evaporative losses and their impact on water availability.

2 OPEN WATER EVAPORATION: BIBLIOMETRIC REVIEW OF ASSESSMENT METHODS AND RECENT ADVANCES

2.1 Introduction and methods

Open water evaporation stands as the second largest component of the global hydrological cycle, second only to precipitation, and plays a critical role in coupling the Earth's water and energy cycle (BEER; LI; ALVERSON, 2018). Projections indicate that the hydrological cycle is poised to intensify in the future due to global warming (HUNTINGTON, 2006; OKI; KANAE, 2006; JUNG *et al.*, 2010). This intensification is expected to manifest through heavier and more extreme precipitation events alongside enhanced surface evaporation, posing significant threats to drinking water resources and elevating the vulnerability of natural ecosystems and agricultural production (TRENBERTH *et al.*, 2014; JANSEN; TEULING, 2020).

Bibliometric studies have become widespread in many fields since 2006. In medical science, this technique has allowed researchers to analyse emerging trends and in economics and finance it has permitted to discover useful information that is not visible using other bibliographical approaches (YE *et al.*, 2020). In the scientific field of evaporation, relevant literature is abundant (over 500 references; see the following sections), but there are not many systematic analyses (to the best of our knowledge, only two reviews were made: (MCMAHON *et al.*, 2013; MCMAHON; FINLAYSON; PEEL, 2016). However, investigations on different approaches were published, such as: methodological and spatial scale issues (TANNY *et al.*, 2008); uncertainty (LOWE *et al.*, 2009); mapping (ZHAO *et al.*, 2022); economic damage (MARTÍNEZ-GRANADOS *et al.*, 2011), among others. The objective of this global review is, thus, to carry out a bibliometric analysis of open water evaporation literature using a well-known worldwide database: Web of Science (WoS).

The WoS is a website that provides subscription-based access to six large, interconnected databases ('Science Citation Index Expanded', 'Social Sciences Citation Index', 'Arts and Humanities Citation Index', among others) and several regional databases that provide worldwide comprehensive citation data for many different academic disciplines. It was originally produced by the Institute for Scientific Information (ISI) and is currently maintained by Clarivate Analytics (previously the Intellectual Property and Science business of Thomson Reuters) (DÍEZ-HERRERO; GARROTE, 2020). WoS was chosen to be our analysis database over other sources such as Scopus (Elsevier) or Google Scholar (Google), because it is the largest available citation database. Moreover, it is more selective in including scientific journal

titles in its ‘Journal Citation Reports’ lists; and Web of Science analytics are the most accurate and trusted source of research evaluation (CLARIVATE ANALYTICS, 2023).

Due to its emphasis on academic publications, the WoS database primarily contains entries from English-language scientific journals published by major academic publishers such as Taylor and Francis, Elsevier, and Nature-Springer. Consequently, it often overlooks literature stemming from the practical application of research in management (e.g., public administrations) and industry (e.g., companies). Nonetheless, WoS offers more standardized and reviewed databases, reducing the necessity to sift through redundant or duplicate records.

At the same time, WoS confers homogeneity to published papers as well as quality, as all of them have been revised in a peer-review. The ‘Core Collection’ of WoS was consulted and several thousand records were extracted using searches to perform a classical bibliometric analysis, using the available tools on the ‘Results Analysis’ menu. These include the fields: research areas, publication years, databases, document types, authors, countries/regions, group/corporate authors, languages, institutions and other categories. For each field of result analysis, a visualisation treemap or bar graph can be shown; and tables sorted by ‘Record count’ or by a ‘Selected field’ can both be downloaded as image files (.jpg) or tab-delimited text files (.txt). All these data have been analysed using a common spreadsheet and other office automation applications; all the bibliometric results and statistics were discussed by comparing scientific literature. Finally, the main conclusions regarding lake evaporation trends are highlighted, as well as the current main topic fields and those that are currently underdeveloped.

2.2 Results

2.2.1 Evolution of evaporation assessment literature

Firstly, the abstracts of the first 50 most cited papers in the field of reservoir evaporation were analysed (Figure 2.1). The most found words were, naturally, evaporation and water. Attention is drawn to highly cited places such as China and the Mediterranean. Moreover, one can get an idea of the methods used, as Penman, Pan and Radiation appear frequently as well. It is noteworthy that the term Eddy does not appear with much prominence, this is related to the fact that nowadays few investigations still offer the possibility to use such an approach.

Figure 2.1 - Word cloud of the most used terms in abstracts from the 50 most cited papers on reservoir/open-water evaporation.

Source: This research

The United States and China stand out as the countries with most studies in this research area (143 and 102 respectively) (Figure 2.2). Brazil appears in a prominent place (third, with 34 references), followed by Australia, Germany, and Iran. Most of these countries have dry regions, a fact that may explain their interest and the relevance attributed to evaporative loss studies in drier climates. It is also notable that in recent years several African countries, especially in the north of the continent, have been increasing the number of research on evaporation.

Figure 2.2 - Global distribution of scientific research involving evaporation in reservoirs/lakes. The recordings are based on the Web of Science database.

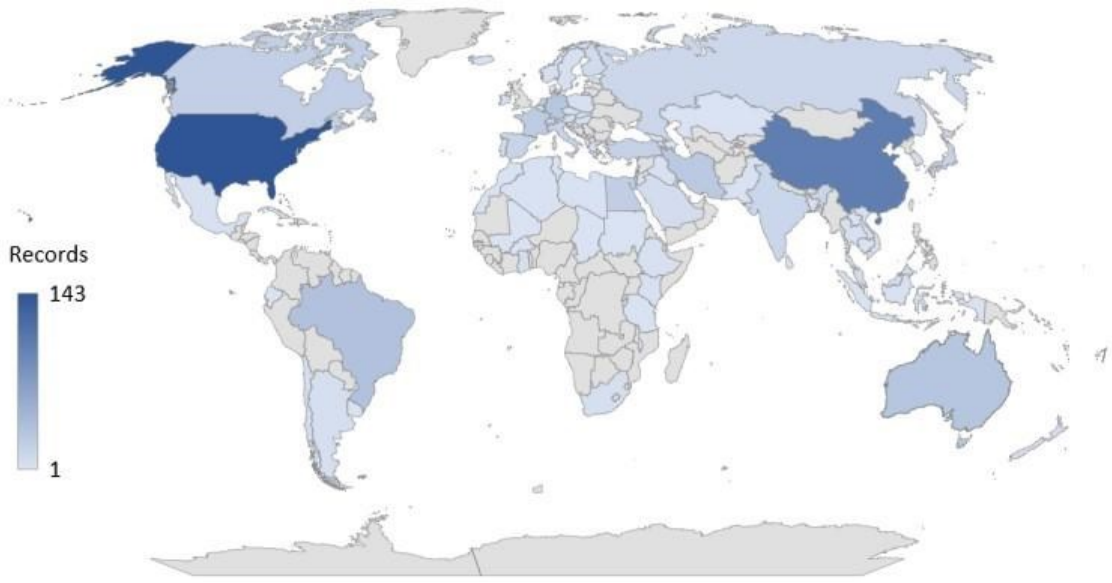

Since 2012 the amount of research in this area has grown considerably (Figure 2.3). Considering the 10 years following 2012, the year 2022 had 54 records compared to 17 in 2012, which represents a growth of 68%. It is reasonable to hypothesise that the significant increase in evaporation-related studies in the last 15 years is due to an increase in available measurement technology, but above all there is an increased interest in the effects of climate change: It may be noted that natural and man-made reservoirs are more closely monitored as the impact of climatic changes is being observed.

Figure 2.3 - References in the area of open water evaporation since the 1980s in the Web of Science database. The line refers to the accumulated values.

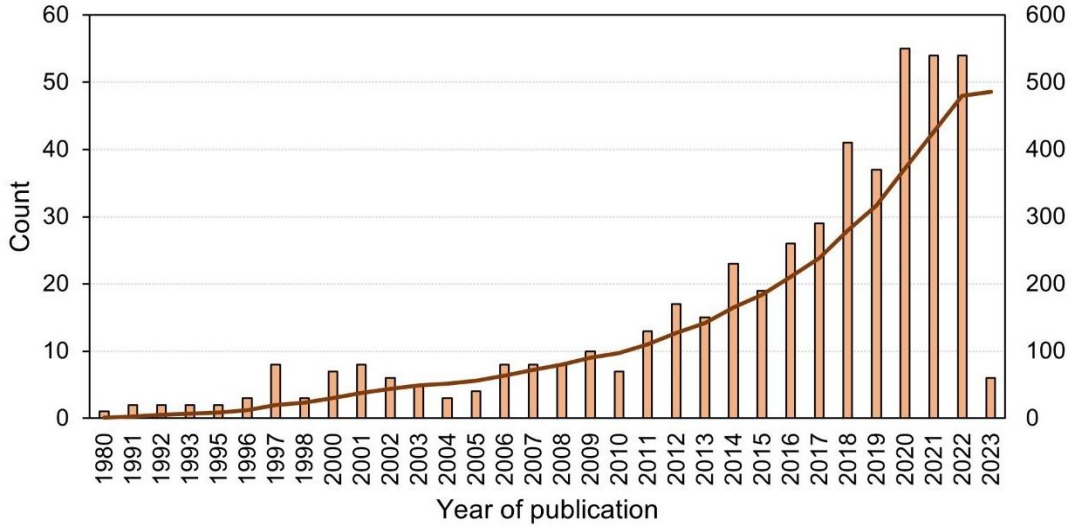

Observing affiliations on a global level reveals the dominance of Chinese institutions. Among the 10 institutions with most publications, four are Chinese. The best Brazilian institutions in this ranking are the Federal University of Ceará, 19th place, and the University of São Paulo, 47th place.

Table 2.1 - Affiliation of major research worldwide, records and relative percentage.

Affiliation	Records	%
Chinese Academy of Sciences	50	10.3
Egyptian Knowledge Bank Ekb	21	4.3
University of Chinese Academy of Sciences	16	3.3
University Of California System	15	3.1
Institute Of Geographic Sciences Natural Resources Research	14	2.9
United States Department Of The Interior	13	2.7
United States Geological Survey	13	2.7
Centre National De La Recherche Scientifique Cnrs	12	2.5

China University of Geosciences	11	2.3
Commonwealth Scientific Industrial Research Organisation CSIRO	11	2.3

Table 2.2 shows which institutions have developed more research in the area of evaporation in Brazil during the analysed period. It can be noted that the Federal University of Ceará has a relevant participation with almost 19% of the total of publications. Most of the ten top publishing institutions in the ranking are located in the South and Southeast of the country, only two are from the Northeast (UFC and Federal University of Pernambuco). In this context we presume that the large scientific contribution from Ceará is directly related to the strong regional hydric question and the need for water management in this region. The state of Ceará has tens of thousands of surface reservoirs (ARAÚJO *et al.*, 2022), which supply more than 9 million people, hence the need for research related to water losses by evaporation and reservoir management is prominent.

Table 2.2 - Affiliation of major research of Brazilian institutes, records and relative percentage.

Affiliation	**Records**	**%**
Universidade Federal Do Ceará	21	18.6
Universidade De São Paulo	12	10.6
Universidade Federal De Viçosa	8	7.1
Universidade Federal Do Rio De Janeiro	8	7.1
Instituto Nacional De Pesquisas Espaciais INPE	6	5.3
Universidade Federal Do Paraná	6	5.3
Universidade Federal Do Rio Grande Do Sul	6	5.3
Petrobras	5	4.4
Universidade Federal De Pernambuco	5	4.4
Universidade Federal De Santa Catarina	5	4.4

The ten main journals which publish evaporation papers are international (Tab. 3), especially the Journal of Hydrology with 4.4% of the references. Only three of the ten favourite journals for publications about evaporation are Brazilian (RBRH, Agriambi and Engenharia Agrícola).

Table 2.3 - Journals in which Brazilian research on open-water evaporation is most frequently published.

Peer-reviewed journal	Records	%
Journal of Hydrology	5	4.4
Journal of Cleaner Production	4	3.5
Water Resources Management	4	3.5
Agricultural Water Management	3	2.7
Anais da Academia Brasileira de Ciências	3	2.7
Energy Conversion And Management	3	2.7
Engenharia Agrícola	3	2.7
Renewable Energy	3	2.7
Water	3	2.7
Engenharia Sanitária e Ambiental	2	1.8

2.2.2 Research challenges

Estimating globe-scale reservoir evaporation losses remains a gap due to the limited accessibility of global long-term and continuous geographic reservoir information. We found two new datasets, Global Lake Evaporation Volume (GLEV, as in ZHAO *et al.,* 2022) and the Reservoir and Lake Surface Area Timeseries (ReaLSAT, as in KHANDELWAL *et al.*, 2022), which try to address this inaccessibility and provide an opportunity to bridge the gap.

In hydrologic practice there are two more approaches to estimate evaporation: the direct and the indirect method. In the direct method, evaporation is directly measured using an evaporation pan. Indirect methods include estimation of evaporation using empirical models that are based on meteorological data. Water evaporation is one of the most difficult components of the hydrologic cycle to measure accurately and there are two basic reasons for this difficulty. First, no instrumentation exists that can truly measure evaporation from a natural surface. Second, none of the indirect methods used for estimation of evaporation is universally accepted across the world (PATEL; MAJMUNDAR, 2016). Estimation of trustworthy or acceptable evaporation values requires either detailed instrumentation or cautious application of climatic and physical data.

2.2.3 Different methods applied for evaporation assessment

Most of the equations used in these methods were developed for specific studies and are most appropriate for use in climates similar to those for which they were developed. Often an equation is chosen because it proved to be satisfactory for some other study, or the equation selected may depend on the respective available data (WARNAKA; POCHOP, 1988). For example, in many hydrological lake studies, evaporation was determined using climate data

from the nearest weather station, which may have been located at some distance from the study lake. In other cases, climate data may have been collected at a land station adjacent to the study lake or reservoir because it was not possible to place or easily service a raft station on the lake or reservoir itself. It is difficult to select the most appropriate evaporation measurement methods for a given study. This is partly because of the availability of so many equations to determine evaporation, the wide array of data types needed and the expertise necessary for using the various equations correctly. More importantly, objective criteria for model selection are lacking. Consequently, the conditions under which one evaporation method would be more suitable than another are not always evident (SINGH; XU 1997). For applications in hydrology and water management, lake evaporation must be computed using indirect methods, such as empirical formulas, equations developed using dimensional analysis and the regression analysis approach.

2.3 Conclusions and outlook

The increase in the number of new studies on open water evaporation is remarkable. New monitoring methodologies are emerging, for example, studies using instrumentation directly placed in the water body and with remote sensing techniques are getting more frequent.

Studies estimating the impact of climate change on evaporation in urban and rural areas are also increasing. The United States and China dominate in the number of studies; however, several African countries (especially Egypt and South Africa) are boosting the scientific production in the area of reservoir evaporation.

Based on the analysis conducted in this chapter, it is possible to recommend several prospects for future research in order to address gaps in current knowledge and inform more effective water resources management strategies. For example:

- Integration of remote sensing techniques: Explore the integration of remote sensing techniques, such as satellite imagery and aerial photography, to improve the accuracy and efficiency of open water evaporation estimation.
- Impact of climate change: Investigate the impact of climate change on open water evaporation trends, considering both historical data and future climate projections. This could involve assessing the influence of changing precipitation patterns, temperature fluctuations, and other climatic variables on evaporation rates.
- Effect of land use changes: Examine how changes in land use, such as urbanization, deforestation, and agricultural expansion, affect open water evaporation dynamics. This research could help understand the interactions between land cover changes and evaporation processes.

- Integration of socioeconomic factors: Integrate socioeconomic factors into open water evaporation research would lead to better understanding of human dimensions of water resources management. Considerations such as water demand, population growth, and policy interventions can influence evaporation dynamics and should be accounted for in future studies.

3 DIRECT MEASUREMENT OF OPEN-WATER EVAPORATION: A NEWLY DEVELOPED SENSOR APPLIED TO A BRAZILIAN TROPICAL RESERVOIR[1]

3.1 Introduction

Knowing about the magnitude of evaporative losses in reservoirs in dry regions is essential for the proper management of consumptive use such as irrigated agriculture, industry and human supply (CRAIG, 2006; DJAMAN *et al.*, 2015). These basic needs are highly dependent on estimating evaporation accurately (MARTÍNEZ ALVAREZ *et al.*, 2008) since quantifying uncertainties can improve the efficiency of water governance (DE ARAÚJO; MAMEDE; DE LIMA, 2018; LOWE *et al.*, 2009; MCJANNET; COOK; BURN, 2013).

Despite numerous approaches developed over the last 200 years to estimate evaporation (MCMAHON; FINLAYSON; PEEL, 2016), there are still uncertainties within evaporation assessment, and the main reasons for this are: the high cost of maintaining the equipment (including personnel training); the numerous parameters needed to apply the equations; and the use of databases located far from the respective water body (for instance, class A pans or meteorological stations).

Bou-Fakhreddine *et al.* (2019) claim that these difficulties are caused by the high costs traditionally linked to data acquisition systems. Abtew and Melesse (2013) state that selecting an evaporation method demands a prior assessment of data generation costs. Indeed, most equations require parameters that need constant and thorough monitoring (ABTEW; MELESSE, 2013) and this is often impossible in the study region ((MCJANNET; COOK; BURN, 2013).

Xu and Singh (2000) argue that evaporation equations are generally more appropriate for climates similar to those where they were developed. Lowe *et al.* (2009) showed that most uncertainties can be reduced by installing evaporation pans near a reservoir rather than using measurements from pans located at a distance. Feitosa, de Araújo e Barros (2021) show that evaporation assessments based on data from inland stations far from the reservoir presented extremely high uncertainty.

While trying to reduce errors and uncertainties in evaporation estimation, increasingly accurate techniques have recently been developed (VIMAL; SINGH, 2022).

[1] A paper derived from this chapter was published as: Rodrigues, GP; Rodrigues, ÍS; Raabe, A; Holstein, P.; de Araújo, JC de. Direct measurement of open-water evaporation: a newly developed sensor applied to a Brazilian tropical reservoir, **Hydrological Sciences Journal**, 68:3, 379-394, https://doi.org/10.1080/02626667.2022.2157278, 2023.

Currently, one of the most reliable evaporation-assessment methods is the eddy covariance (FRIEDRICH *et al.*, 2018), which has a robust physical basis (SHUTTLEWORTH *et al.*, 1988); BLANKEN *et al.*, 2000; BRUTSAERT, 2005). Yet, variables may not be easily measurable. Evaporation measurements with eddy covariance techniques usually relate to limited periods (DUAN; BASTIAANSSEN, 2015). Furthermore, given their complexity and expense (VELLAME *et al.*, submitted), long-term studies are uncommon for small reservoirs. In fact, water regulatory agencies in most developing countries usually either lack the necessary apparatus or have it installed but in conditions of poor spatial distribution (YASEEN *et al.*, 2020; MOAZENZADEH *et al.*, 2018). Evaporation assessment is usually based on class A pans installed far from water body, on water balance and hydrological modelling (HELFER; LEMCKERT; ZHANG, 2012; MESQUITA *et al.*, 2020; WURBS; AYALA, 2014).

Evaporation assessments based on the water balance are often inaccurate (KAMPF; BURGES, 2010; FOWE *et al.*, 2015). During the dry season, however, acceptable results for monthly steps may be obtained from the water balance of semiarid reservoirs (FEITOSA; DE ARAÚJO; BARROS, 2021). Contrastingly, in the rainy season, the method yields poor results mainly due to diffuse water in- and outflows, as well as to groundwater fluxes.

Jansen and Teuling (2020) studied the effects of various evaporation parameterizations on shorter-term local water management (from hourly to decadal time step). Tan *et al.* (2007) modelled hourly and daily open-water evaporation rates in areas with an equatorial climate in Singapore. Other similar research efforts which adopted such time steps were almost exclusively dedicated to estimating evaporation for vegetated surfaces. For hourly open-water evaporation it is more common to find micrometeorological measurements that use eddy covariance systems (MIRANDA RODRIGUES *et al.*, 2020; TANNY *et al.*, 2011). There have been less attempts to apply these methods to estimations of open-water evaporation. As stated by Granger and Hedstrom (2011), evaporation from open water remains largely unmeasured as a course of routine. The major source of difficulty is the fact that the required meteorological variables are rarely measured over water surfaces, and the thermal lag between lake and land surfaces makes the use of land-based measurements ineffective in parameterising open water evaporation.

The aforementioned issues are particularly significant in densely inhabited areas that are sensitive to environmental and land use changes (TIAN *et al.*, 2021), such as the one-million km² Brazilian semiarid, located in the northeastern part of the country (MARENGO; BERNASCONI, 2015; MARENGO *et al.*, 2018). In this region, annual potential evaporation rates exceed 2,000 mm, annual precipitation averages 700 mm, groundwater is scarce and often

salty, and rivers are intermittent (GAISER et al, 2003; DE ARAÚJO; PIEDRA, 2009). During the dry season in the region, which lasts about 8 months, open-air reservoirs are the main water sources for human consumption and agriculture (PETER *et al.*, 2014).

Given this context, four open-air reservoir evaporation measurement methods were applied to a tropical reservoir for the present study: (i) Penman equation (1948) with variables measured in a floating meteorological station; (ii) an adaptation of the Dalton (1802) equation (RAABE *et al.*, 2020), also based on variables measured in the floating station; (iii) a standard pressure gauge installed in a floating pan inside the lake; and (iv) a novel sensor, derived from the echo-sound principle and installed in a floating pan inside the lake as well (RAABE *et al.*, 2021). This work intends to demonstrate to what extent two sensors and two physically-based models estimate evaporation of a tropical reservoir. Besides, we investigated the accuracy of each method with emphasis on the proposed acoustic sensor. Our interest was to assess which approach presents potential to improve water management in dry regions.

3.2 Methodology

3.2.1 Study area

The equipment was installed in the Gavião reservoir (2.7×10^7 m³, 6.18 km²), located in the State of Ceará, northeastern Brazil (NEB) (Figure 3.1). This lake is set on a sedimentary and crystalline base (IPECE, 2015), surrounded by perennial tropical coastal vegetation and some residential properties, and entirely located in a Tropical Savannah (As) climate according to the Köppen classification.

Many studies report the water deficit conditions in almost the whole territory of the NEB (KROL; BRONSTERT, 2007; MARENGO *et al.*, 2018; ALVALÁ *et al.*, 2019), which is 85% semiarid. Historically, dams have been built to provide water for the population during periods of drought, which generally last eight months (MAMEDE *et al.*, 2012); PETER et al, 2014). In Ceará, there are about 30,000 dams (GAISER *et al.*, 2003), and Gavião is the most downstream reservoir of the 300 km long metropolitan system, supplying water to four million inhabitants (RODRIGUES *et al.*, 2021)

Figure 3.1 - Study area and location of the floating weather station.

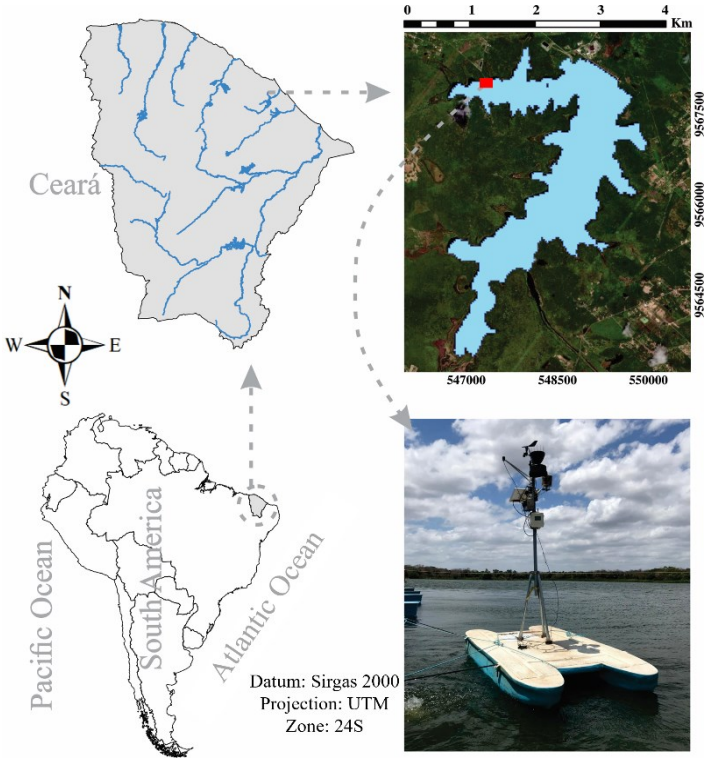

3.2.2 Installed setup

The equipment was positioned on the surface of the reservoir, about 30 m from the shore. The setup consisted of a weather station affixed on a raft (in Fig. 1, approximately 1.5 x 3 m) and two pan evaporimeters made of galvanised steel, both also floating and each with a sensor inside. The pans were designed according to the recommendations of the Word Meteorological Organization (DVWK[2], 1996; WMO, 2018; dimensions in Fig. 2). In order to reduce the wind-induced movement of the water surface, both pans have a stilling well. Given that the acoustic sensor is more sensitive to movement, a wave containment cylinder was placed around the pan (Figure 3.2, item a). Both sensors have a resolution of 0.1 mm (0.1 $kg.m^{-2}$).

[2] "DVWK" stands for "Deutscher Verband für Wasserwirtschaft und Kulturbau" (German Association for Water Management and Land Improvement). This association was responsible for setting standards and guidelines in the field of water management in Germany before it merged with ATV (Arbeitsausschuss für Technik im Wasserwesen) to form the DWA (Deutsche Vereinigung für Wasserwirtschaft, Abwasser und Abfall) in 2000. Therefore, "DVWK" represents the previous organization responsible for these guidelines.

Figure 3.2 - Floating pans with (a) the acoustic sensor and (b) the pressure sensor; (c) schematic sketch with the pan for the acoustic sensor and the wave-breaker cylinder; and (d) the pan for the pressure metre.

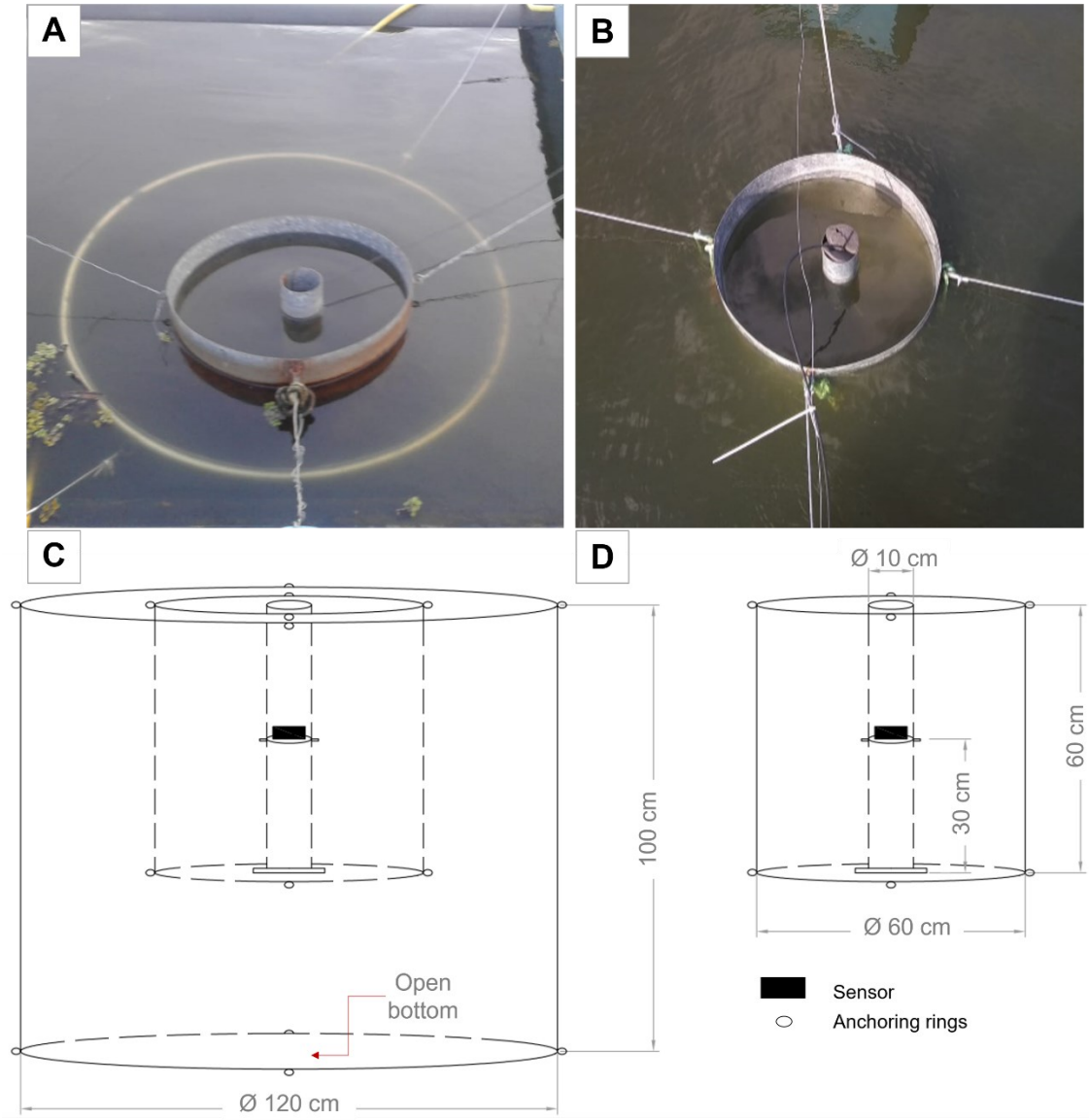

The raft was constructed of fibreglass; it is hollow, filled with plastic bottles and has four anchoring points. The weather station apparatus is described in Table 1. The data logger is a HOBO RX3000 model that sends information remotely to a website (https://hobolink.com/) where the data is downloaded in .xls format.

Table 3.1 - General information on the meteorological variables obtained from the onboard station.

Variable	Resolution	Data recording resolution
Water and air temperature, dew point	0.02 °C	10 min
Solar radiation	1.25 W/m²	
Precipitation	0.2 mm	
Relative humidity	0.1 %	
Wind speed and direction	0.1 m/s 1°	

The entire monitoring period extended from 16/Oct/20219 to 28/Feb/2020. There were, however, some failures in the sensors, notably the acoustic one. As the station was assembled before the sensors, the meteorological variables were collected earlier, except for water temperature, a necessary data for the Dalton equation, that's why calculation began only on 18/Oct. In order to easily understand and highlight the individual records of each method, Figure 3.3 was drawn up.

Figure 3.3 - Overview of the monitoring period for each approach (first day: 15 October 2019; last day: 29 February 2020). White spaces are missing data.

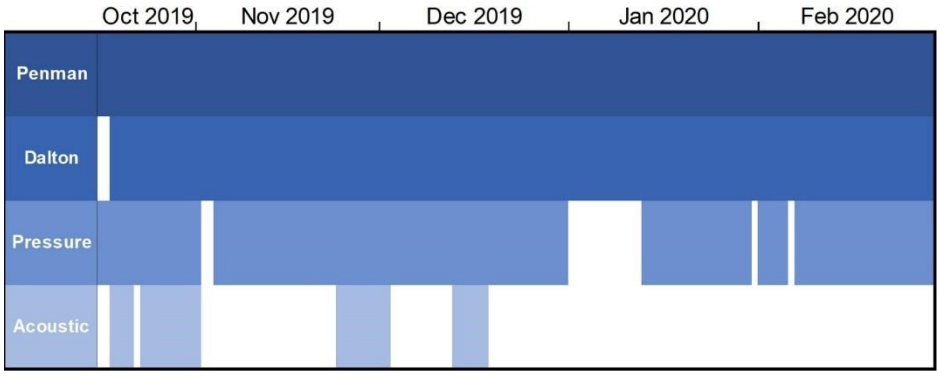

Due to the sensitivity of the sensors to reservoir water movement (mainly the acoustic sensor), not all the days could be recorded, so that some approaches have more data available than others. We, therefore, used for comparison only the days of simultaneous measurement from 17/10/2019 to 18/12/2019. Data provided by the floating station represented the input for the two equations - Penman and Dalton.

3.2.3 Evaporation assessment using Penman equation (E_{Pen})

Over the years, the Penman equation has undergone adaptations (VALIANTZAS, 2013) but in this work we strictly follow the steps described by Allen *et al.* (1998) and McMahon *et al.* (2013), used as a standard for situations in which data for radiation, wind, relative humidity, air and water temperatures, dew point temperature and altitude are available. All other parameters are derived from these. The Penman proposition (1948) for estimating open-water evaporation is defined in Equation 1.

$$E_{Pen} = \frac{\Delta}{\Delta + \gamma} \cdot \frac{R_n}{\lambda \rho} + \frac{\gamma}{\Delta + \gamma} \cdot E_a \quad (1)$$

In which, E_{Pen} is open-water evaporation (mm h^{-1}), R_n is net radiation at the water surface (MJ m^{-2} h^{-1}), E_a (mm h^{-1}) is a function of wind speed, saturation vapour pressure and average vapour pressure. The term Δ is the slope of the saturation vapour pressure curve (kPa K^{-1}) at air temperature (T, in °C), as in equation 2:

$$\Delta = \frac{4098 \cdot \left[0.6108 \cdot \exp\left(\frac{17.27 \cdot T}{T+237.3}\right)\right]}{(T+237.3)^2} \quad (2)$$

In Eq. 2, γ is the psychrometric coefficient (~0.0665 kPa K^{-1}), ρ is water density (1000 kg m^{-3}), and λ is the latent heat of vaporisation (~2.5 MJ kg^{-1}). The procedure to obtain γ and λ is described in Annex 2 of the FAO 56 protocol (Allen et. al, 1998).

According to Allen *et al.* (1998), saturation vapour pressure (es) and actual vapour pressure (ea) were estimated by Eqs. 3 and 4 (both terms in hPa). Since dew point temperature was recorded each 10 min, we assumed in this study the term e_a equal to saturation vapour pressure at dew point temperature (T_D), as recommended in (McMahon *et al.*, 2013):

$$e_s = 6.107 \cdot 10^{\frac{7.5 \cdot T}{237.15+T}} \quad (3)$$

$$e_a = 6.107 \cdot 10^{\frac{7.5 \cdot T_D}{237.15 + T_D}} \quad (4)$$

To obtain E_a (mm·h^{-1}) we adopted the Penman (1956) form of the wind function f(u), with the vapour pressure deficit ($e_s - e_a$) in kPa and average hourly wind speed at 2 m height (m s^{-1}) (Eq. 5). Somewhat different wind speed functions are given in literature (TANNY *et al.*, 2011); for this investigation we decided to apply the one suggested by McMahon *et al.* (2013). Thus, the wind dependent function was calculated as can be seen in Equation 6:

$$E_a = f(u)_{Pen} \cdot (e_s - e_a) \quad (5)$$

$$f(u)_{Pen} = 0.00547 + 0.00575 \cdot u \quad (6)$$

Net radiation (R_n) is given as the difference between net incoming shortwave radiation (R_{ns}) and net outgoing longwave radiation (R_{nl}), as shown in Equation 7:

$$R_n = R_{ns} - R_{nl} \quad (7)$$

The term R_{ns} depends on the measured incoming solar radiation (R_s) obtained directly from the weather station. All radiation terms are given in MJ m^{-2} h^{-1}. An appropriate albedo value (α) should be used. For this study we applied $\alpha = 0.065$ according to Jensen (2010) (Equation 8), whose work shows that albedo for water has a seasonal pattern and also varies with latitude:

$$R_{ns} = (1 - \alpha)\, R_s \quad (8)$$

The term R_{nl} is estimated in function of actual vapour pressure, average hourly temperature, the Stefan Boltzmann constant ($\sigma = 2{,}0412 \times 10^{-10}$ MJ K^{-4} m^{-2} h^{-1}) and the K ratio, as shown in Equation 9:

$$R_{nl} = \sigma\,(0.34 - 0.14 \cdot e_a^{0,5}) \cdot (T+273.2)^4 \cdot K \quad (9)$$

The factor K (expressed by $1.35\frac{Rs}{Rso} - 0.35$) is a correction dependent on the relation between measured incoming solar radiation (R_s) and clear sky radiation (R_{so}). The latter can be calculated with both geographical (elevation above sea level, latitude) and extra-terrestrial information (inverse relative distance Earth-Sun, sunset hour angle, solar declination), but the formulation is quite lengthy. Details are fully described by McMahon *et al.* (2013) and available in the supplementary material, section S3.

3.2.4 Evaporation assessment using Dalton equation (E_{Dal})

The second indirect method to estimate reservoir evaporation was an equation based on Dalton's principle (DALTON, 1802) and recommended by the World Meteorological Organization (RICHTER, 1975; RAABE *et al.*, 2020). In contrast to Penman, the Dalton formula uses the saturation deficit between a possible moisture content if air and water temperature were equal, and the observed air humidity. So here water temperature is required as a measured variable. The mass of evaporated water within a certain time depends on wind speed, relative humidity, and the difference between water vapour pressure on the water surface

and in the air (e_s - e_a) (Equation 10). Vapour pressure at water surface was obtained as the saturation value for water temperature, and water vapour pressure in the air corresponds to that of the dew point.

$$E_{Dal} = f(u)_{Dal} \cdot (e_s - e_a) \quad (10)$$

E_{Dal} is water surface evaporation ($mm.h^{-1}$), f(u) is the wind function of the horizontal wind velocity.

Like in the Penman formulation, the wind function f(u) accounts for the advective drying effects of wind and is is given in Eq. 11 (u in $m.s^{-1}$):

$$f(u)_{Dal} = a + b \cdot u \quad (11)$$

The parameters a and b need to be adapted to the respective measurement area (WMO, 1996); thus, the evaporation estimate over a period of one hour ($mm.h^{-1}$) for the investigated region was obtained with the parameters a = 0.00542 and b = 0.00392.

Due to its robust physical background, relative simplicity and reasonable accuracy (ELSAWWAF; WILLEMS; FEYEN, 2010; LIU *et al.*, 2016), Dalton is one of the most widely used models for calculating free water surface evaporation and served as a reference for the development of the following mass-transfer models.

3.2.5 Evaporation assessment using a pressure sensor (E_{Pre})

This approach employs a differential pressure sensor (UTK - EcoSens GmbH; see Figure 3.4) as a benchmark method: It is a commercially available sensor used for water monitoring purposes, such as water level difference or discharge, for example. The sensor is a KELLER 46X in a 30 hPa version and contains a ceramic measuring cell for low pressure ranges. The signal values from the pressure and temperature sensors are also computed with 10 min frequency and 0.1 mm resolution. These values can be displayed and saved on a personal computer and later programmed. The cell's reference chamber is connected to ambient pressure via a capillary tube integrated in the cable. The sensor is connected to a module that guarantees power supply and internet connection.

Figure 3.4 - Pressure sensor and its components (a) and schematic drawing of the measurement cell (b).

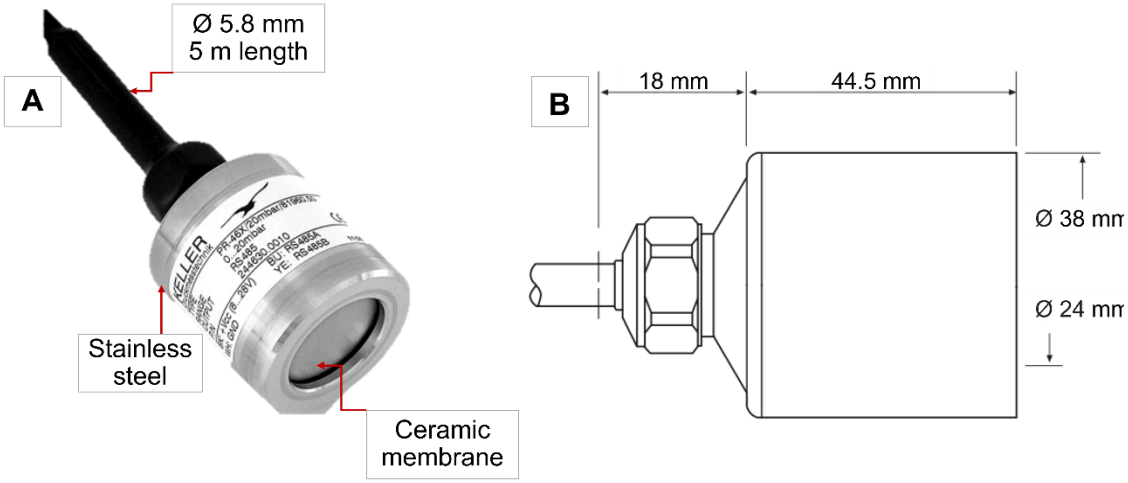

Source: Keller® company

The sensor measures the hydrostatic pressure exerted by the water column inside the pan, as well as local atmospheric pressure. For this reason, it is possible to calculate the level changes in the pan (Δh, in mm) (Eq. 12), considering that the reduction in water level is evaporation (E_{Pre}, in mm). Rainfall values (H) are deduced as shown in equation 13:

$$\Delta h = \frac{\Delta p}{\rho \cdot g} \quad (12)$$

$$E_{Pre} = \Delta h + H \quad (13)$$

In Equation 12, Δp is the difference between hydrostatic pressure, exerted by the water column, and atmospheric pressure ($N \cdot m^{-2}$); ρ is water density ($kg \cdot m^{-3}$); g is gravity ($m \cdot s^{-2}$); and H represents precipitation (mm) for the same time interval as the pressure measurements (Pa).

3.2.6 Evaporation assessment using an acoustic sensor (E_{Aco}, CORVO-AQUA)

This approach consists of a newly developed acoustic sensor attached to the bottom of an evaporation container floating in open water (as described in section 2.2). This sensor is used to determine the transit time of short ultrasonic signals between its position in the evaporation pan and the water surface (Figure 3.5). Hence, it measures the distance to the surface via the speed of sound in water (i.e. an echo sounder principle). 2 MHz sound signals are used by the sensor to determine the acoustic signal transit time between their respective position in the evaporation pan and the water surface. Theoretically, this method can measure transit time with an accuracy of 2 ps. Two temperature sensors register the water temperature

inside and outside the pan.

Figure 3.5 - Schematic drawing and measuring principle of the CORVO-AQUA sensor (a) and its components (b).

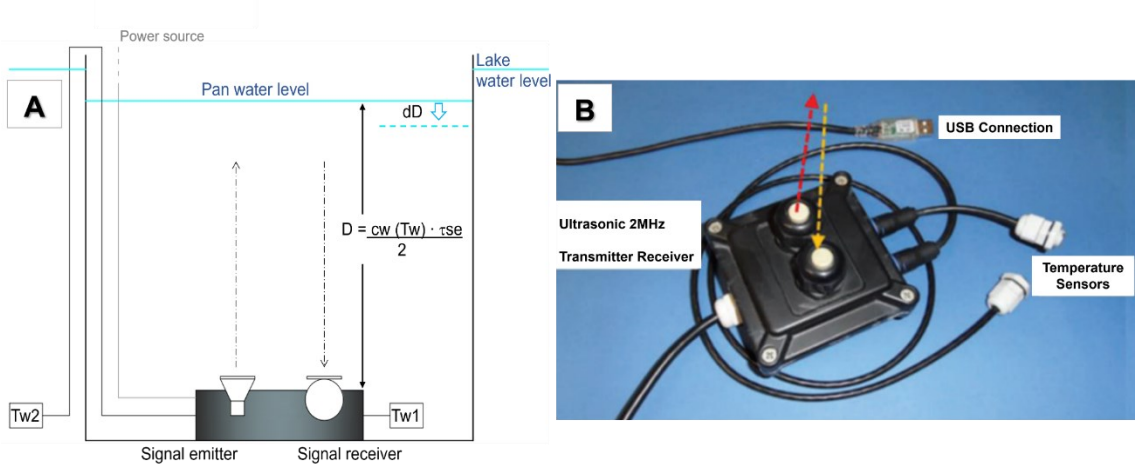

Equation 14 determines sound speed (c_W, $m.s^{-1}$) for the water in the evaporation pan:

$$c_w = 1402.95 + 5.044 \cdot T_w - 0.056 \cdot T_w^2 \quad (14)$$

Here T_w is water temperature (°C). Distance to the water surface is then calculated from the measured transit time of sound signals (τ_{SE}, in µs) and sound speed, as shown in Equation 15.

$$D = \frac{c_w(T_w) \,.\, \tau_{SE}}{2} \quad (15)$$

The evaporated water column E_{Aco} (in mm per unit of time, Eq. 16) is then obtained from the changing water level (dD) over a certain time (dT).

$$E_{ACO} = -\frac{dD}{dt} \quad (16)$$

3.2.7 Overview of evaporation measurements

Evaporation is given by the simple water balance, which corresponds to the reduction in height of the water column less precipitation. The pans were replenished whenever the water surface reached a very low level, which would have impeded sensor measurements. Precipitation events have similar effects (water level increase), so these events were considered when determining water level decrease. The on-board station was only 5 m away from the pans, so that any rainfall at the site was accurately measured.

To assess the performance of the methods, the Pearson correlation coefficient (r) and the root mean square error (RMSE) were used.

The root mean square error (Eq. 17) indicates standard deviation of the model prediction error.

$$RMSE = \sqrt{\frac{1}{N}\sum_{i=1}^{N}(S_i - O_i)^2} \quad (17)$$

While r varies between zero (no match) and 1 (perfect agreement), the ideal RMSE is zero and a large value suggests a bad adaptation of the model.

3.2.8 Sensitivity and uncertainty analysis

In order to estimate the impact of changes in the parameters of the Penman and Dalton equations, we performed a one-at-a-time sensitivity analysis on the parameters obtained from the weather station. The sensitivity analysis of Penman equation parameters had already been examined, the first respective studies date from the 1970s (BEVEN, 1979). Yet, it is known that some parameters vary according to the region (MAMASSIS *et al.*, 2014) and that literature has focused more on reference crop evapotranspiration than on open-water evaporation.

Measurement uncertainty is defined as an indication of how much the estimated value differs from the true value of the measurand in terms of probability; according to standard uncertainty, it is deemed to be the confidence interval for 95% of measurements (Eq. 18):

$$\sigma = \sum_{j=1}^{k}\sqrt{\frac{(\bar{y}_j - y_j)^2}{k}} \quad (18)$$

In Equation 18, σ is standard uncertainty; k stands for the number of points observed; y_j is each of the observations made with the acoustic sensor; and $\bar{y}_j$ the value for observations made with the standard sensor.

Measurement uncertainty of the other approaches was calculated by using Equation 19:

$$U = \frac{\frac{\sigma.t}{\sqrt{n}}}{x} \quad (19)$$

where U = Measurement uncertainty, σ = standard deviation, t = Student's coefficient for n measurements at a fixed value of reliability, n = number of measurements, and x = variable

value. The minimum number of measurements (n) was obtained by Equation 20.

$$n = \left(\sqrt{\frac{\sigma . t}{U}} \right)^2 \quad (20)$$

3.3 Results

3.3.1 Comparison of direct evaporation measurements

The accumulated evaporation recorded was 157.3 mm for the pressure sensor and 140.4 mm for the pressure-metre during the period from 17/Oct to 18/Dec. Recordings differed between 21/10 and 25/10 (Figure 3.6, item a) due to water inflow into the container which could not be corrected afterwards to obtain evaporation rates. From December 3rd to December 12th the acoustic sensor stopped operating (Figure 3.6, item b) because of technical issues but it continued data collection as usual until December 18th.

Figure 3.6 - Water level decrease for both the acoustic and the pressure sensor. Measurement period: a) 17/10/2019 to 01/11/2019; and b) 24/11/2019 to 18/12/2019.

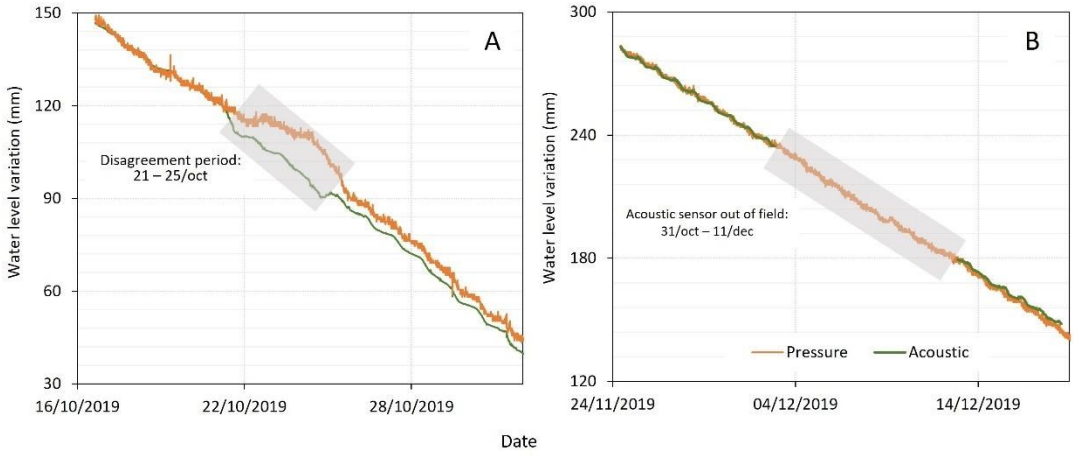

To illustrate the daily course of evaporation, we used 10 min step recordings to compose hourly averages. Higher variations were evident in the case of the pressure sensor (Figure 3.7); this is due to water movement caused by wind action (on average, 4.32 m s^{-1} at daytime and 1.64 m s^{-1} during nighttime for the study period). While the acoustic sensor stopped recording if subjected to angles greater than 6°, the pressure sensor continued to record data, and this affected the average and required correction. During that period, the average evaporation rate was: 0.38 ± 0.31 mm h^{-1} at daytime and 0.21 ± 0.21 mm h^{-1} at nighttime for the pressure sensor; and 0.35 ± 0.23 mm h^{-1} at daytime and 0.19 ± 0.13 mm h^{-1} at nighttime for the acoustic sensor.

Figure 3.7 - Hourly evaporation in the Gavião Reservoir based on the acoustic and the pressure sensor (17/10/2019 – 18/12/2019).

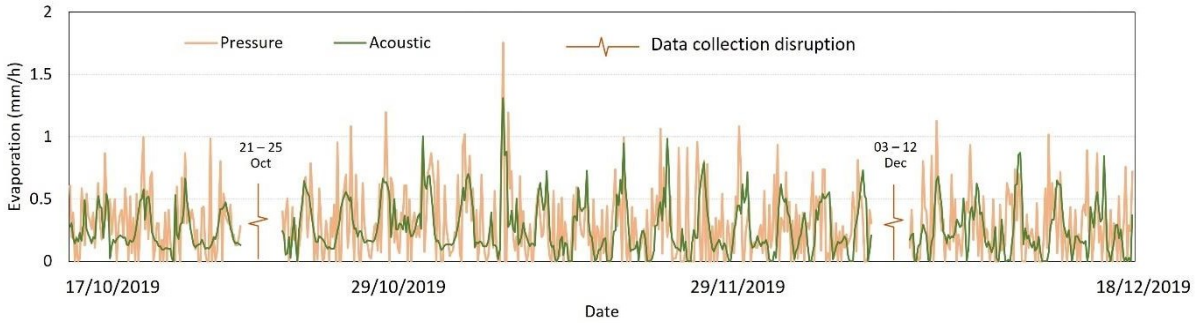

With the objective to assure data quality, we used values considered as missed input such as registers below zero and those between the 21st and 25th of October. It is relevant to mention the impact of this quality criteria on data loss: In the case of the acoustic sensor, 31.6% of raw data were lost due to recording errors caused by wave movement while the pressure sensor registered only 22.5% of lost data.

Daily evaporation obtained through 10-min time steps is presented in Figure 3.8 for the 22 measurement days. During that period, the average evaporation rate was 6.38 ± 1.00 mm day^{-1} for the acoustic sensor and 7.15 ± 1.01 mm day^{-1} for the pressure sensor (Figure 3.8).

Figure 3.8 - Average daily evaporation for both the acoustic and the pressure sensor. Measurement period: 17/10/2019 to 18/12/2019.

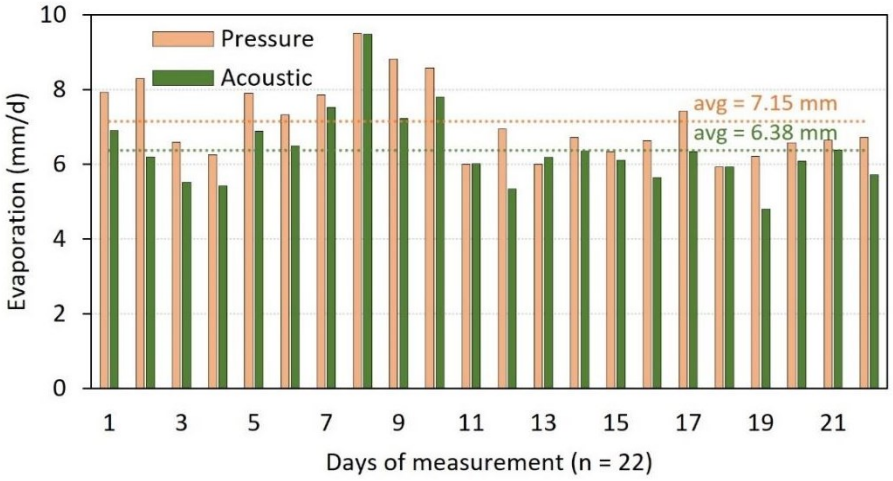

3.3.2 Evaporation assessment by equations

The evaporation rates gauged by the Dalton and the Penman equation also evidence a difference in the results of hourly steps and some similarity in the daily average. During that period, the average evaporation rate was: 0.35 ± 0.11 mm h^{-1} at daytime and 0.16 ± 0.06 mm h^{-1} at nighttime for the Dalton-modified equation; and 0.53 ± 0.33 mm h^{-1} at daytime and 0.03 ± 0.04 mm h^{-1} at nighttime for Penman.

Yet, when analysing hourly evaporation with the Penman equation, daytime peaks (over 1.0 mm h^{-1}) can be noticed and no more than a negligible night evaporation (0.01 mm h^{-1} on average) (Figure 3.9). This behaviour differs from all other approaches, which recorded some nighttime evaporation. Overestimation results of the Penman equation have already been observed in previous studies on free water surfaces, such as in Althoff *et al.* (2019), in which Penman overestimated the evaporation value in all the simulations performed in comparison with class A pan data. Lensky *et al.* (2018) showed that during summer evaporation is characterised by a diurnal double peak with one of these peaks related to radiative heat supply and the other to high wind speed during nighttime. This phenomenon could explain the difference between Penman and the other methods; still, a more focused investigation would be necessary, and this was beyond the scope of our research.

Figure 3.9 - Hourly evaporation from the Gavião Reservoir based on Penman and Dalton equations (17/10/2019 – 18/12/2019).

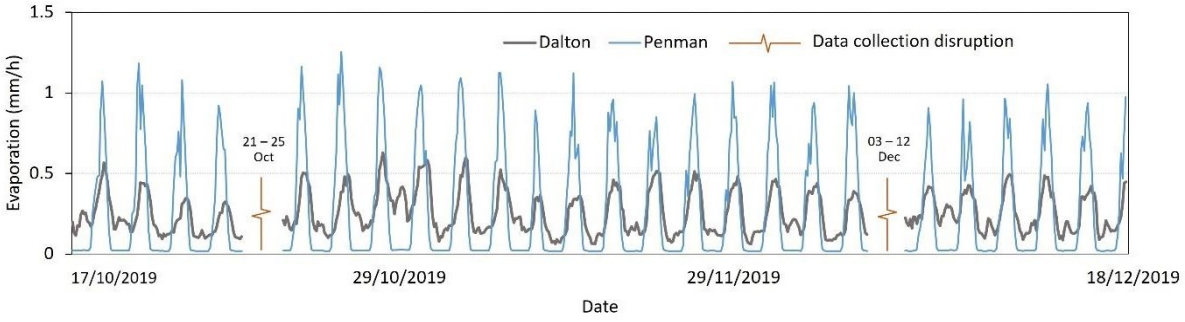

Daily evaporation rates are quite similar between Dalton and Penman (6.04 ± 1.09 mm day^{-1} and 6.83 ± 0.57 mm day^{-1}, respectively), but for physical process studies one needs a model which can precisely reproduce daily activities, such as an approach that uses the micrometeorological turbulence equation as in Raabe *et al.* (2021).

3.3.3 Comparison between all approaches

We compared the indirect methods and the acoustic sensor with the reference sensor (pressure-metre) at various time steps spanning 1h and 24h (Table 3.2 - Performance of evaporation estimation methods compared to the pressure sensor (benchmark) for different time steps. Bold numbers correspond to satisfactory performance ($r \geq 0.6$).). The acoustic sensor did not mimic hourly evaporation events measured by the pressure sensor, but it provided acceptable values from 4 h ($r > 0.6$) onwards. The modified Dalton model estimated values over 3 h time steps similar to those measured by the pressure sensor. The Penman model showed good results ($r > 0.7$) only for the 12 h time step or daily evaporation. Presumably, the reason lies in the fact that the Penman equation was developed for daily time steps and does not represent sub-daily evaporation activity properly. Indeed, Metzger *et al.* (2018) state that some approaches developed for longer time intervals are not applicable for sub-daily calculations and suggest the use of the Penman method only for longer time steps as its prediction skill improves with increasing time intervals.

Table 3.2 - Performance of evaporation estimation methods compared to the pressure sensor (benchmark) for different time steps. Bold numbers correspond to satisfactory performance ($r \geq 0.6$).

		Acoustic	**Dalton**	**Penman**
t	**n**		**r**	
1 h	590	0.36	0.37	0.27
2 h	299	0.46	0.55	0.36
3 h	196	0.53	**0.65**	0.44
4 h	147	**0.64**	0.73	0.36
5 h	115	0.62	0.79	0.53
6 h	97	0.68	0.80	0.53
12 h	46	0.73	0.82	**0.66**
24 h	22	0.82	0.76	0.66

t = time step; n = number of measurements; r = Pearson's coefficient.

As a matter of comparison, Feitosa *et al.* (2021) computed in a recent investigation for the same region of our study daily averages of approximately 7 mm day^{-1} with the Penman equation and data from an on-board meteorological station. Rodrigues *et al.* (2021) assessed evaporation for Gavião and other reservoirs nearby using the AquaSEBS algorithm (ABDELRADY *et al.*, 2016), which is based on the energy balance. The researchers noted underestimation by the algorithm when they compared it with the Penman equation and suggested that this fact might be due to a known tendency of the Penman model to overestimate (+2%) evaporation in tropical regions (as observed by MCJANNET *et al.*, 2013).

On a daily basis, evaporation overestimation is not large but consistent (Figure 3.10); yet it might lead to large errors when evaporation rates are aggregated over longer time periods. Apparently, despite overestimation during daytime, the very low night-evaporation rates which are basically caused by the aerodynamic effect (LENSKY *et al.*, 2018) compensate for the total volume in the Penman approach (Table 3.3). When comparing the evaporated volume during the days when the sensors collected data simultaneously, it was observed that Dalton registered 17.5 mm more than Penman.

Figure 3.10 - Evaporation from the Gavião Reservoir based on Penman and Dalton equations, as well as pressure and acoustic sensors (n = 22), for 24 h time steps. Measurements performed simultaneously using all methods (18/10/2019 – 18/12/2019).

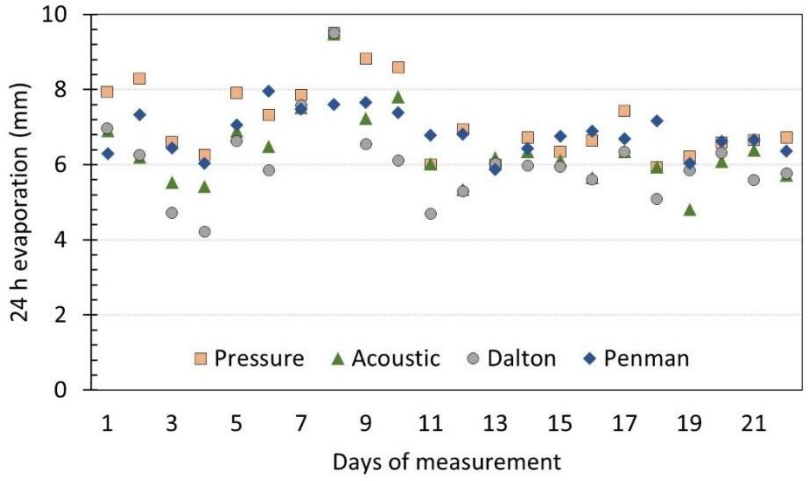

Table 3.3 - Accumulated and 24 h evaporation for recordings performed simultaneously by all methods (17/10/2019 – 18/12/2019).

n	Date	Pressure	Acoustic	Dalton	Penman
1	17/10/2019	7.93	6.91	6.97	6.30
2	18/10/2019	8.29	6.20	6.26	7.33
3	19/10/2019	6.60	5.53	4.71	6.44
4	20/10/2019	6.26	5.42	4.22	6.03
5	26/10/2019	7.91	6.89	6.62	7.06
6	27/10/2019	7.32	6.49	5.86	7.96
7	28/10/2019	7.86	7.52	7.58	7.48
8	29/10/2019	9.51	9.48	9.50	7.60
9	30/10/2019	8.83	7.23	6.55	7.66
10	31/10/2019	8.59	7.81	6.10	7.38
11	25/11/2019	6.01	6.02	4.69	6.78
12	26/11/2019	6.94	5.34	5.29	6.82
13	27/11/2019	6.00	6.18	6.03	5.88
14	28/11/2019	6.72	6.35	5.97	6.43

15	29/11/2019	6.34	6.11	5.95	6.75
16	30/11/2019	6.64	5.65	5.61	6.90
17	01/12/2019	7.43	6.35	6.34	6.68
18	02/12/2019	5.94	5.94	5.09	7.16
19	15/12/2019	6.22	4.81	5.85	6.04
20	16/12/2019	6.58	6.09	6.31	6.63
21	17/12/2019	6.65	6.39	5.59	6.66
22	18/12/2019	6.72	5.73	5.78	6.36
Accumulated		157.28	140.44	132.86	150.31
Average		7.15	6.38	6.04	6.83

An additional point of analysis was the effect of precipitation on both evaporation rates and data collection. Five rainfall events were recorded during the dry measurement period (Figure 3.11). We adopted the 25/Dec event as the threshold between the rainy period and the end of the dry season because from then on evaporation rates decreased remarkably and less than a week later a series of rainy days started that made the pans sink and compromised measurements.

Figure 3.11 - Evaporation from the Gavião Reservoir based on Penman equation (n = 142), Dalton-modified (n = 142) as well as pressure (n = 122) and acoustic sensors (n = 22), for the period 17/Oct/2019 – 29/Feb/2020).

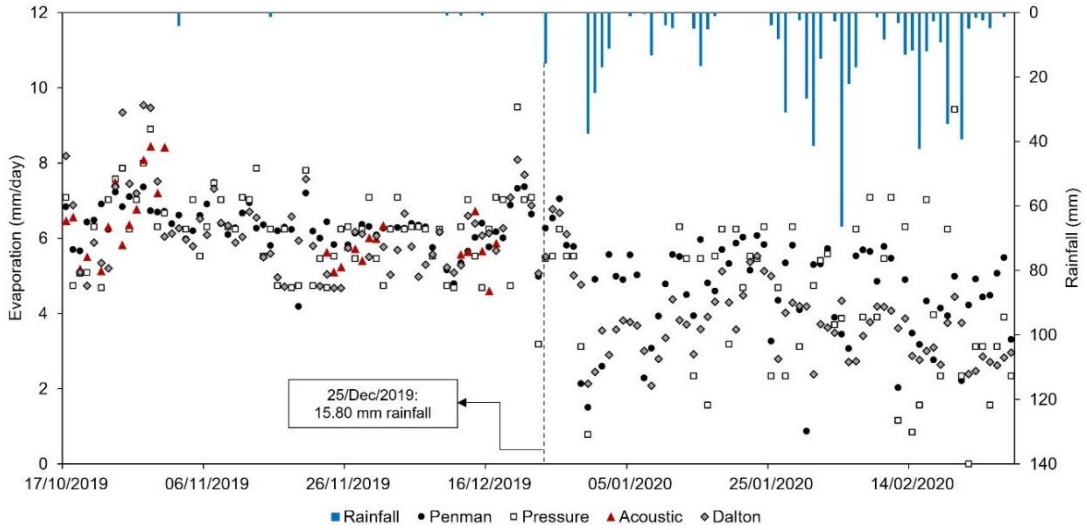

This negative correlation between precipitation and evaporation was also observed by Chen and Buchberger (2018), who analysed 259 data items from climatological stations located in various regions of the USA: The results revealed that 93 % of the weather stations exhibited a pattern of reduced evaporation when the rainy season started.

The humidity rate (%) is positively related to the formation of precipitation, while evaporation is inversely related to humidity (PENMAN, 1948; ALLEN *et al.*, 1998). As a result,

precipitation and evaporation will tend to exhibit a negative correlation and, according to Bouchet (1963), this is even more the case in semiarid or arid regions than in humid areas.

Figure 3.11 indicates that uncertainties in evaporation measurements increase considerably in the rainy season. The pressure sensor presented the biggest variations in this period, followed by the Dalton and Penman methods. It was not possible to obtain records with the acoustic sensor.

The comparison of different evaporation approaches is essential to determine which method is more accurate to estimate evaporation in this study area. Moreover, to the author's knowledge, evaporation has never been measured with these four methodologies as well as with such accuracy in the Brazilian Northeast, which makes this work unprecedented. A more precise understanding of this hydrological process is still missing in literature although it is undoubtedly crucial for water resources management, especially in water-scarce regions.

3.3.4 Sensitivity and uncertainty analysis

The relative change in hourly evaporation due to relative changes in the meteorological parameter is presented in Figure 3.12. The most sensitive parameter in Dalton's equation is water temperature (T_W): A change of only 5% already alters evaporation by 22% in a positive and linear manner. The least sensitive parameter was wind speed (±5% engender a ±2% change in evaporation). For Penman, the most sensitive parameter was global radiation with ±5% producing a ±3.8% change in evaporation, slightly followed by air temperature (±5% lead to a ±3.4% change in evaporation).

Evaporation values reveal the relevant influence of temperature in both approaches, while wind speed does not exert great influence (in the Dalton equation 4% cause a 5% alteration; in Penman 1% cause a 5% alteration).

Figure 3.12 - Sensitivity analysis for the Dalton-modified (a) and Penman (b) parameters directly obtained from the weather station. In the legend, Tw is water temperature, Ta is air temperature, Rs is global radiation, RH is relative humidity and u is wind speed.

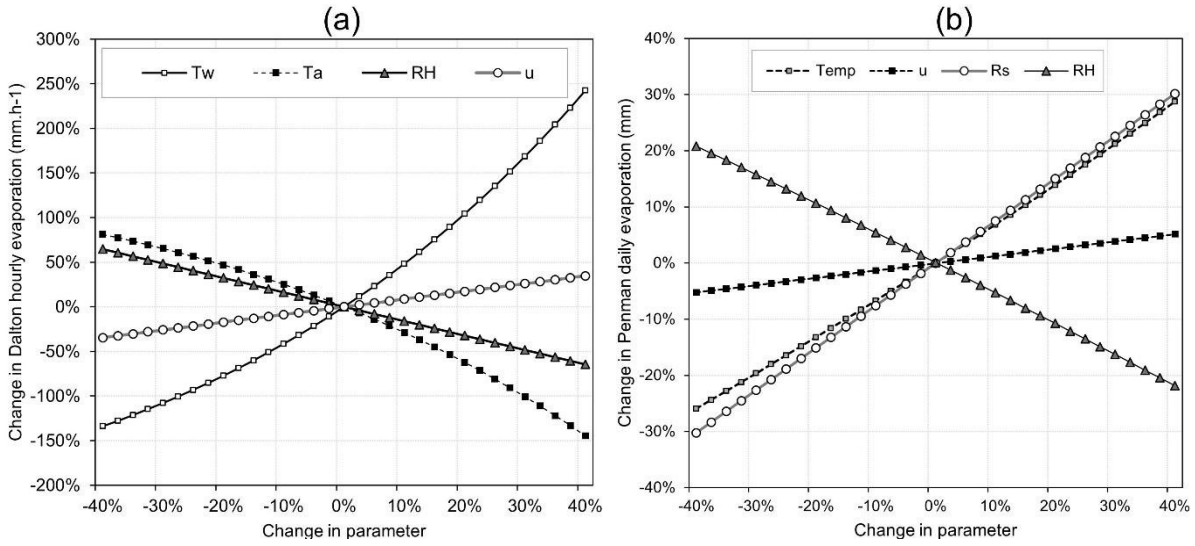

These findings can help to quantify the impact of climatic variations on evaporation, estimate the accuracy of predicted evaporation compared with that obtained from meteorological instruments, and investigate alternative methods in case of no adequate data.

The results plotted in Figure 3.9 above (Section 3.3.3) show the variability of the pressure sensor (explained by wave movement) and the minor dispersion of the Penman method (as seen in the metrics in Table 3.4). It is important to mention that this does not mean that the latter has fewer sources of uncertainty or is more accurate. It should be considered that the Penman equation is strongly influenced by the radiation factor, which during the study period did not vary (daily average of 241.48 ± 25.5 W m^{-2}) even on cloudier days. At first glance, all the evaporation estimation methods appear equally valid. Yet, it should be emphasised that the Penman equation besides requiring meteorological information also demands astronomical data which, from a practical and organisational point of view, makes it more difficult to implement. Dalton's equation, on the other hand, requires easily obtainable information (as long as there are hourly water temperature measurements, of course).

Table 3.4 - Descriptive statistics for sensors, Penman and Dalton equations regarding 24 h evaporation (all terms in mm). Measurements performed simultaneously using all methods (17/10/2019 – 18/12/2019, n = 22).

	Pressure	**Acoustic**	**Dalton**	**Penman**
Median	6.72	6.19	5.96	6.77
Minimum	5.94	4.81	4.22	5.88
Maximum	9.51	9.48	9.50	7.96
Standard deviation	1.01	1.00	1.09	0.57

For the acoustic sensor, individual runtime measurements with unchangeable environmental conditions and uncertainties of 0.003 µs are shown (see RAABE *et al.*, 2020). An accuracy of 0.1 µs is attainable given the water movement; this leads to an expected uncertainty in distance measurement of ± 0.11 mm.

Uncertainty analyses for a single measurement exhibit a good performance of the acoustic sensor (± 0.11 mm, same as in RAABE *et al.*, 2020) compared to the standard sensor (± 0.6 mm according to benchmark information); this makes it sensitive enough to record the daily course of evaporation although waves caused by the wind may influence measurement quality and long-term monitoring.

The minimum number of measurements with the acoustic sensor to obtain this level of uncertainty is 307 (Figure 3.13). In this case, uncertainty is 1.1% for 1h steps. These results serve as a basis for future approaches to assess the spatial variation of evaporation and wind on the lake; they might highlight the minimal number of instruments needed to gauge the spatial variability of evaporation.

Figure 3.13 - Relationship between number of field measurements (n) and the respective uncertainty (U) for the acoustic sensor.

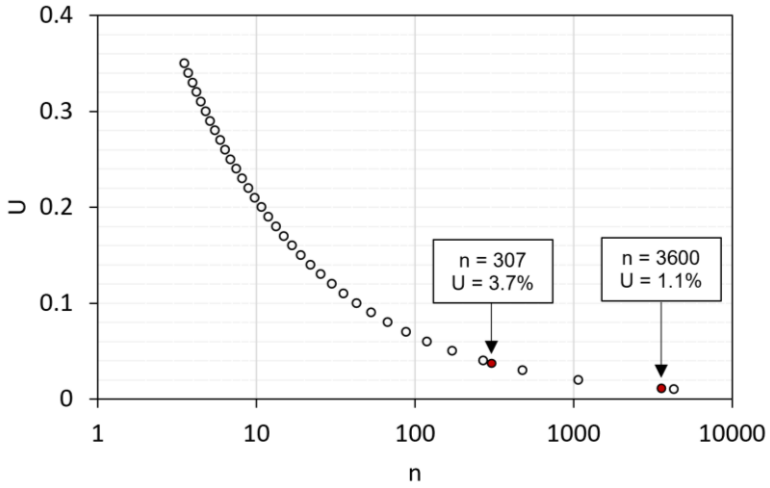

3.4 Discussion

3.4.1 Sources of uncertainty in evaporation assessment

Two common and relatively simple approaches to estimate evaporation are the class A pan method and measurements of standard meteorological parameters applied to equations. The difference in evaporation between a class A pan and a neighbouring reservoir was shown by Tanny *et al.* (2008) to be large, mainly because of the huge difference in water volumes and related heat storage between the pan and the reservoir.

In most cases, meteorological data are obtained from stations that are distant from the water body, sometimes tens of kilometres away. Our results revealed that the average daily evaporation by the novel method (acoustic sensor) differs 5% from the one of indirect methods (Penman and Dalton) which use floating station data. We recommend using information from meteorological stations that are close to the water body when monitoring evaporation if direct measuring sensors cannot be used. Our study corroborated for example the results of Feitosa *et al.* (2021), which conveyed overestimation of evaporation when making use of data from a station that is far from the reservoir. Neglecting the critical impact of reservoir evaporation could result in serious overestimation of water availability and therefore underestimation of the required storage capacity to support water management (MAYS, 2011).

The present paper describes direct and indirect methods to estimate lake evaporation. These models vary in complexity and data requirements. When selecting an appropriate model, analysts should consider the uncertainty of any available method.

Errors in lake evaporation estimates due to transposed data were studied by Rosenberry *et al.* (1993) for a lake in Minnesota, United States during 4 years of measurements. Their key conclusions were that replacing raft-based air temperature or humidity data with data from a land-based near-shore site affected computed estimates of annual evaporation between +3.7% and −3.6%. In their study, obtaining lake shortwave solar radiation, air temperature and atmospheric vapour pressure from a site 100 km away resulted in errors of +6% to +8 %.

The present study shows that even the choice of albedo generates an impact on evaporation calculations: 0.08 as recommended by McMahon *et al.* (2013) instead of 0.065 as suggested by Cogley (1979) led to underestimating evaporation by 2% and disregarding the effects of latitude and time of year on surface reflectance.

Investments in water saving measures are becoming common practice in water resources management. Managers are trying to reduce inefficiencies in water supply systems, including the evaporative loss of reservoir water (LOWE *et al.*, 2009). This explains why it is not uncommon to find recent studies in literature that aim to reduce reservoir evaporation losses

(MADY *et al.*, 2021).

The present study was conducted in a hot tropical region which is not semiarid, but still has high evaporation rates during about two thirds of the year. In addition, the Gavião reservoir is part of a reservoir network that provides water to about 4 million people (the most populated urban area in the Brazilian Northeast according to the most recent census, IBGE (2022)). In an environment in which climate change scenarios predict an increase in extreme events (heavy and more concentrated rainfall, flash droughts, for instance) during the coming decades (MARENGO *et al.*, 2022), investment in techniques that assess evaporative losses as effectively as possible becomes imperative.

3.4.2 Limitations of the instrumentation setup

The ideal situation for installing evaporation monitoring instruments depends mainly on two factors: i) knowledge of the measurement uncertainties of the apparatus used, and ii) knowledge of the spatial variation of evaporation from the lake in question. The latter happens because the evaporation rate tends to be higher on the shores, i.e., measurements made exclusively there are not representative of the entire water body and would be an overestimation (RODRIGUES *et al.*, 2021; ZHANG *et al.*, 2017).

We understand, of course, that the structure used in our study cannot be reproduced in most of the other reservoirs worldwide: An anchoring structure is required that is robust enough to prevent the sinking of a tank or dislocation of the floating meteorological station, and it needs to be positioned as far away from the shore as possible. In addition to heat flow being different near the shoreline, an installation positioned as close as possible to the reservoir centre also avoids the presence of animals, aquatic plants, and other disturbance factors near the equipment. If such an arrangement is not possible, a weather station installed as close as possible to the water body (but at a safe distance from an eventual flooding area) can also provide consistent results.

Our findings show the difference between direct methods (ideal) and indirect ones, such as through commonly used equations. Deviations are small at first sight, but if the accumulated values are multiplied by 7 (months of drought in the study area, from June to December) the deviation is around 170 mm per year. If water regulating agencies are provided with this kind of information, they perceive the order of magnitude of the deviation between measured and modelled values. The intention of this investigation was to test the performance of high-resolution sensors (0.01 mm) in the field with recording every 5 min. This procedure

illustrates the daily course of evaporation but generates a large data volume. Since instantaneous values of real evapotranspiration are not interesting for water managers, daily 24h values are computed as well. From the viewpoint of hydrological monitoring daily steps are sufficient for water yield and usage regulation, for example. Additionally, remote sensing tools can assist in monitoring evaporation (GUO *et al.*, 2019) and water volume loss in general (ZHANG *et al.*, 2021). A good match between reservoir size and spatial resolution of satellite imagery is always essential, because a mismatch can compromise estimations.

3.4.3 Outlook and further investigations

Overall, the four parameters provided by a weather station to be applied in evapo(transpi)ration calculations are: temperature, relative humidity, global solar radiation, and wind speed. Solar radiation is the parameter, which is least influenced by local surface conditions, while wind speed is the most affected factor (JIA, 2007). Referring to wind speed above 2 m s^{-1} Allen (2006) stated that temperature and relative humidity measurements are not conditioned by the surface surrounding the station with adequate fetch as required by the standard, but by the fetch distance upwind of the weather station.

Naturally, the equipment position in the reservoir and the representativeness of evaporation data for the entire water body deserve some debate given the spatial evaporation variations resulting from factors such as lake depth and proximity to the edge.

Overall, few studies have examined the classical ‘oasis effect’ for open-water conditions, only for vegetated surfaces. Regarding lake evaporation, Baldocchi *et al.* (2016) reported on six years of rice crop evaporation measurements based on the eddy covariance method. During this period, the authors noticed a strong (15%) decrease in annual evaporation. After inspecting trends in variations of biophysical variables (net radiation, temperature, leaf area index), they discovered the influence of an oasis-effect that cooled down the site. So, the amount of water lost by rice per unit area was a function of the size of the surrounding fields. This being said, an approach for wind measurement at different heights and different distances would be ideal to analyse the uncertainties related to fetch width and its influence on evaporation.

The resolution of both pressure and acoustic sensors in relation to other traditional methods does not vary much: It is 0.02 mm for a Class A pan and 0.1 mm for a Piché evaporimeter, since each evaporated ml cm^{-3} corresponds to a loss of 1 litre per m^2. The advantage is, however, in the equipment position within the water body and in the automation

of the evaporation recording process. Therefore, in addition to functionality, one should also take into account the financial aspects of monitoring compared to traditional methods. For data collection, both sensors require a power source (a solar panel feeding a 12V battery is the most practical option), a material protection structure (a sealed box for datalogger and cables) and adequate anchoring.

Precise knowledge of reservoir evaporation rates is essential to manage water resources, and some techniques may be implemented on the reservoir surface in a manner to reduce water losses by evaporation. Some examples are floating photovoltaic panels (RODRIGUES *et al.*, 2020), chemical covers and monolayers (BARNES, 2008), porous metallic materials (ALVAREZ *et al.*, 2006), counterweighted spheres (HAN *et al.*, 2020), as well as suspended shade cloth cover (GALLEGO‐ELVIRA *et al.*, 2011). Reduced evaporation rates occur as a consequence of shading the water body, and also of reducing the aerodynamic effect on the reservoir surface. Yet, the main advantage of floating photovoltaic panels compared with the other methods is the fact that they generate energy (SAHU *et al.*, 2016). Even though the above-mentioned methods can reduce evaporation rates, reservoir water quality may drastically decline as a consequence of the shading effect which interferes in all the parameters: the physical (e.g. water temperature, electrical conductivity, dissolved oxygen, total dissolved solids, turbidity, etc.), chemical (e.g. cations, anions, etc.) and also microbiological ones (e.g. faecal coliforms, *Escherichia coli*, etc.) (MAESTRO-VALERO *et al.*, 2011; MAESTRO-VALERO *et al.*, 2013).

It should also be recalled that climate change scenarios are predicting impacts on water availability in semiarid regions (EHSANI *et al.*, 2017; HUANG *et al.*, 2019); better accuracy in evaporation measurements is, thus, fundamental to foster respective simulations. We suggest the most precise measurements possible, close to the lake and preferably on top of the water body. One of the advantages of our floating-pan method is that evaporation measurements are independent of changes in the reservoir level due to outflows (e.g. irrigation, seepage) or inflows (precipitation).

3.5 Conclusions

The present study demonstrated to what extent two sensors (pressure and acoustic) and two physically-based models (Penman and modified Dalton) estimate evaporation of a tropical reservoir. The main conclusions drawn from the investigation are:

Wind-induced waves in the reservoir often disturbed the measurements using both pressure (uncertainty of ± 0.6 mm) and acoustic (uncertainty of ± 0.1 mm) sensors, causing flaws (respectively 22.5% and 31.2% of the 10-min records) and affecting continuous monitoring.

The acoustic sensor did not mimic hourly courses of evaporation measured by the pressure sensor, considered the benchmark method; yet it provided acceptable values over 4 hours ($r > 0.6$) or more.

The Penman model, based on data from a floating station, showed good results ($r > 0.7$) for 12 h time steps or daily evaporation.

The modified Dalton model, based on data collected with a floating station, estimated values over 3 h courses of evaporation similar to those measured by the pressure sensor.

4 CLIMATE-CHANGE IMPACT ON RESERVOIR EVAPORATION AND WATER AVAILABILITY IN A TROPICAL SUB-HUMID REGION, NORTH-EASTERN BRAZIL [3]

4.1 Introduction

The increasing atmospheric concentration of greenhouse gases is changing the Earth's climate more rapidly than ever before (KONAPALA *et al.*, 2020). Expected changes in climate variables such as rainfall and temperature may result in alterations in the hydrological cycle and, thus, in reservoir management strategies (MINVILLE *et al.* 2010). As climate changes, it is imperative to identify its impact on water supply, especially in the context of open-water reservoirs located in drylands.

As stated by Adrian *et al.* (2009), lakes, reservoirs and other inland open-water surfaces are likely to serve as good sentinels for current climate change because (1) lake ecosystems are well defined and continuously studied; (2) lakes respond directly to climate change and also incorporate the effects of climate-driven changes occurring within the catchment; (3) lakes integrate responses over time, which can filter out random noise; and (4) lakes are distributed worldwide and, as such, can act as sentinels in many different geographic locations and climatic regions, capturing different aspects of climate change (e.g., rising temperature, glacier retreats, permafrost melting). Indeed, several investigations worldwide have highlighted the impact of climate change on water resources. Reservoirs are essential infrastructures for the economic and social development of a region, their evaporation losses are significant for the water system and can severely impact water availability and allocation (MALVEIRA; ARAÚJO; GÜNTNER, 2012; MAMEDE *et al.*, 2012; PETER *et al.*, 2014).

The state of Ceará in the Brazilian semiarid region is supplied by a dense network of surface-water reservoirs and they are vulnerable to droughts and water deficit (MEDEIROS; DE ARAÚJO, 2014). The accurate knowledge of evaporation, which corresponds to 30%-50% of the water budget, is fundamental to manage the water resources and to assess the impacts of climate change on water availability.

In hydrology and in studies relating to water availability, free-surface evaporation is essential. Climate change plays a critical role in water resource planning: The water cycle is expected to be accelerated because of increasing temperatures, among others. In warm

[3] A paper derived from this chapter was accepted for discussion: Rodrigues, G. P., Brosinsky, A., Rodrigues, Í. S., Mamede, G. L., and de Araújo, J. C.: Climate-change impact on reservoir evaporation and water availability in a tropical sub-humid region, north-eastern Brazil, **Hydrology and Earth System Sciences.** [preprint], https://doi.org/10.5194/hess-2023-189, in review. Publication: 2024.

atmospheric conditions, climate change is expected to worsen water shortage episodes. Investigations reveal the sensitivity of lakes to climate and convey how rapidly physical, chemical, and biological lake properties respond to climate-related changes (ADRIAN *et al.*, 2009; ROSENZWEIG *et al.* 2007).

Climate change is studied by means of global circulation models, usually with coarse spatial resolution of hundreds of kilometres, disregarding regional factors in the modelling (CHOU *et al.*, 2014; NAVARRO-RACINES *et al.*, 2020). Hence the importance of regional climate models (RCMs), which have a smaller scale (usually tens of kilometres) and consider local factors such as topography, land cover and land use. One of the issues addressed refers to the resilience of metropolitan areas to climate change. Major problems may be related to rapid changes in urban mobility and the supply of water and energy (LYRA *et al.*, 2018).

The Metropolitan Region of Fortaleza (MRF) has a population of over 4 million inhabitants (IBGE, 2022) and is one of the most densely-populated areas in Brazil. Its water supply is highly dependent on an extensive network of open-water reservoirs, almost entirely located in the semiarid region (MAMEDE *et al.*, 2018; PETER *et al.*, 2014). Despite the well-known sensitivity of dry regions to changes in climate, little is yet known about the impacts on water resources in this region and how water availability may be affected in the future. With this investigation we intend to increase the amount of information currently existing on the possible impacts of climate change on water resources in Northeast Brazil. Although several studies in this region focus on temperature variation (MARENGO, 2009) and precipitation (ALMAGRO *et al.*, 2020), our analysis might contribute to the growing body of knowledge on surface water reservoirs and demonstrate how lake systems respond to climate change.

The objective of this research was, then, to analyse the impact of climate change on reservoir evaporation and its respective water availability in a densely populated urban area located in northeastern Brazil. To achieve our goals, we (i) assessed historical and present evaporation by means of a meteorological station and remote sensing calculations, (ii) compared them to historical and future simulations based on four climate change scenarios, and (iii) investigated the impact of climate change on water availability through stochastic modelling.

4.2 Study area

The state of Ceará is situated in the northeastern region of Brazil (Figure 4.1), it is mostly semiarid (BSh, according to Köppen classification) and a dryland where various studies on the impacts of climate change have shown susceptibility to severe climate extremes, especially droughts (ALVALÁ *et al.*, 2019; MARENGO *et al.*, 2017, 2022; VIEIRA *et al.*, 2020). The average annual rainfall in the region is about 800 mm (of which 80% occurs between January and April); average annual temperature is 26 °C and relative humidity 78% (INMET, 2019; RODRIGUES *et al.*, 2021). This region has high water vulnerability resulting from irregular rainfall associated with ephemeral rivers, high potential evaporation rates exceeding 2000 mm per year and shallow soils over crystalline basement (DE ARAÚJO; PIEDRA, 2009; MEDEIROS; DE ARAÚJO, 2014). This soil-feature allows only limited storage of water (ALVALÁ *et al.*, 2019) which, when present, is often salty because of the prevalence of fissural aquifers in crystalline bedrock.

Figure 4.1 - Location of the reservoirs that supply the Metropolitan Region of Fortaleza, hydrographic network and INMET station.

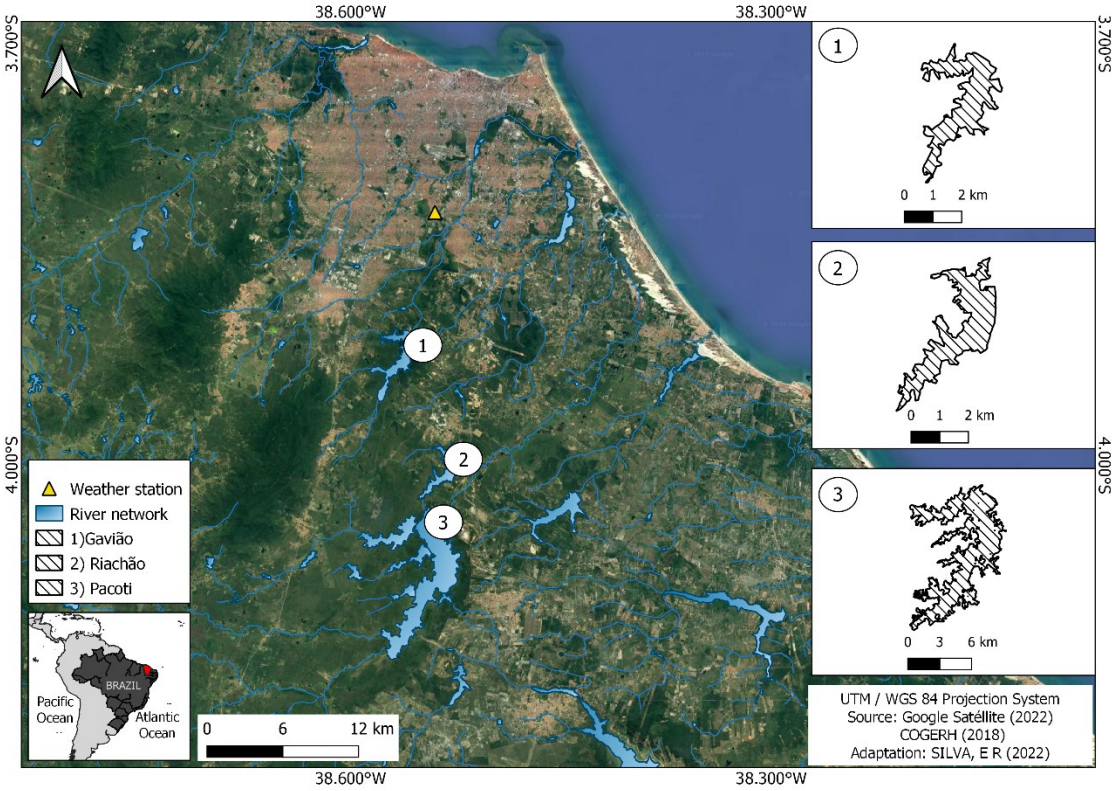

The reservoirs under analysis in this study (Pacoti, Riachão and Gavião, see Table 2.1) are responsible for supplying water to approximately 4.2 million inhabitants and comprise the downstream sector of a network of reservoirs located in a sub-humid territory. Unlike the reservoirs that supply them, the water level of these three reservoirs does not decrease

substantially during the dry season, due to a transposition system that provides water.

Table 4.1 - Technical characteristics of Pacoti, Riachão, and Gavião reservoirs.

	Pacoti	**Riachão**	**Gavião**
Capacity (hm^3)	380.0	47.9	33.3
Catchment area (km^2)	1,110	34	97
Hydraulic basin (km^2)	37.0	5.7	6.2

Source: Secretariat for Water Resources, SRH (2015).

4.3 Methodology

To assess the impact of climate change on reservoir evaporation and the consequent water availability in the Fortaleza Metropolitan Region, we analysed three supply reservoirs: Pacoti, Riachão, and Gavião (Figure 4.1). We used the regional Eta model (MESINGER *et al.* 2012) nested to two Global Circulation Models (CanESM-2 and MIROC5) and in the context of Representative Concentration Pathways 4.5 and 8.5. The investigation was performed in three phases: the first consisted of simulating regional evaporation patterns with bias correction; the second involved the combined application of remote sensing and *on-site* measurement to assess open-water evaporation; and in the third we analysed the impact of evaporation changes on water availability for four scenarios. For ease and convenience, the four scenarios are hereafter referred to as C4 (model Eta-CanESM2, Pathway 4.5), C8 (model Eta-CanESM2, Pathway 8.5), M4 (model Eta-MIROC5, Pathway 4.5) and M8 (model Eta-MIROC5, Pathway 8.5). The methodological framework is presented in Figure 4.2.

It is outside the scope of this work to study the effects on the general hydrology of the study area, but rather focus on a single hydrological process, which is a major cause of water losses in the whole region.

Figure 4.2 - Methodological flowchart for the simulation of evaporation with climate models and assessment of water availability.

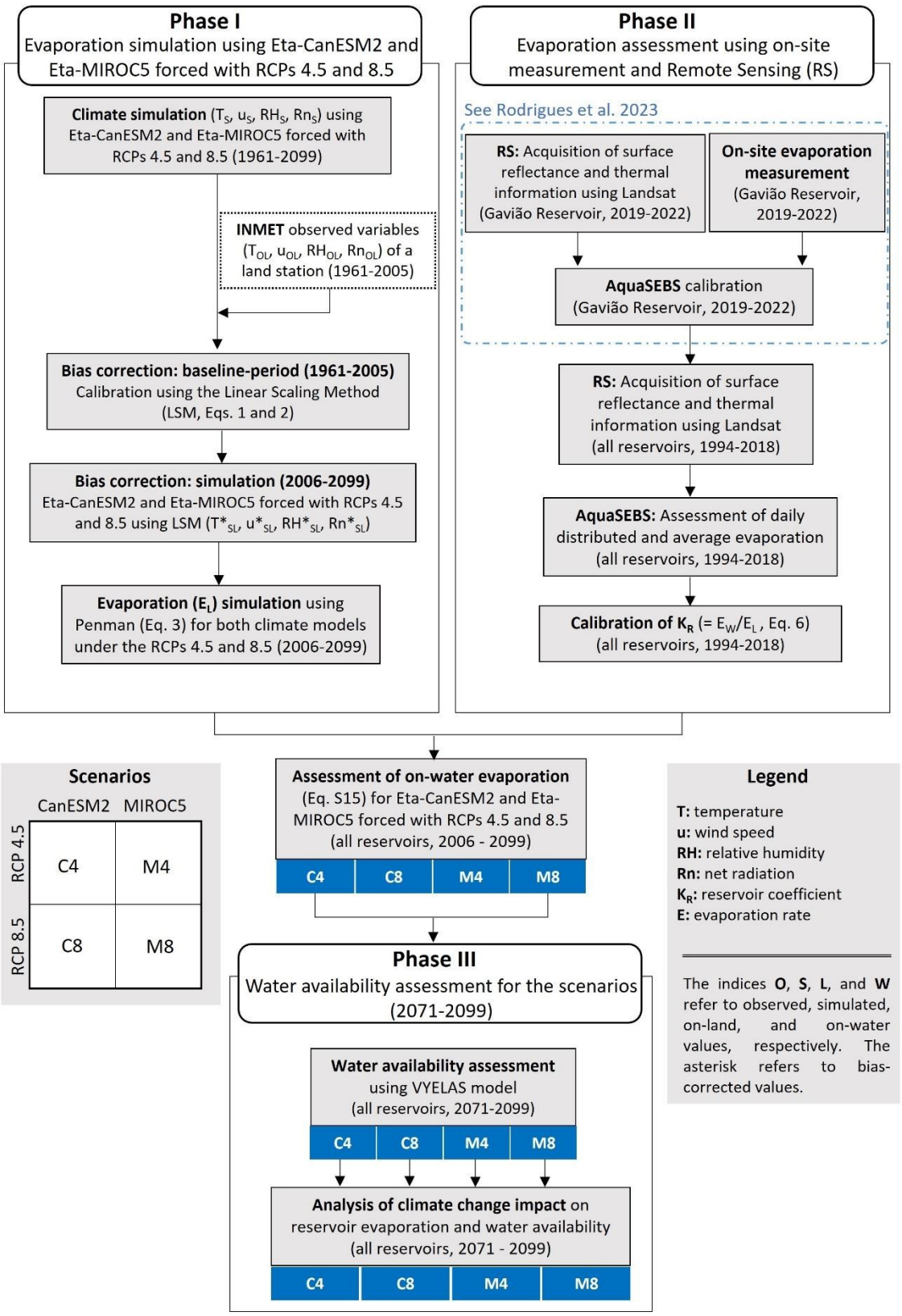

4.3.1 Phase I: Evaporation simulation forced with RCPs 4.5 and 8.5

Using the regional model Eta (MESINGER *et al.* 2012) of the Brazilian National Institute for Space Research (INPE), we assessed daily meteorological variables such as net radiation, wind speed, mean temperature and relative humidity. The Eta model is nested to the Japanese MIROC5 (The University of Tokyo Centre for Climate System Research, WATANABE *et al.*, 2010) and to the Canadian CanESM-2 (Canadian Centre for Climate Modelling and Analysis, CHYLEK *et al.*, 2011). According to Chou *et al.* (2014), the Brazilian model has been used operationally at INPE since 1997 for weather forecasts, and since 2002 for seasonal climate forecasts. The model was set up with a spatial resolution of 20 km, covering both South and Central Americas.

Since the Fifth Assessment Report (AR5) from the Intergovernmental Panel on Climate Change (IPCC 2014), the greenhouse gas concentration scenarios are based on the Representative Concentration Pathways (RCP), which are expressed in terms of radiative forcing toward the end of the twenty-first century. In this study, the downscaled products were simulated based on RCP4.5 and RCP8.5. The first provides a climate forcing that reaches 4.5 W m^{-2} by 2050 with further stabilisation; the latter provides continued growth of the radiative forcing to reach 8.5 W m^{-2} by 2100 (BJØRNÆS, 2013). All simulated data were extracted from the INPE Portal "Climate Change in Brazil" and made available on the PROJETA Platform (https://projeta.cptec.inpe.br).

Outputs from regional climate models are often prone to systematic errors (biases), therefore, bias correction is recommended (GRAHAM *et al.*, 2007) for simulation reliability purposes (TEUTSCHBEIN; SEIBERT, 2012). To correct bias, we applied the Linear Scaling Method (LSM), often used in studies of hydrological impacts of climate change (ALTHOFF *et al.*, 2020; OLIVEIRA *et al.*, 2017; FISEHA *et al.*, 2014). The correction is based on the identification of biases between observed and simulated climate variables. Temperature (T) is corrected with an additive factor ($\overline{T}_{obs}$- $\overline{T}_{sim}$, Equation 1, where both terms are the monthly average), whereas the remaining meteorological variables (represented by the letter C) are corrected with a multiplicative factor ($\overline{C}_{obs}$ / $\overline{C}_{sim}$, Equation 2, where both terms are the monthly average). Equations 1 and 2 were used for both the baseline (1961-2005) and scenarios simulation (2006-2099) periods.

$$T^{*}_{(t)} = T_{(t)} + \overline{T}_{obs} - \overline{T}_{sim} \quad (1)$$

$$C^{*}_{(t)} = C_{(t)} \cdot \left(\frac{\overline{C}_{obs}}{\overline{C}_{sim}}\right) \quad (2)$$

In Equations 1 and 2, the variables to which C refers are relative humidity (%), wind speed at 2 m height (m s^{-1}), and net radiation (MJ m^{-2} day^{-1}); the asterisk indicates the climate variable values after bias correction. Daily observed meteorological variables from a station of the Brazilian National Institute of Meteorology (INMET) were used to correct bias of the climate model in the period from 1961 to 2005 (station code: 82397 - Fortaleza). The station was chosen due to two aspects: it is the nearest weather station to the reservoirs, and it has produced longer historical series with fewer flaws. To assess evaporation, we used the Penman (1948) Equation 3:

$$E = \frac{\Delta}{\Delta + \gamma} \cdot \frac{R_n}{\lambda v} + \frac{\gamma}{\Delta + \gamma} \cdot f(u) \cdot (e_s - e_a) \quad (3)$$

In Equation 3, E is the open-water evaporation rate (mm d^{-1}); R_n is net radiation at water surface (MJ m^{-2} d^{-1}); Δ is the slope of the saturation vapour pressure curve (kPa $^oC^{-1}$) at air temperature; γ is the psychrometric coefficient (assumed 0.0665 kPa $^oC^{-1}$); ρ is water density (1000 kg m^{-3}); λv is the latent heat of vaporisation (assumed 2.5 MJ kg^{-1}); (e_s - e_a) is the difference between saturation and partial water vapour pressure (kPa), and f(u) is a function used to account for the advective drying effects of wind (mm $d^{-1}kPa^{-1}$). In Equation 4, u is the wind speed at 2 m height (m s^{-1}). We have adopted the Penman (1956) form of the wind function:

$$f(u) = 1.313 + 1.381 \cdot u \quad (4)$$

A trend analysis was carried out using the Mann-Kendall method (KENDALL, 1975; MANN, 1945). The null hypothesis states that there is no trend in the series. The three hypotheses evaluated are: i) no trend, ii) positive trend, iii) negative trend. A significance level of p = 0.05 was adopted. The magnitude of the changes was evaluated by the nonparametric Sen's slope and Kendall's tau (τ) coefficient, which describes the relationship between variables.

4.3.2 Phase II: Evaporation assessment using on-site measurement and Remote Sensing

The on-water evaporation rate was estimated utilising the remote sensing algorithm AquaSEBS (Surface Energy Balance of Fresh and Saline Waters, see ABDELRADY *et al.*, 2016). The algorithm is a modification from Su (2002) and was developed to estimate heat fluxes by integrating satellite data and hydro-meteorological field data. It was validated in the study region (RODRIGUES *et al.*, 2021b, 2021a), and requires three sets of data as input: (i) remote-sensing data, including emissivity, surface albedo and surface temperature; (ii) meteorological data; and (iii) radiative forcing parameters such as downward shortwave and

long-wave radiations. The following Landsat bands were used for a temporal estimation of evaporation: bands 1 to 5 (reflectance) and band 6 (thermal) from Landsat 5 (Thematic Mapper - TM) and bands 1 to 7 (reflectance) and band 10 (thermal) from Landsat 8 (Optical Land Imager - OLI). Due to the technical characteristics of the sensors (radiometric, spectral, and thermal band spatial resolutions), methodological adjustments were necessary to define some parameters in the model application (see APPENDIX B - AQUASEBS OVERVIEW).

AquaSEBS uses the energy balance to calculate instantaneous latent heat flux of evaporation (Equation 5), thus, evaporation is calculated for each pixel of the image. The energy balance of the water surface can be expressed as it follows:

$$E_w = \frac{R_n - G_w - H}{\lambda v \cdot \rho} \quad (5)$$

In Equation 5, R_n is net radiation on the water surface, G_w is the water (or ground for land surfaces) heat flux, and H is sensible heat to the air. All terms are expressed in W m^{-2}. Detailed information about the algorithm and the meteorological input is provided in the Supplementary Material 1 of this manuscript. To assess the on-water evaporation rate (E_w) in the scenarios, we used Equation 6, in which E_L stands for the on-land evaporation rate and K_R is a coefficient. E_L refers to a value provided by the models Eta-CanESM2 and MIROC5, whose bias was corrected using data from an on-land meteorological station. The coefficient K_R was calibrated using AquaSEBS to assess E_w and Penman Equation 3 to estimate E_L based on data from a meteorological station located on-land.

$$E_w = K_R \cdot E_L \quad (6)$$

For calibration purposes, AquaSEBS utilised images of the three studied reservoirs and the time span from 1994 to 2018. A total of 24 scenes were used, eighteen from Landsat 5 and six from Landsat 8 (Figure 4.3), all acquired from the United States Geological Survey portal (https://earthexplorer.usgs.gov/, last accessed 09/08/2022). We made use of images exclusively from the dry season (June to December) due to the following reasons: (i) cloud-free images are easier to obtain in these months; (ii) the water-availability model only considers evaporation of the dry period; and (iii) this is the period when evaporation is more intense and, thus, more relevant for water management purposes.

Figure 4.3 - Temporal distribution of Landsat images applied to assess on-water evaporation using AquaSEBS and, thus, to calibrate the KR coefficient. Years shown in grey did not have cloud-free images.

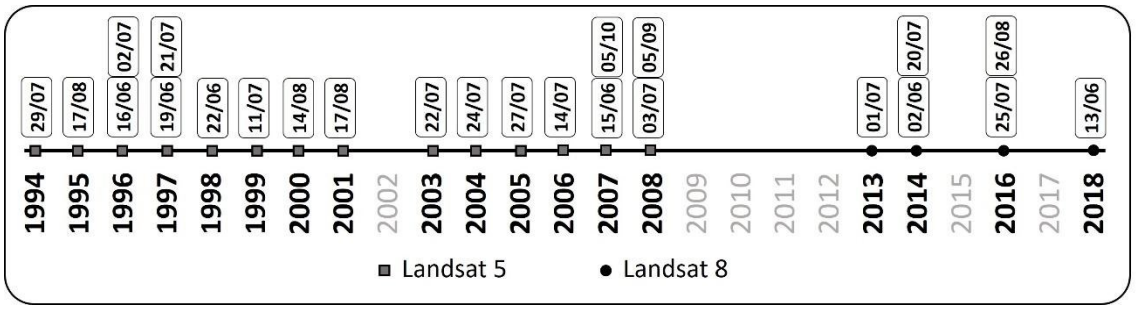

4.3.3 Phase III: Water availability assessment for scenarios in the long-term future (2071-2099)

The VYELAS model (Volume-Yield-Elasticity, as in DE ARAÚJO *et al.*, 2006) was applied to simulate water availability. River inflow to the reservoir is generated by a stochastic procedure, using the inverse of the two-parameter gamma probability density function (see MCMAHON; MEIN, 1986; and CAMPOS, 1996). Distribution parameters were derived from the average and standard deviation of historical annual inflow to the reservoir. A 10,000-year synthetic series was generated for each of the three reservoirs, which reproduced the historical average and the coefficient of variation of annual inflow as given in Table 2. VYELAS simulates the reservoir water balance for a large synthetic series, corresponding to the number of annual water-balance simulations (Equation 7). Each set of simulations is associated with a withdrawal discharge (Q_w). The model calculates the annual reliability level (G), which corresponds to the annual probability of providing the target withdrawal discharge; the respective formula is $G = 1 - N_S/N$, where N_S is the number of successful years and N the total number of years in the simulation (CAMPOS, 2010, MCMAHON; MEIN, 1986). In this context, a successful year is one in which the target water withdrawal can be integrally met without leaving the reservoir reserve below the minimum operational volume (DE ARAÚJO; MAMEDE; DE LIMA, 2018). Campos (2010) states that the water balance of reservoirs in semiarid environments is approximately:

$$\frac{\Delta V}{\Delta t} \approx Q_{in} - Q_{E,\,dry} - Q_s - Q_w \tag{7}$$

In Equation 7, V is the water storage volume in the reservoir, t represents time, Q_{in} the inflow from the river network into the reservoir, $Q_{E,dry}$ the water loss due to evaporation in the dry season, Q_S the reservoir outflow over the spillway, while Q_w stands for water withdrawal

from the reservoir (all variables in $hm^3\ year^{-1}$). The model assumes that water input by rainfall directly onto the reservoir surface, together with groundwater discharge into the reservoir, is compensated by wet season evaporation and outflow due to seepage. VYELAS demands data of seasonal water inflow (average and standard deviation), precipitation, evaporation, storage capacity (SC), alert volume, and the morphological parameter α ($SC = \alpha \cdot y^3$, where y is the water maximum depth) (CAMPOS, 2010).

Simulated long-term evaporation rates (last 30 years of the century) of the two models were adjusted by the K_R coefficient (see Equation 6) and used as input in the VYELAS model. The input data required to run the model are listed in Table 4.2.

Table 4.2 - Input data for the VYELAS model for the three reservoirs.

	Gavião	**Riachão**	**Pacoti**
Average inflow ($hm^3\ yr^{-1}$) [a]	32.6	7.8	254.5
Coefficient of variation annual inflow [b]	0.8	0.8	0.8
Reservoir-shape coefficient [c]	17927	5007	31174
Evaporation in the dry season ($m\ yr^{-1}$) [d]	1.3	1.3	1.3
Maximum storage capacity (hm^3) [a]	33.3	47.9	380.0
Minimum operational volume (hm^3)*	5.0	7.2	57.0
Initial volume in the first simulation year (hm^3)**	16.3	3.9	127.2

Source of data: [a]COGERH (2020); [b]Macêdo (1981); [c]Feitosa et al (2021); [d]Calculated in this study.
*The minimum operational volume was assumed as 15% of the reservoir storage capacity (de Araújo *et al.*, 2018).
**Initial volume is the smallest value between half of maximum storage capacity and half of the annual average inflow (Campos, 2010)

To calculate how water availability varies with evaporation rate changes, we use the concept of elasticity (ε, as in DE ARAÚJO; GÜNTNER; BRONSTERT, 2006; DE ARAÚJO; MAMEDE; DE LIMA, 2018), represented by Equation 8, in which Q_{90} is water availability with 90% annual reliability and E stands for the evaporation rate. According to this concept an increase in elasticity leads to a proportionally more significant impact of evaporation on water availability. The asterisk refers to the reference values.

$$\varepsilon(Q_{90}:E) = \frac{\Delta Q_{90}/Q_{90}^*}{\Delta E/E^*} \quad (8)$$

The VYELAS model has been used in hydrological studies with the objective to assess the effects of water quality on evaporation (MESQUITA *et al.*, 2020), reservoir operating rules (DE ARAÚJO *et al.*, 2018), reservoir water balance (Feitosa *et al.*, 2021) and reservoir silting (DE ARAÚJO; GÜNTNER; BRONSTERT, 2006; LÓPEZ-GIL *et al.*, 2020).

4.4 Results

4.4.1 Evaporation assessment using on-site measurement and Remote Sensing

Table 4.3 shows the comparison between on-land (E_L) and on-water (E_w) evaporation rates. Average daily evaporation rates generally differ by 27% with on-land evaporation rates being constantly higher than on-water evaporation rates: E_w averages 7.12 mm d^{-1} against 5.24 mm d^{-1} by E_L (Figure 4.4 - Daily evaporation estimated with the AquaSEBS algorithm (E_w) and calculated based on variables obtained from the INMET station (EL). The analysed period is from 1994 – 2018, 24 days of measurement.). The correction value K_R averages 0.73 (Figure 5). Studies report that remote sensing algorithms tend to underestimate evaporation in high-temperature areas (GOKOOL *et al.*, 2017; RODRIGUES *et al.*, 2021a), such as tropical-coastal Northeast Brazil. This feature may have influenced on-water evaporation which was assessed with the help of AquaSEBS. It is shown in Table 3 that the pixel count varies. This is mainly driven by two factors, the presence of clouds and reservoir water level. The first factor, however, is more strongly related to the final number of pixels used because the reservoirs are maintained full (above 80% of the storage capacity) even during dry season, which affects the spatial representation less than gaps produced by cloudiness. We also examined the data in order to detect a possible correlation of K_R values with the period of the year when evaporation rates were estimated (for example, higher ratios at the end of the dry season). No correlation was found between the coefficient and the period of assessment, though. Most of the highest K_R values (above 0.85) were registered in the first years of monitoring; six of the seven ratios at this threshold are from before 1999. Future investigations may look into the correlation of this fact with aspects not addressed in this paper, such as features on the satellite sensor, for instance.

Table 4.3 - Evaporation in the three reservoirs Gavião, Riachão and Pacoti (1994-2018): comparative results of on-water (Ew) and on-land (EL) daily rates. The lower part of the table shows statistical parameters.

n	Date	Pixel count*	E_L (mm d^{-1})	E_w (mm d^{-1})**	K_R
1	29/07/1994	27350	6.89	6.65	0.96
2	17/08/1995	48980	8.08	7.19	0.89
3	16/06/1996	57108	7.23	5.40	0.75
4	02/07/1996	47735	6.92	6.24	0.90
5	19/06/1997	38887	6.98	5.61	0.80
6	21/07/1997	36370	7.69	6.97	0.91
7	22/06/1998	23277	7.25	6.23	0.86

8	11/07/1999	17344	7.39	5.43	0.73
9	14/08/2000	34668	8.31	5.82	0.70
10	17/08/2001	32373	8.24	5.61	0.68
11	22/07/2003	55487	7.31	4.37	0.60
12	24/07/2004	53372	7.18	3.70	0.52
13	27/07/2005	41088	7.54	4.74	0.63
14	14/07/2006	39100	7.16	4.15	0.58
15	15/06/2007	38071	7.47	4.70	0.63
16	05/10/2007	34419	8.48	5.60	0.66
17	03/07/2008	38744	6.93	3.84	0.55
18	05/09/2008	41943	8.55	6.38	0.75
19	01/07/2013	35519	6.19	4.88	0.79
20	02/06/2014	31122	6.09	3.94	0.65
21	20/07/2014	30688	6.20	4.60	0.74
22	25/07/2016	26976	6.20	5.38	0.87
23	26/08/2016	27823	6.80	4.62	0.68
24	13/06/2018	28585	6.21	4.69	0.75
	Average	35934	7.22	5.28	0.73
	Median	35945	7.20	5.39	0.74
	Min	27350	6.09	3.70	0.52
	Max	57108	8.55	7.19	0.96
	Std	12183	0.74	0.99	0.12
	CV	0.27	0.10	0.19	0.17

* Number of reservoir pixels in the raster
** Each value refers to the pixel average in the three reservoirs

Figure 4.4 - Daily evaporation estimated with the AquaSEBS algorithm (E_w) and calculated based on variables obtained from the INMET station (EL). The analysed period is from 1994 – 2018, 24 days of measurement.

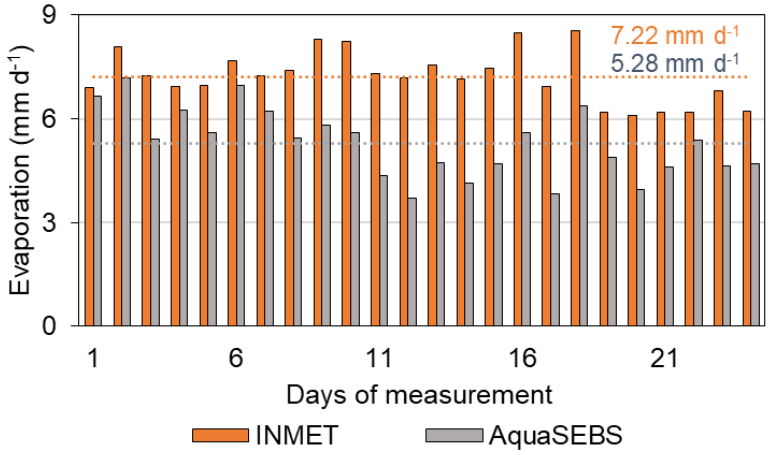

Figure 4.5 - Relationship between daily evaporation estimated with the AquaSEBS algorithm

(Ew) and calculated based on variables obtained from the INMET station (EL). The analysed period is from 1994 - 2018.

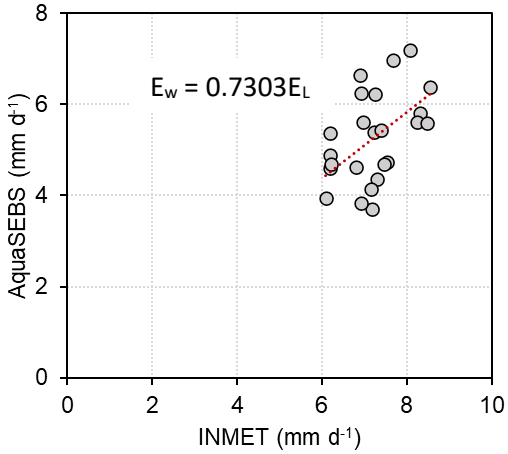

4.4.2 Spatialised evaporation rate in the reservoirs with AquaSEBS

Figure 4.6 shows spatialised evaporation in the reservoirs Gavião, Pacoti and Riachão. It is noticeable that over the last decades of monitoring lower evaporation rates (greenish tones) occur more frequently. The highest evaporation rates are found from 1994 to 2000, which suggests a declining evaporative pattern in the reservoirs over the last decades. In fact, in a recent study, Rodrigues *et al.* (2021a) evidenced such a downward trend for the same study region (− 0.26 to − 0.08 mm/34 years, spanning 1985 to 2018). From 2000 onwards, one can notice scenes where the evaporation rate is low (about 3 mm day $^{-1}$), as in the scene obtained in the year 2004. This is due to atypically rainy years in Ceará State (MEDEIROS; DE ARAÚJO, 2014; MEDEIROS; SIVAPALAN, 2020), like the above-mentioned year, when the historical average rainfall (800 mm yr^{-1}) was exceeded by over 40% (FUNCEME, 2023). Although the images were obtained in the dry season of each year with low cloudiness, factors such as lower surface temperature and lower relative humidity may have influenced the final product of the algorithm.

Figure 4.6 - Daily evaporation rates in the Fortaleza Metropolitan Region reservoirs (Gavião, Riachão and Pacoti) obtained with the AquaSEBS algorithm between 1994 and 2018.

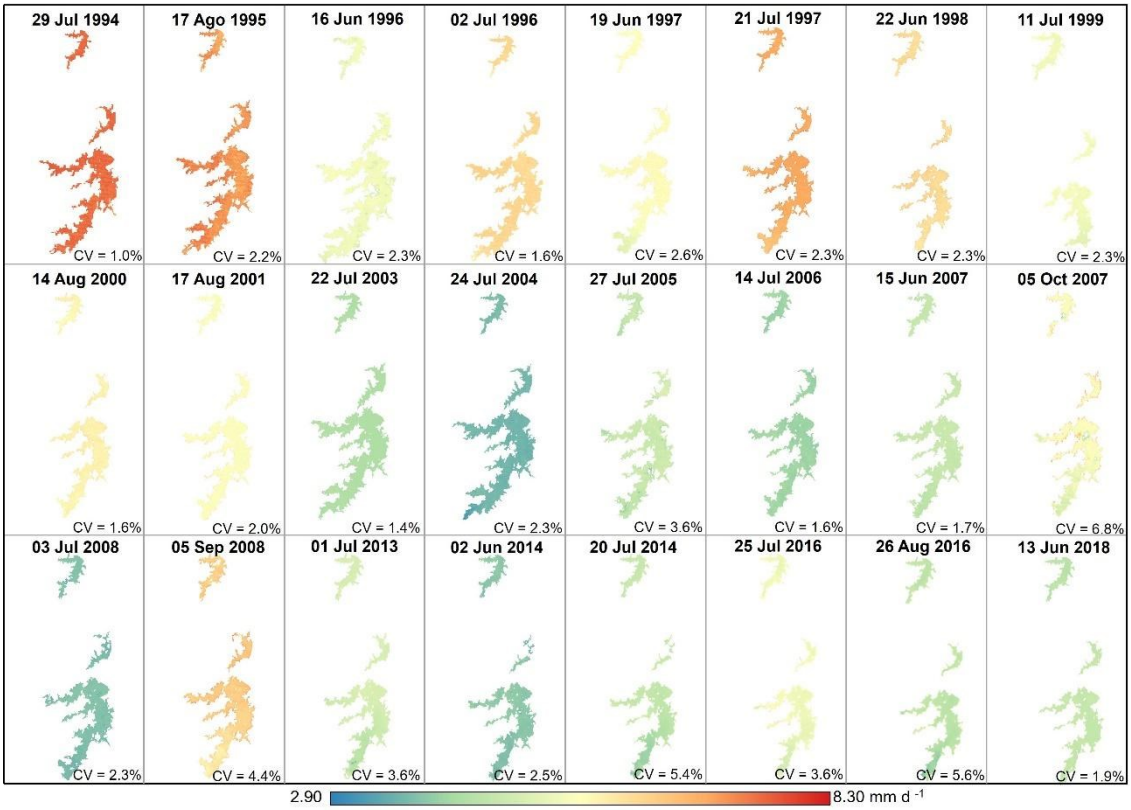

Different reservoirs have different evaporation rates due to several drivers, such as depth, surface area and water transparency. The first two factors influence the change in water heat storage and the phase lag between energy and evaporation rate; the latter is directly related to the albedo, which depends on water quality and the resulting changes of surface reflection properties (MCMAHON *et al.*, 2016; MESQUITA *et al.*, 2020). However, after evaluating the reservoir pixels with AquaSEBS, we observed that daily evaporation rates and variation coefficient did not differ substantially (see Figure 4.5), regardless of whether reservoir evaporations were assumed separately or as a single raster. Thus, we assumed that the reservoirs are subject to the same evaporation rate. Regarding the spatial variability of evaporation within the water bodies, it is necessary to highlight the uncertainty in the result related to only-water pixels. This is caused by the presence of aquatic plants or exposed soil on some of the reservoir banks, which are captured by the Landsat pixels (spatial resolution = 30 m) and this hindered assessment accuracy.

4.4.3 Evaporation simulation under four climate change scenarios

Figure 4.7 shows the behaviour of monthly evaporation rates for the following four temporal slices: historical (1961-2005), near term (2006-2040), midterm (2041-2070), and long term (2071-2099). The two scenarios derived from the MIROC5 model (M4 and M8) presented similar behaviour, varying only in the magnitude of the evaporation rates. In summary, both scenarios predict a reduction in the evaporative rate during the first two months of the year, stability until the middle of the dry season, and a reduction in the last two months of the year. April was the only month that showed a consistent evaporation rate increase, 3% and 4% for the scenarios M4 and M8, respectively. The months of November and December show the greatest expected reduction in evaporation, ranging from -3% to -10%, respectively.

The scenarios derived from the Eta-CanESM2 model (C4 and C8) show a possible increase in the evaporative rate throughout the whole year. However, the greatest increment is expected in the rainy season for the long-term future (2071-2099) under the C8 scenario. The largest absolute variations are expected in March and April of the long-term future (8 and 10% increase respectively). The C4 scenario shows stability for the near future (2006-2040) during the dry (from -1% in September to 1% in December) and in the wet season (-1% in February and 2% in March and April). The C8 scenario also shows the largest absolute variations in March and April, but the increase is 34% and 35%, respectively, for the long-term future. It is possible that a combination between a reduction in relative humidity and a temperature increase during the rainy season explains this difference in evaporation behaviour between the two seasons (QIN *et al.*, 2021). Moreover, the downscaling done by the regional models for the C4 and C8 scenarios indicate that wind speed is expected to increase in the rainy season and decrease in the summer season. Relative humidity decreases systematically throughout the year but is more pronounced during the rainy season.

Figure 4.7 - Scenarios of monthly evaporation rates for the Historical (1961-2005) and RCP (2006-2099) periods in the Metropolitan Region of Fortaleza. The rates refer to on-water evaporation (Ew).

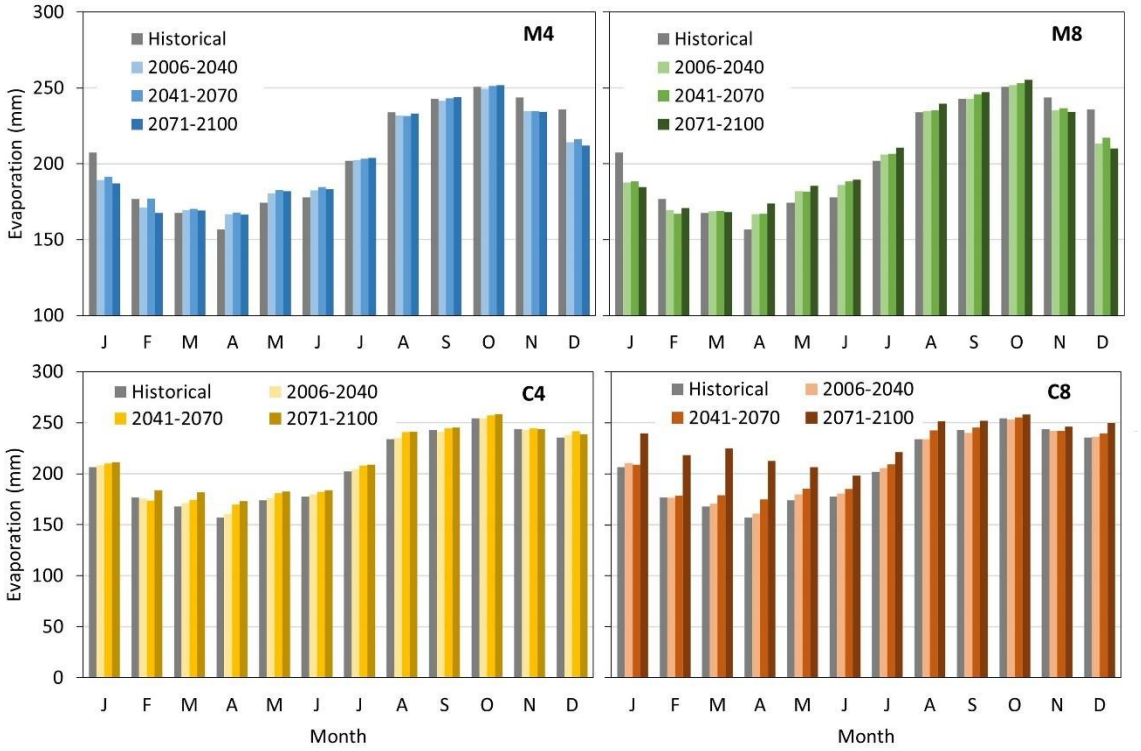

Figure 4.8 shows an overview of annual evaporation rates for the historical periods and the four climate change scenarios. A distinct pattern of the models is evident if the 10-year average is considered: the scenarios C8 indicates an upward behaviour, whereas C4, M4 and M8 show a stabilisation followed by a decrease. From Figure 7 one can depict that there is an increasing behaviour for all the scenarios in the beginning of the 2010s. Afterwards, a downward trend is observed for M4 and M8. Except for the C8 scenario (which shows a substantial increase), all tend to maintain the evaporation rate in the long-term future. Over the last decade of simulation (2090s), the M4 scenario presents a more abrupt decrease, while M8 and C4 remain steady. A notable feature is the uncertainty intrinsic to the climate models themselves. They do not differ much when simulating the historical period (Eta-MIROC5 with 16.2% difference from the observed data and Eta-CanESM2 with 16.4%). However, when the RCP experiment starts, the four model-derived scenarios behave in different directions. The high variability found in the simulations is attributed to external climate factors such as solar radiation, Earth orbit, atmospheric concentrations of greenhouse gases and internal factors within the GCMs themselves (KUNDZEWICZ *et al.*, 2018).

Figure 4.8 - Simulated annual on-water evaporation for the Metropolitan Region of Fortaleza. The dashed lines represent the Historical (1961-2005) period, and bold lines refer to the 10-year moving averages.

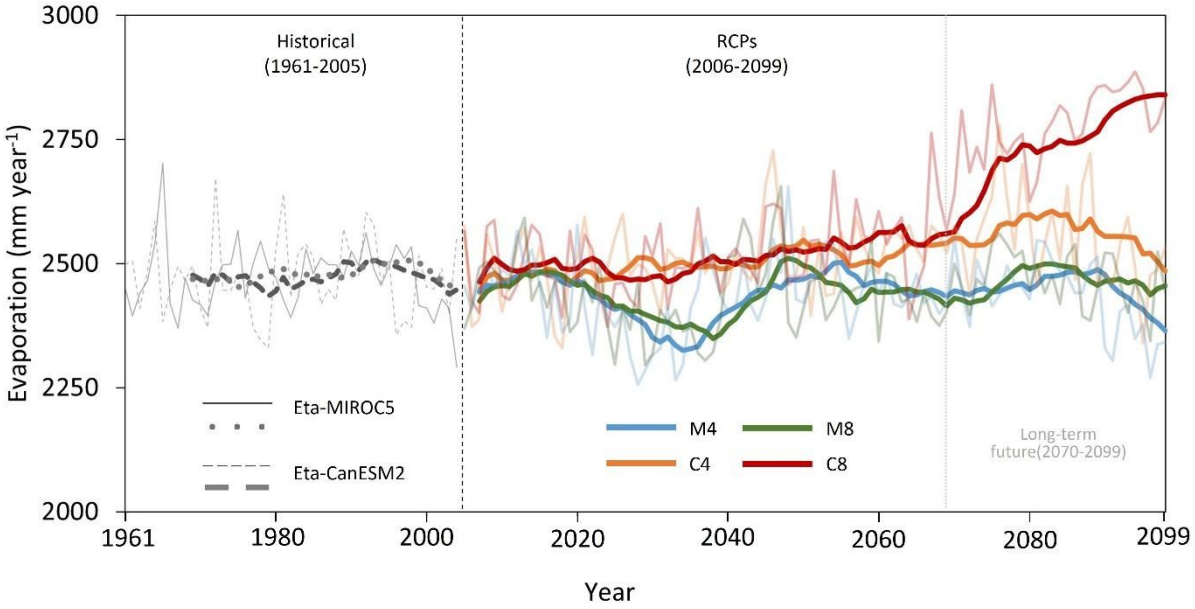

Table 4.4 presents the statistical metrics related to the evaporation trends for all the scenarios in the Historical and RCP experiments. The results indicate no statistically significant variation for the historical simulation of both models (p-value > 0.05). The M8, C4 and C8 scenarios envisage an increase in reservoir evaporation rates during the period from 2006 to 2099. However, the Mann-Kendall test detected significant variation simulated by Eta-CanESM2 only: + 0.40 mm yr^{-1} for the C4 scenario and + 4.30 mm yr^{-1} for C8. The M4 scenario is the only one that projects an evaporation decrease (-0.01mm yr^{-1}), yet with no significant trend.

Table 4.4 - Mann-Kendall statistics for annual evaporation projected by the regional models for Historical (1961-2005, n = 45), and RCP (2006-2099, n = 93) experiments. Bold numbers are statistically significant (p-value < 0.05). The p-values were determined using a two-sided Kendall tau test (KENDALL; GIBBONS, 1990).

	Historical		**Scenarios**			
	Eta-MIROC5	**Eta-CanESM2**	**M4**	**M8**	**C4**	**C8**
tau	0.008	0.010	-0.003	0.105	0.192	0.582
p-value	0.945	0.930	0.969	0.136	0.600	< 0.001
Sen's slope (mm yr^{-1})	0.07	0.04	-0.01	0.42	0.40	**4.30**

Based on the above findings, we can therefore state that the best scenario in terms of evaporative rate is scenario M4 (-2%) and the worst-case scenario is C8 (+6%), since they respectively reduce and increase the evaporative rate in the dry season in the Fortaleza

Metropolitan Region. It is worth noting that these rates change when average annual evaporation is considered (i. e. including both rainy and dry seasons): -1% under the M4 scenario and +12% under C8.

4.4.4 Water availability assessment for the scenarios (2071-2099)

Figure 4.9 depicts the relation among water yields with their respective annual reliabilities for the investigated reservoirs in the long-term future. The dashed line refers to the current water availability of the Gavião-Riachão-Pacoti system, whose water yield with 90% annual reliability (Q_{90}) is 127 hm³ yr^{-1}. For scenario C4, the Q_{90} is 119 hm³ yr^{-1}, and for C8 it is 116 hm³ yr^{-1}, which represents reductions of 6% and 9%, respectively. For scenario M4, on the other hand, the Q_{90} increases to 129 hm³ yr^{-1}, resulting in a 1increase in the water availability of the reservoir system. Scenario M8 projects no change in the future evaporation rate, hence it is not displayed. It is also noteworthy in Figure 4.9 that, for higher reliability levels (e.g., 99%), there is less variation in water availability between the scenarios, while for smaller reliability levels (e.g., 75%), the differences become more pronounced. This means that the impact of evaporation is greater in regimes of reduced water reliability.

Figure 4.9 - Water availability as a function of annual reliability level for the reservoirs Gavião, Riachão and Pacoti. Each curve represents a different evaporation rate: current historical average (1961-2005) and four climate change scenarios (M4, M8, C4, and C8) at the end of the 21st Century.

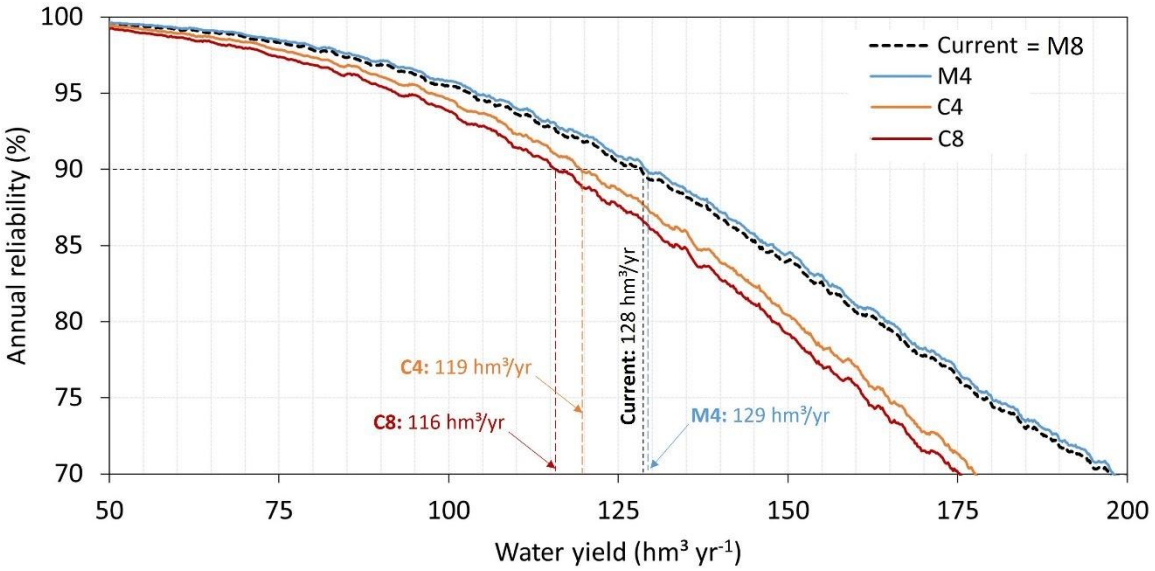

The impact on water availability can be reported from two perspectives: first, as a change in reliability for a predefined withdrawal volume and, second, as a change in the

available withdrawal volume for a given reliability level (DE ARAÚJO; GÜNTNER; BRONSTERT, 2006). For example, 128 $hm^3\ yr^{-1}$ could be taken from the reservoir system with 90% reliability under the current climate conditions, but only 116 $hm^3\ yr^{-1}$ could be withdrawn with the same reliability under scenario C8 conditions. This reduction in water availability corresponds to a substantial loss of water resources: under the assumption of per capita consumption of 150 L day^{-1}, the difference in water yield would be enough to supply around 200 000 people per year, 6% of the FMR's population.

It is noteworthy in Figure 4.9 that, although the C8 scenario reports a + 6% change in evaporation rate and the M4 scenario reports -2%, water availability does not respond linearly to such variations. Table 5 shows the influence of evaporation on water availability for the case of the Fortaleza Metropolitan Region reservoirs. The results indicate that evaporation has a relevant impact on water availability in the region depending on the scenario. Consequently, the reservoir capacity to supply water with high reliability is reduced. It is relevant to stress that global average elasticity is -0.83, and this value is comparable to siltation impacts observed in reservoirs of the semiarid region (-0.80, as found by DE ARAÚJO; GÜNTNER; BRONSTERT, 2006).

Table 4.5 - Elasticity (ε) for the current conditions of water availability in the Metropolitan Region of Fortaleza and for the climatic scenarios in the period 2070-2099. The lower part of the table shows average elasticity.

Scenarios	**M4**		**M8**		**C4**		**C8**	
$\Delta E/E^{*}$[1]	**$\Delta Q_{90}/Q^{*}_{90}$**	**ε**	**$\Delta Q_{90}/Q^{*}_{90}$**	**ε**	**$\Delta Q_{90}/Q^{*}_{90}$**	**ε**	**$\Delta Q_{90}/Q^{*}_{90}$**	**ε**
- 0.15	0.099	-0.657	0.092	-0.615	0.052	-0.346	0.023	-0.153
- 0.10	0.072	-0.725	0.059	-0.588	0.015	-0.154	0.000	0.000
- 0.05	0.045	-0.896	0.000	0.000	-0.016	0.317	-0.049	0.984
+ 0.05	-0.024	-0.480	-0.041	-0.813	-0.103	-2.069	-0.143	-2.857
+ 0.10	-0.058	-0.579	-0.085	-0.847	-0.153	-1.532	-0.185	-1.852
+ 0.15	-0.103	-0.690	-0.133	-0.885	-0.196	-1.308	-0.255	-1.699
Average[2]	-0.014	-0.674	-0.040	-0.627	-0.091	-0.949	-0.126	-1.085

[1] The asterisk refers to the reference values. E* – M4: 977, M8: 997, C4: 1016, C8: 1052 (all values in mm yr^{-1}). Q*90 – M4: 136, M8: 134, C4: 119, C8: 116 (all values in $hm^3\ yr^{-1}$)

[2] The global average is -083.

4.5 Discussion

4.5.1 Evaporation analysis

Our findings show two opposite trends for the same study area: one climate model shows an increase in evaporative rate when compared to the historical period and the other shows a decrease. In fact, there are records around the world of positive and negative trends in evaporation. Liu *et al.* (2004) found that the evaporation of 85 Class A pans in China, between 1955 and 2000, had decreased at an average rate of 29.3 mm per decade. Roderick and Farquhar (2004) observed in regions with large industrial centres in Australia that evaporation reduced by an average of 4.3 mm between 1970 and 2002. This reduction in evaporation was also observed in Canada (BURN; HESCH, 2007), India (CHATTOPADHYAY; HULME, 1997) and Italy (MOONEN *et al.*, 2002). The findings of Zhao *et al.* (2022) show an increasing trend of evaporation at global scale by 0.9% per decade for the period 1985 to 2018. Positive trends in reservoir evaporation was also observed in Benin, West Africa (HOUNGUÈ *et al.*, 2019), Austria (DUETHMANN; BLÖSCH, 2018), Australia (HELFER *et al.*, 2012; FUENTES *et al.*, 2020), centre-west Brazil (ALTHOFF *et al.*, 2019), Czech Republic (MOZNY *et al.*, 2020) and in other parts of the world, generally associated with countries or regions with low rates of gas-emissions/industrialization (WANG *et al.*, 2014; MIRALLES *et al.*, 2014). These different trends of evaporation increase and decrease in various regions of the planet have been called an "evaporation paradox" (BRUTSAERT; PARLANGE, 1998).

One of the main limitations of the original Penman (1948) equation is its simplifying assumptions and empirical coefficients, which may not fully capture the complexities of evaporation processes in tropical climates. For example, the Penman equation assumes constant conditions over a 24-hour period, neglects the effects of diurnal variations in temperature, humidity, and radiation, and may not adequately account for the specific atmospheric and surface characteristics of tropical regions. However, has undergone adaptations (VALIANTZAS, 2013) and in this work we strictly follow the steps described by Allen et al. (1998) and McMahon et al. (2013). Studies such as those by Donohue et al. (2010) and Elsawwaf et al. (2010) report that Penman (1948) produces the most realistic estimates of evaporation and is the most comparable to energy balance estimates using the Bowen ratio. In a recent study, Rodrigues et al. (2023) demonstrated to what extent two direct-measurement sensors and two physically-based models (Penman and modified Dalton) accurately estimate the evaporation of a tropical reservoir (same study region of the present paper). The Penman (1948) model, based on data from a floating station, showed good results ($r > 0.7$) for the 12 h time step or daily evaporation, comparing with the direct measurements.

A priori it seems a matter of mere model selection to make important water management decisions in a region sensitive to climate change. Indeed, temperature is rising on a global level (SOLOMON *et al.*, 2007; DARSHANA *et al.*, 2013; QIN *et al.*, 2021), and this is expected to be directly related to an increase in evaporation rates. Be that as it may, it should be considered that the historical simulation of both the Eta-CanESM2 and Eta-MIROC5 models was quite similar to what was recorded by the INMET stations (overestimates of 16.2 % and 16.3 %, respectively). Rodrigues *et al.* (2021b) analysed the evaporation trend in Ceará reservoirs for the period 1985 - 2018 using the AquaSEBS model and assessed negative trends (− 0.26 to − 0.08 mm/34 years). According to the authors, such behaviour was attributed to the impact of regional air pollution, analogous to the global dimming effect of reduced evaporation in reservoirs located closer to nearby industrial areas (around 2000, according to IPECE, 2017). This causes an increase in the number of clouds and reduces the influence of solar radiation heating on the evaporation of the water body. However, although Figure 4.6 shows a similar pattern to the results of the authors op cit, our results do not have sufficient basis to affirm this. Especially when considering the more continuous modelled data, this trend of a reduction in the evaporative rate is not evident.

4.5.2 Water availability

Campos (2010) states that in Brazil the annual reliability discharge of 90% is commonly used for water resources planning and can be interpreted as the reference water availability of the reservoir. Recio-Villa *et al.* (2018) also used annual reliability to establish reference water availability, however, they recommend a reliability level of 75% for reservoirs located in a humid tropical climate, which is the case of the region where the weirs studied in the present paper are located. Despite this recommendation, we used Q_{90} as a rule for two main reasons: i) the reservoirs of the Metropolitan region of Fortaleza are supplied by a long network of reservoirs located in a semiarid region with water deficit during two thirds of the year and high rainfall uncertainty; ii) the water from these reservoirs is mainly used for industries, agriculture and for the direct supply of about 4 million inhabitants. It should be considered that such a simulated water availability is affected by changes in the evaporation rate. In Ceará, the reservoirs usually suffer a process of reduced storage capacity mainly due to sediment deposition in the lakes (DE ARAÚJO *et al.*, 2022) because of erosion; and also due to the high rate of water pollution, mostly caused by eutrophication (MESQUITA *et al.*, 2020). Our study highlights another important factor affecting water availability, which is the evaporation rate

influenced by climate changes (elasticity concept, as in DE ARAÚJO *et al.*, 2006).

As stated by Krol *et al.* (2003), climate impacts are not merely an effect of changes in water availability but emerge from the confrontation between availability and societal demands, and also the role these demands play in society. This explains why a study should include not only the physical understanding of climate impacts on the water balance, but also the analysis of water use, agricultural economy, and societal impacts. This clearly demonstrates that the study of climate change impacts in developing semiarid regions calls for an integrated approach.

Besides the uncertainty associated with future water availability, there is substantial uncertainty regarding future water demand (KUNDZEWICZ *et al.*, 2018). The findings of De Araújo *et al.* (2004) indicate that 60 % of the municipalities of the state of Ceará may suffer from long-term water scarcity by 2025. On average, the probability of these municipalities facing water shortage ranges from 9 % to 20 % annually. Silva *et al.* (2021) analysed climate change impacts and population growth rates in a basin whose sole reservoir provides water to an urban area of 1 million inhabitants in northeastern Brazil. The rates of change in population growth for the period from 2015 to 2030 varied between 0.9% and 0.8%. Water recycling and more efficient technologies can decrease overall water demand. In fact, the results of the investigation by Rodrigues et al (2020) in a tropical reservoir in northeast Brazil indicated that the investment in building a floating photovoltaic power generation system is fully recovered in eight years, and water losses due to evaporation can be reduced by approximately 2.6×10^6 m^3 $year^{-1}$, enough to supply about 50,000 people. Indeed, cooling techniques for electricity generation are among the most influential climate change mitigating factors affecting future water demand.

4.5.3 Uncertainties

In this research, observed evaporation was assessed in two manners: by the Penman equation (1948) with data from a meteorological station; and by remote sensing. The station, used to correct the bias in simulated data and to calculate evaporation, is 20 km away from the reservoirs. In most cases, meteorological data are obtained from stations distant from the water body, sometimes tens of kilometres away. Feitosa *et al.* (2021) compared measurements on the lake (using a floating raft) with a station 30 km away from the reservoir. Their results showed overestimation of open-water evaporation when using data from the ground station. Mays (2011) warns that neglecting the impact of reservoir evaporation can result in considerable overestimation of water availability and consequent underestimation of the storage capacity

required to support water management decisions. Rodrigues *et al.* (2023) also found results supporting this statement. Measurements made directly with sensors in a reservoir showed lower averages than historical measurements or previous studies for the same area (Fortaleza Metropolitan Region). The authors recommend monitoring evaporation based on information obtained from meteorological stations as close as possible to the water body when direct measurements cannot be done. Since the late 1990s remote sensing tools contribute to the monitoring of water losses (BASTIAANSSEN, 2000; BASTIAANSSEN *et al.*, 1998), however the application to lakes and reservoirs is more recent, and this is particularly true for northeastern Brazil. Except for the investigation of evaporation trends in Brazilian tropical reservoirs by Rodrigues *et al.* (2021a) and the assessment of spatial variability and impact of riparian vegetation by Rodrigues *et al.* (2021b) there are no applications like the one in this research for monitoring open water evaporation with remote sensing.

In the present study, we also show the limitations of monitoring during the rainy season: It is impractical since cloudiness impedes visualising the surface. Moreover, some reservoirs are not so large and medium resolution images (e.g. Landsat) may show better results than lower resolution ones like MODIS due to contamination of water pixels. One should also take into consideration limitations due to the absence of field data. This is because AquaSEBS, as well as other models for estimating energy balance and turbulent fluxes (SEBAL, BASTIAANSSEN *et al.*, 1998; SEBS, SU, 2002), require three sets of information as inputs. The first set consists of land surface albedo, emissivity and temperature. The second set comprises air pressure, temperature, humidity and wind speed. The third data set is composed of downward solar radiation and downward longwave radiation. As stated by Su (2002), conventional techniques that employ point measurements to estimate the components of energy balance are representative only of local scales and cannot be extended to large areas because of the heterogeneity of land surfaces and the dynamic nature of heat transfer processes. Remote sensing is probably the only technique which can provide representative measurements of several relevant physical parameters at scales from a point to a continent. Techniques using remote sensing information to estimate atmospheric turbulent fluxes are therefore essential when dealing with processes that cannot be represented by point measurements only.

The climate simulations revealed great variations between the regional model outputs and within the historical series of each model. Indeed, climate models mimic the physical mechanisms of the planet, however, data-based representation is not always satisfactorily accurate, particularly when dealing with complex hydrological processes such as lake evaporation. There are external climatic factors such as solar radiation, the Earth's orbit,

atmospheric concentrations of greenhouse gases and other atmospheric factors that increase uncertainty. Besides, there are internal factors in the model system that diminish or amplify the effects and generate a high variability (KUNDZEWICZ *et al.*, 2018).

CanESM2 (CHYLEK *et al.*, 2011) and MIROC5 (WATANABE *et al.*, 2010) have some differences in their model configurations, parameterizations, and simulation outputs, namely: i) Model Physics and Dynamics: CanESM2 and MIROC5 use different atmospheric and oceanic dynamical cores, which can lead to differences in the representation of atmospheric and oceanic processes. For example, differences in how convection, cloud formation, and ocean circulation are parameterized can influence simulated climate patterns and variability; ii) Forcing Scenarios: CanESM2 and MIROC5 may be driven by different historical and future greenhouse gas emissions scenarios and external forcings. Variations in the scenarios used to force the models can lead to differences in simulated climate responses, particularly for future projections of temperature, precipitation, and other climate variables; iii) Model Calibration: Each model undergoes a process of calibration and tuning to ensure that its simulations are consistent with observed climate variability and change. The specific calibration and tuning procedures used for CANESM2 and MIROC5 may differ, leading to differences in model behaviour and performance; iv) Data Assimilation and Initialization: Differences in how observational data are assimilated into the models and how initial conditions are initialized can also lead to divergent simulation outcomes. Variations in data assimilation techniques and initialization procedures can affect the skill and reliability of model simulations.

These differences between CanESM2 and MIROC5 can contribute to divergent climate projections, particularly at regional scales and for specific study areas. Understanding these distinctions is important for interpreting and contextualizing model results and for assessing the robustness of climate change projections.

Chou *et al.* (2014) state that, before using climate models as tools to estimate future climate change impacts, the systematic errors of current climate simulations need to be estimated in order to assign some degree of confidence to future climate scenarios. Climate models simulate different future climates which are equally plausible for the same period (in the present case, up to the end of the 21st century). By using bias correction methods, the aim is to bring model simulations closer to real world measurements over a given reference period (baseline). A bias correction method that is valid for the historical validation period should then remain valid for future climate change impact studies (Chen *et al.*, 2020). This assumption has been widely accepted in climate change impact studies (FISEHA *et al.*, 2014; KUNDZEWICZ *et al.*, 2018; TEUTSCHBEIN; SEIBERT, 2012). Yet the performance of bias correction can be

affected by climate models with different sensitivities to the real system (CHOU *et al.*, 2014). Regionally, although driven by a single GCM, various downscaling methods may lead to different future climate scenarios (ADACHI; TOMITA 2020; KENDON *et al.* 2017; MARAUN, 2013; TANG *et al.* 2016). Downscaling regional climate simulations is another source of uncertainty. While much attention has been paid to the uncertainties of future projections associated with the choices of GCMs (MOGES *et al.* 2021), fewer analyses have quantified downscaling uncertainty (AHMADALIPOUR *et al.* 2018). Generally, it is recommended to use an ensemble of simulations by multiple GCMs and downscaling techniques for reliable regional climate projections (DIBIKE *et al.* 2017; PIERCE *et al.* 2013). Despite the systematic errors inherent in all simulations, the development of regional models for Brazil is essential, as this increases the possibility to better understand the impacts of climate change in various regions, given that it is a country of continental dimensions (8,5 million km²) with climatic, environmental, social, and economic particularities. Our results show that Eta-CanESM2 and Eta-MIROC5 data for Brazil have various biases, which can be originated from the driving GCMs, introduced by the downscaling RCM and related to uncertainties in observational data. It is expected that such biases, due to generalised information about the region, are also present in our results, and if output data are not corrected, any hydrological application will be compromised. Future analyses can be carried out for the study region of this research, such as analysis of the change in the aridity index or the impact of changes in other hydrological processes of relevance for dry regions. Naturally, spatialised and continuous field information can improve the simulations of regional models, as they serve as basis for bias correction and ground truth.

4.6 Conclusions and outlook

Climate simulations made with the regional models Eta-CanESM2 and Eta-MIROC5 showed different trends in the future evaporation of a reservoir network. Similarly, these trends affected regional water availability in opposing patterns. Four scenarios derived from the RMs were evaluated, and the following conclusions can be drawn from the results.

The scenarios derived from the Eta-CanESM2 model (C4 and C8) indicate an increase in dry season evaporative rates: 2% and 6% respectively. The total annual increase, i.e., including both rainy and dry seasons, indicate 12% for the worst-case scenario. Unlike the above scenarios, the ones derived from the Eta-MIROC5 model (M4 and M8) display a decrease in the dry season evaporative rate (-2% in the M4 scenario) and no change in M8. All

in all, there is a statistically significant evaporation trend only for the scenarios C4 (+ 0.87 mm yr^{-1}) and C8 (+ 4.30 mm yr^{-1}). Regarding the impact of simulated evaporation on water availability: For a 90% reliability level, the expected range of change in water availability is -7% to +9%. The scenario C8 envisages the highest reduction in annual water flow while model M4 predicts the highest decrease.

To reduce uncertainties in modelling future water availability an adaptive management strategy is recommended, in combination with continuous monitoring of climate change and regional development, as it directly affects water demand. Because model-based projections of climate impact on water resources can be quite divergent, it is necessary to develop adaptations that do not need quantitative projections of changes in hydrological variables, but rather ranges of projected values. Adaptive planning should be based on ensembles and probabilistic approaches from multiple models rather than, for example, a single scenario or a single-value projection. Naturally, improvements on evaporation measurements are needed to feed climate models and remote sensing algorithms, which are highly dependent on measured data. Spatialised and continuous field information can improve the simulations of regional models, as they serve as basis for bias correction and ground truth, and thereby increase their reliability. We believe our findings can complement an estimation of water availability, which is especially important during the dry season of the year (June to December) in north-eastern Brazil.

The present research assessed the impact of evaporation from reservoirs on water availability, although the impact of water quality, silting, and increase in per capita consumption should also be taken into consideration in future investigations. It is necessary, therefore, that water management agencies propose adaptation measures for different scenarios, and this study contributes to decision-making aimed at water security during the dry season. Further investigations in densely-populated areas situated in dry regions may find in these results a reference for studies that take into account other variables which were not addressed in our study.

To achieve an integrated approach for integrating physical climate impacts with societal demands and water use it would be firstly necessary to understand the local context and the specific needs of each region, economic sectors, and water resource managers. Then, a comprehensive assessment of the projected impacts of climate change on regional water resources, considering extreme weather events and changes in hydrological regimes. An accurate assessment of the current and future availability of water resources is essential, taking into account surface and groundwater, water quality and its demand. Hydrological models and

reliable field data to quantify water availability under different climate scenarios are essential.

Identifying social demands and vulnerabilities is also crucial, so the main social demands for water should be identified, including agricultural, industrial, urban, ecological, and recreational use, etc. Analysing social vulnerabilities related to water availability, considering factors such as poverty, social inequality, access to water resources and resilience to climate change. Vulnerable populations, marginalised groups, and areas prone to adverse impacts from water scarcity need to be identified. It is necessary to actively involve local stakeholders, including communities, community leaders, non-governmental organisations, the private sector, and government authorities, at all stages of the analysis and planning process. Promote inclusive participation, interdisciplinary dialogue and consensus building around adaptation and water management strategies.

Finally, there must be constant monitoring and evaluation systems to follow up on the implementation of adaptation strategies and assess their impacts on water availability and welfare. We recommend the work of Sivapalan *et al*. (2012) as a starting point on that matter: "Socio-hydrology: a new science of people and water", and Medeiros and Sivapalan (2020) as complementary reading, whose work evaluates the dynamic nature of human adaptation to droughts since the beginning of the 20th century in the Jaguaribe Basin (89,000 km^2) in semi-arid Brazil.

5 INFLUENCE OF FLOATING MACROPHYTE *EICHHORNIA CRASSIPES* ON EVAPOTRANSPIRATION: PRIMARY RESULTS AND PROPOSAL FOR FURTHER RESEARCH

5.1 Introduction

The continuous increase of water demand has been subject of concern, requiring increasingly efficient management systems, particularly in water-scarce regions such as the Brazilian semiarid, a one million km² area and home to 25 million inhabitants.

Since it is an area with a long dry season (around 8 months), the population depends heavily on water supply from reservoirs. However, several driving forces lead to the consistent decline of network water availability, such as reservoir silting (DE ARAÚJO *et al.*, 2006) and pollution (ZUO *et al.*, 2015). The intensive growth of aquatic plants (macrophytes) is often related to a high load of nutrient pollutants in reservoirs and this condition is named eutrophication. Macrophytes can considerably restrict water functions.

A eutrophication process is the result of the transfer of sediments and nutrients from the basin to the reservoirs, resulting in high concentrations of nutrients, mainly phosphorus and nitrogen (LIRA *et al.*, 2020). Reservoir water quality is directly related to nutrient content, which also directly influences macrophyte growth. Although sediment deposition reduces storage capacity and therefore makes the reservoir more susceptible to evaporation losses (DE ARAÚJO *et al.*, 2006), nutrient input into reservoirs can nonetheless decrease the evaporation rate because it reduces light penetration due to high turbidity (MESQUITA *et al.*, 2020). The presence of floating macrophytes is common in reservoirs in Ceará State, hence understanding the effect of macrophyte growth on evaporation is crucial for better water management.

Observations of the water bodies and statements by locals indicate a strong and increased coverage of the reservoirs by standing and floating macrophyte species. Yet a uniform quantitative record of these plants is not available (WEBER, 2020).

At the beginning of the 20th century, Otis (1914) observed that areas colonised by aquatic macrophytes usually showed higher water losses when compared with open water surfaces. The author observed a great difference between areas colonised by various macrophytes and attributed this fact to differences in the internal and external morphology of the species. Brezny *et al.* (1973) discussed several works, evidencing the importance of climatic factors in the relation of water losses between areas colonised by macrophytes and those with a free surface.

It is clear that there is still no consensus on the real impacts of macrophytes on lake evaporation. Data observed in literature vary greatly depending on various climatic factors and

the conditions of the plants evaluated.

The main objective of this chapter is to investigate the effect of macrophytes on open-water evaporation in meso-scale (~ 20 m²) reservoirs.

5.2 Methodology

2.1 Study Area

The investigation was carried out in the Agrometeorological Station of the Federal University of Ceará. The study area is located in Fortaleza, Ceará, Brazil. It is a coastal region with an average annual rainfall of 1338 mm concentrated predominantly in the period between January and May, with two defined seasons (rainy and dry) and a sub-humid hot tropical climate, with an average temperature ranging from 26 to 28 °C (CEARÁ, 2016), a maximum monthly temperature of 30.7 °C and a minimum of 22.4 °C, with an average annual total evaporation of 1435 mm and an average wind speed of 3.2 $m \cdot s^{-1}$ (MESQUITA *et al.*, 2020; INMET, 2009). Figure 5.1 shows the location of the agrometeorological station boundaries and the tank.

Figure 5.1 - Study area (UFC Agrometeorological station) and location of the evaporation tank (T1).

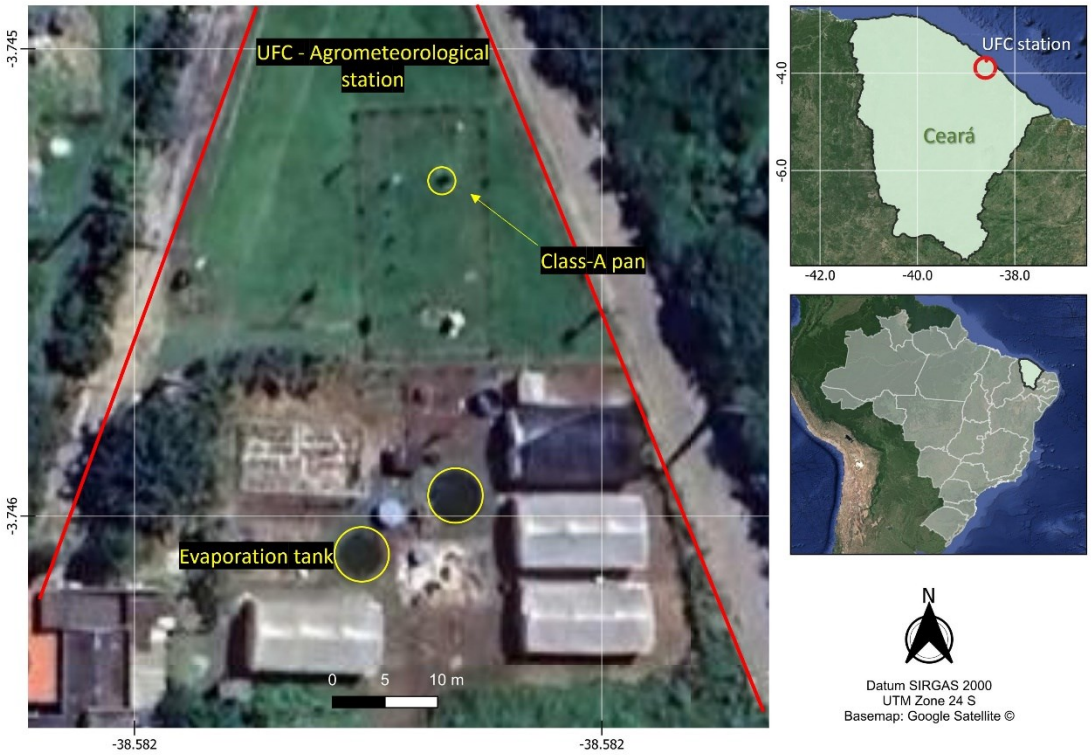

Samples of macrophyte *Eichhornia crassipes* were collected from a nearby reservoir (Santo Anastácio, about 900 m) where it is abundant, and placed in an evaporation tank (Figure 5.2). Santo Anastácio has a water surface area of 16.00 ± 2.60 ha and depth of 4.79

± 0.56 m, this makes it a shallow reservoir. Due to eutrophication the lake surface is partially (24 ± 6.2%) covered by macrophytes (MESQUITA *et al.*, 2020). The tank is 2.5 m deep (49.1 m^3) and its surface was 100% covered (19.63 m^2) with plants.

Figure 5.2 - Five-metre diameter evaporation tank in the experimental area with free surface (a), and with macrophyte cover (b), Fortaleza, Brazil.

The study was developed from August to December 2022, encompassing only the dry season of the region. Every 30 days the plants were removed and placed in a neighbouring tank (T2, Figure 5.3, also see Figure 5.1); the water was replenished monthly as well, always on the same day. Evaporation was directly measured with a differential pressure sensor (UTK - EcoSens GmbH) installed in Tank 1 (see chapter 3 of this thesis). Since it works under low pressure ranges, the pressure sensor was placed in a 40-cm-high still well. The signal values of the pressure sensor were computed with 10 min frequency and 0.1 mm resolution. The sensor was connected to power supply and internet connection.

Figure 5.3 - Experimental design representing the measurement period and the different coverages. The hatched circles refer to the tank with macrophytes, and the blank circles refer to no coverage.

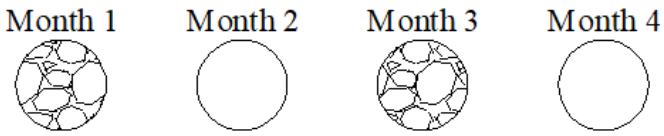

5.3 Results and discussion

Figure 5.4 shows the variation of water in the tank recorded by the pressure sensor every 10 min. The steep rises refer to the days when the plants were relocated or removed, and the water level was replenished. It is noticeable that in the first month of monitoring (August-September) the pattern of water variation is not altered, while it did change in the following months. For example, a plateau is noted from October 5 on. Most probably, cloudiness played a role in this. From the second half of October onwards some minor (< 5mm day $^{-1}$) rainfall events are recorded. By the end of December, rainfall became more frequent and more intense (pre-rainy season) and the recordings turned more uncertain due to the movement caused in the water.

Figure 5.4 - Water level variation in the evaporation tank. Recording period: 27 August 2022 to 31 December 2022.

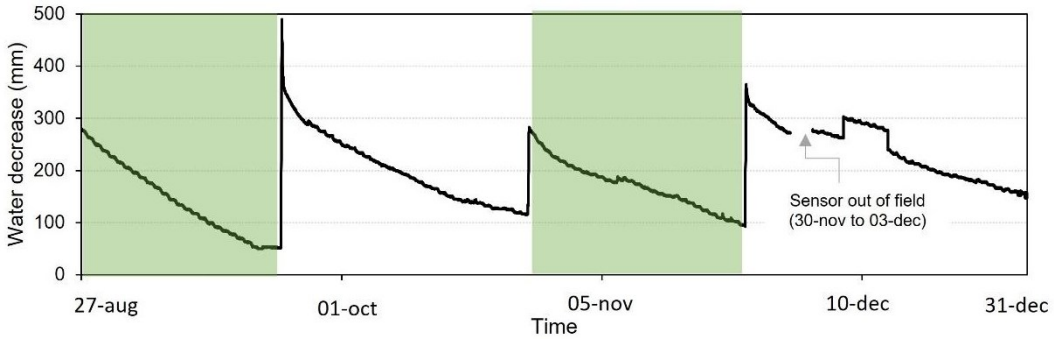

Figure 5.5 shows the 24-hour evaporation for the monitoring period (August to December). The gaps between one set of measurements and the other refer to missed data shortly after water change and replenishment of plants in the tank. The reason is a shape feature: cracks near the edge of the tank cause water to evaporate at a faster rate (15mm 24h^{-1} on average) when the tank is almost full; therefore, data from the three days following maintenance were excluded. On average, evaporation with macrophyte cover exceeded open water evaporation by 16%. According to Brezny *et al.* (1973), aquatic plants evapotranspirated 26% more water than a free water surface. Anda *et al.* (2016; 2018) showed that the presence of submerged aquatic

macrophytes increases evaporation of Class A pans by an average of 21.3%. Jiménez-Rodríguez *et al.*, (2019) reported that *E. crassipes* are influenced mainly by radiation and vapor pressure deficit.

Figure 5.5 - Evapotranspiration (mm $24h^{-1}$) recorded with the pressure sensor in the evaporation tank. Period of measurement: 30 Aug 2022 – 30 Dec 2022. Green bars refer to evaporation with macrophytes, black bars to open-water evaporation.

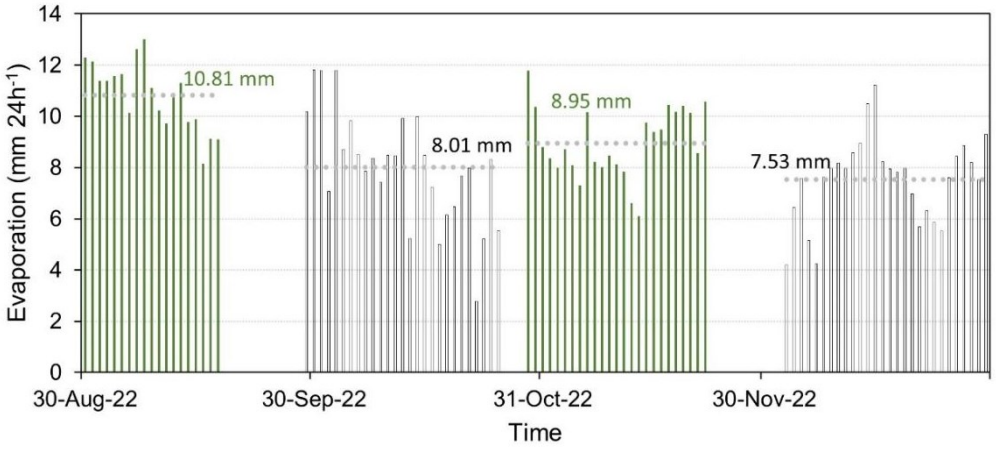

From Table 5.1 one can depict that with macrophyte presence the tank evaporated 9.71 mm daily on average, and 8.14 mm daily with a free surface, which results in a ratio of 0.84 between both approaches. Evaporative rates in the meso-scale reservoirs without macrophytes are similar (on average only 4.6% higher) to those of the class A pan for the same period and at the same site (respectively 8.14 and 7.78 mm d^{-1}). However, the average evaporation rate in the reservoir with macrophytes exceeds that of the class A pan by 25%. The average of the ratio between evapotranspiration and free surface evaporation (E_M/E_{PAN} and E_O/E_{PAN}) is 1.25. It is believed that the tank may be subjected to intense wind action and possibly heating of the soil or surrounding structures. Wind speed is the most affected factor by local surface conditions (JIA, 2007). Allen (2006) proposed that when wind speed is higher than 2 m s^{-1}, temperature and relative humidity measurements are not conditioned by the surface surrounding the station with adequate fetch as required by the standard, but by the fetch distance upwind of the weather station. The months have different numbers of recording (n) due to measurement flaws; nineteen days of measurement were used in each repetition.

Table 5.1 - Variation of average evaporation (mm $24h^{-1}$) in the evaporation tank for the four months of monitoring. The lower part of the table shows statistical parameters.

n	Date	E	E_{PAN}	E/E_{PAN}
		Without macrophytes		
1	29/09/2022	10.19	8.00	1.27
2	30/09/2022	11.81	8.10	1.46
3	01/10/2022	11.79	8.70	1.36
4	02/10/2022	7.07	1.20	5.89
5	03/10/2022	11.78	11.70	1.01
6	04/10/2022	8.71	8.80	0.99
7	05/10/2022	9.82	5.20	1.89
8	06/10/2022	8.49	8.00	1.06
9	07/10/2022	7.84	9.60	0.82
10	08/10/2022	8.37	5.70	1.47
11	09/10/2022	7.43	7.40	1.00
12	10/10/2022	8.47	8.60	0.99
13	11/10/2022	8.45	9.50	0.89
14	12/10/2022	9.92	7.80	1.27
15	13/10/2022	5.23	10.30	0.51
16	14/10/2022	10.00	9.10	1.10
17	15/10/2022	8.47	6.70	1.26
18	16/10/2022	7.23	11.90	0.61
19	17/10/2022	5.00	10.30	0.49
20	03/12/2022	4.20	8.10	0.52
21	04/12/2022	6.44	8.00	0.80
22	05/12/2022	7.59	10.00	0.76
23	06/12/2022	5.15	8.40	0.61
24	07/12/2022	4.26	7.00	0.61
25	08/12/2022	7.61	11.60	0.66
26	09/12/2022	7.95	6.90	1.15
27	10/12/2022	8.16	8.40	0.97
28	11/12/2022	7.96	8.50	0.94
29	12/12/2022	8.57	10.90	0.79
30	13/12/2022	8.95	9.10	0.98
31	14/12/2022	10.48	9.10	1.15
32	15/12/2022	11.22	7.40	1.52
33	16/12/2022	8.24	7.80	1.06
34	17/12/2022	7.95	6.10	1.30
35	18/12/2022	7.80	8.80	0.89
36	19/12/2022	7.96	10.30	0.77
37	20/12/2022	6.97	7.20	0.97
38	21/12/2022	5.68	8.10	0.70
Average		**8.14**	**8.38**	**1.12**
Minimum		4.20	1.20	0.49
Maximum		11.81	11.90	5.89
STD		1.96	1.97	0.85

With macrophytes				
1	30/08/2022	12.29	7.10	1.73
2	31/08/2022	12.14	5.40	2.25
3	01/09/2022	11.37	11.70	0.97
4	02/09/2022	11.38	9.90	1.15
5	03/09/2022	11.56	2.70	4.28
6	04/09/2022	11.65	8.90	1.31
7	05/09/2022	10.14	9.40	1.08
8	06/09/2022	12.62	10.10	1.25
9	07/09/2022	13.01	6.00	2.17
10	08/09/2022	11.11	9.50	1.17
11	09/09/2022	10.22	8.90	1.15
12	10/09/2022	9.71	8.50	1.14
13	11/09/2022	10.90	8.50	1.28
14	12/09/2022	11.31	9.00	1.26
15	13/09/2022	9.78	7.90	1.24
16	14/09/2022	9.88	9.00	1.10
17	15/09/2022	8.15	8.40	0.97
18	16/09/2022	9.11	7.50	1.22
19	17/09/2022	9.11	8.60	1.06
20	29/10/2022	11.78	8.10	1.45
21	30/10/2022	10.36	7.70	1.35
22	31/10/2022	8.79	10.60	0.83
23	01/11/2022	8.34	4.70	1.78
24	02/11/2022	8.00	4.10	1.95
25	03/11/2022	8.72	11.10	0.79
26	04/11/2022	8.09	4.60	1.76
27	05/11/2022	7.30	3.90	1.87
28	06/11/2022	10.15	5.30	1.92
29	07/11/2022	8.23	7.90	1.04
30	08/11/2022	8.01	4.10	1.95
31	09/11/2022	8.48	7.00	1.21
32	10/11/2022	8.13	9.00	0.90
33	11/11/2022	7.85	9.80	0.80
34	12/11/2022	6.62	6.90	0.96
35	13/11/2022	6.09	7.80	0.78
36	14/11/2022	9.75	7.10	1.37
37	15/11/2022	9.40	7.20	1.30
38	16/11/2022	9.48	7.60	1.25
Average		**9.71**	**7.67**	**1.40**
Minimum		6.09	2.70	0.78
Maximum		13.01	11.70	4.28
STD		1.72	2.13	0.62

Some authors have proposed using the ratio of macrophyte evaporation (E) to open water evaporation (E_W) as an alternative to the crop coefficient in wetland ecosystems. For instance, *E. crassipes* in the Nile Delta exhibits a ratio of E/E_W of 2.12 (ALI; KHEDR, 2018), while in the experiment conducted by Jiménez-Rodríguez *et al.* (2019), this ratio is reported as 1.15. The crop coefficient, commonly employed in agriculture for irrigation management (AYARS *et al.*, 1999; JENSEN; ALLEN, 2016), can also be utilized in hydrological modelling of agricultural wetlands (BACHAND *et al.*, 2014).

It is known that the transpiration rate of plants, including aquatic plants, depends on the species, phenological state and environment in which the plant is located (BREZNY, 1973). The constantly higher rates with the presence of macrophytes are possibly linked to their evapotranspiration demand, even though the plants provide surface overlay and protection from the effects of wind and solar radiation. Sánchez-Carrillo *et al.* (2004) state that macrophyte cover has a marked spatiotemporal variation which determines the variability of evapotranspiration. From our findings, it may be concluded that changes from open water towards a vegetated cover imply an increase in the total evaporation flux, including the evaporation from open water bodies and transpiration from vegetated surfaces.

This study naturally contains some sources of uncertainty, mainly related to the time and reproduction of the experimental plots. At least one more tank measuring evaporation in parallel and within the same study area would be necessary. Repetitions would contribute to the replicability of the study, and this would give the findings more trustworthiness.

Studies analysing the relationship between macrophyte/open water evaporative rates carried out in dry environments are still scarce in literature. Strong fluctuations in evapotranspiration can be expected in semiarid environments given their pronounced wet and dry periods with significant changes in the emergent cover/open water ratio, and this topic should be addressed. Remote sensing algorithms that estimate evapotranspiration with acceptable uncertainty are being improved (GAO *et al.*, 2020). In addition, remote sensing might also be used to estimate macrophyte cover (dynamics) on many reservoirs and/or on remote ones. It is expected that the findings of this study may also support remote sensing applications adapted to macrophyte-rich reservoirs, since these tools rely heavily on reliable and continuous field data.

Earlier, it was believed that floating macrophytes like *E. crassipes* could lower evaporation from open water surfaces due to their shading effect (SNYDER; BOYD 1987). Nevertheless, this presumption overlooked the transpiration process, which actually raises evaporation rates from *E. crassipes* plants compared to open water surfaces (SAMBASIVA

RAO, 1988; WEERT; KAMERLING, 1974).

5.4 Conclusions and further investigations

The aim of this study was to obtain information on the relationship between macrophytes evapo(transpi)ration and open-water evaporation. We present incipient results of evaporation estimation in an evaporation tank with 100% of the water surface covered with macrophytes and with free surface. It is expected that additional investigations will be made covering a longer period and under different climatic conditions, since evaporative rates depend on weather conditions and the phenological conditions of the plant. Due to the limited in-depth nature of this study and remaining uncertainties, the conclusions made here should be considered with care until more long-term research on the topic is conducted to solve some of the many remaining uncertainties.

We recommend more comprehensive studies on the relationship between macrophytes and open water evaporation rates. Investigate how different types of macrophytes, weather conditions, and phenological stages influence evapotranspiration processes in aquatic ecosystems;

- **Longitudinal studies on macrophyte-rich reservoirs:** "Longitudinal studies" refer to research designs where data is collected from the same subjects repeatedly over time. Instead of just taking a snapshot of a situation at one point in time (cross-sectional study), longitudinal studies track changes in variables of interest over an extended period. To better understand the dynamics of evaporation and evapotranspiration processes in these ecosystems, it might be helpful to investigate how changes in macrophyte abundance and distribution affect water balance and ecosystem functioning over time;

6 SUMMARY AND CONCLUSIONS

This section summarises the findings of the previous chapters and relates them to the outlined objectives of the dissertation.

The first chapter aimed at carrying out a bibliometric survey of research on evaporation in open water since the 1980s based on the Web of Science database. The growing number of new studies in the field of open water evaporation is remarkable. Studies using instrumentation directly placed in the water body and with remote sensing techniques have been emerging since the beginning of the 2010s. Experiments estimating the impact of climate change on evaporation in urban and rural areas are also increasing. The United States and China dominate in the number of studies, but several developing countries, namely Brazil, Egypt and South Africa, are boosting the scientific production in the area of reservoir evaporation.

The second chapter demonstrated to what extent two sensors (pressure and acoustic) and two physically-based models (Penman and modified Dalton) estimate evaporation from a tropical reservoir. The resolution of both pressure and acoustic sensors in relation to other traditional methods does not vary much: It is 0.02 mm for a Class A pan and 0.1 mm for a Piché evaporimeter. The advantage lies, however, in the equipment position in the water body and in the automation of the evaporation recording process. Therefore, in addition to functionality, one should also consider the financial aspects of monitoring compared to traditional methods. We recommend that the equipment position in the reservoir take into account the representativeness of evaporation data for the entire water body, since there is spatial variation in evaporation depending on factors such as lake depth and proximity to the borders. Remote sensing applications are helpful to take this decision.

The third chapter intended to analyse the impact of climate change on reservoir evaporation and on water availability in a densely populated urban area located in northeastern Brazil. Climate change was simulated using two regional climate models and future water availability was quantified with a stochastic model. We show that remote sensing is a good support for water management and can complement the monitoring done by land stations. According to the findings, the impact of evaporation on the water availability of the studied reservoir system is substantial, and in the long-term future (from 2070 onwards) the region may suffer from water scarcity. It is important to stress that only the impact of evaporation was estimated, and that the impact of pollution, increased water demand and silting should also be contemplated.

The fourth chapter aimed to obtain information on the relationship between macrophytes evapo(transpi)ration and open-water evaporation. We present incipient results of

evaporation estimation in a tank with 100% of the water surface covered with macrophytes and with free surface. It is expected that additional investigations will be made covering a longer period and under different climatic conditions, since evaporative rates depend on weather conditions and the phenological circumstances of the respective plants. Studies analysing the relationship between macrophytes, and open water evaporative rates carried out in dry environments are still scarce in the literature. It is expected that the findings of this study may also support investigations in macrophyte-rich reservoirs, since the tools employed rely heavily on reliable and continuous field data. Due to the limited in-depth nature of this last experiment and the remaining uncertainties, the conclusions made here should be pondered with care until more long-term research on the topic is conducted to solve some of the many remaining uncertainties. We believe that the products of this thesis can serve as a reference for subsequent research in the field of reservoir evaporation and water management in dry regions.

7 SUGGESTIONS FOR FUTURE RESEARCH

These suggestions aim to build upon the findings and insights presented in this thesis and address gaps in knowledge identified during the research. Additionally, they offer opportunities for further exploration and advancement in the field of water resources management and climate change adaptation.

- **Long-term monitoring of evaporation trends:** Conduct long-term monitoring studies to track evaporation trends in open water bodies over several years. This can provide valuable insights into the long-term impacts of climate change and other environmental factors on evaporation rates;
- **Comparative studies of evaporation measurement methods:** Compare the accuracy and reliability of different evaporation measurement methods, including traditional methods and newer technologies such as sensors and remote sensing techniques. Investigate how factors such as equipment positioning, and automation affect the results;
- **Regional climate change impact assessments:** Expand climate change impact assessments to other regions and reservoir systems, particularly in areas with high population density and water scarcity issues. Explore the potential impacts of climate change on water availability and develop adaptation strategies to mitigate these effects. Moreover, the use of other regional models applied to the study areas of this research;
- **Integration of remote sensing in water management:** Explore further the integration of remote sensing technologies in water management practices. Investigate how remote sensing data can complement traditional monitoring methods and improve water resources management strategies;
- **Study on the relationship between macrophytes and evaporation:** Conduct more comprehensive studies on the relationship between macrophytes and open water evaporation rates. Investigate how different types of macrophytes, weather conditions, and phenological stages influence evapotranspiration processes in aquatic ecosystems;
- **Interdisciplinary research on water resource management:** Encourage interdisciplinary research collaborations between hydrology, ecology, climate science, and engineering disciplines to address complex water resource management challenges. Explore innovative approaches to sustainable water management that consider the interactions between climate, land use, and ecosystem dynamics;

- **Longitudinal studies on macrophyte-rich reservoirs:** "Longitudinal studies" refer to research designs where data is collected from the same subjects repeatedly over time. Instead of just taking a snapshot of a situation at one point in time (cross-sectional study), longitudinal studies track changes in variables of interest over an extended period. To better understand the dynamics of evaporation and evapotranspiration processes in these ecosystems, it might be helpful to investigate how changes in macrophyte abundance and distribution affect water balance and ecosystem functioning over time;
- **Assessment of non-evaporative factors on water availability:** Expand assessments to consider the impacts of non-evaporative factors such as pollution, increased water demand, and sedimentation on water availability in reservoir systems. Investigate how these factors interact with evaporation processes and contribute to overall water scarcity issues.

REFERENCES

ABDELRADY, A.; TIMMERMANS, J.; VEKERDY, Z.; SALAMA, M. Surface energy balance of fresh and saline waters: AquaSEBS. **Remote Sensing.** v. 8, n. 7, p. 583-600. 2016.

ABTEW, W.; MELESSE, A. **Evaporation and evapotranspiration**: estimations and measurements. Dordrecht, Heidelberg: Springer, 2013

ADACHI, S. A.; TOMITA, H. Methodology of the constraint condition in dynamical downscaling for regional climate evaluation: A review. **Journal of Geophysical Research: Atmospheres** v. 125, n. 11, 2020.

ADRIAN, R. *et al.* Lakes as sentinels of climate change. **Limnology and Oceanography**, v. 54, n. 6, p. 2283–2297, 2009.

AHMAD, F.; SULTAN, S.A.R. Equilibrium temperature as a parameter for estimating the net heat-flux at the air-sea interface in the central red-sea. **Oceanologica Acta.** v. 17, n. 3, p. 341-343, 1994.

AHMADALIPOUR, A.; MORADKHANI, H.; RANA, A. Accounting for downscaling and model uncertainty in fine-resolution seasonal climate projections over the Columbia River Basin. **Climate Dynamics.** v. 50, p. 717–733, 2018.

ALI, Y.M.; KHEDR, I.S.E.D. Estimation of water losses through evapotranspiration of aquatic weeds in the Nile River (Case study: Rosetta Branch). **Water Sci**. v. 32, p. 259–275, 2018.

ALLEN, R.G., *et al.* Crop evapotranspiration: guidelines for computing crop water requirements. *In*: **FAO Irrigation and drainage paper 56**. Rome: FAO, 1998. Available in: https://www.fao.org/3/x0490e/x0490e00.htm#Contents. Accessed in: 8 Dec 2021.

ALLEN, R.G., TASUMI, M. Evaporation from American Falls reservoir in Idaho via a combination of Bowen ratio and eddy covariance. *In*: PROCEEDINGS OF THE 2005 EWRI CONFERENCE, 2005, Anchorage. **Anais [...]**. Anchorage, 2005. p. 1–17.

ALLEN, R.G. Footprint analysis to assess the conditioning of temperature and humidity measurements in a weather station vicinity. *In*: ASCE-EWRI 2006 ANNUAL MEETING, 2006, Omaha. **Anais [...]**. Omaha, 2006.

ALMAGRO, A.; OLIVEIRA, P.T.S.; ROSOLEM, R.; HAGEMANN, S.; NOBRE, C.A.; 2020. Performance evaluation of Eta/HadGEM2-ES and Eta/MIROC5 precipitation simulations over Brazil. **Atmospheric Research.** v. 244, n. 1, p. 105053, 2020.

ALTHOFF, D.; RODRIGUES, L. N.; AND DA SILVA, D. D.: Evaluating Evaporation Methods for Estimating Small Reservoir Water Surface Evaporation in the Brazilian Savannah, **Water**, v. 11, p. 1–17, 2019.

ALTHOFF, D.; RODRIGUES, L. N.; AND DA SILVA, D. D.: Impacts of climate change on the evaporation and availability of water in small reservoirs in the Brazilian savannah, **Climatic Change**, v. 159, p. 215–232, 2020.

ALVALÁ, R.C.S. *et al.* Drought monitoring in the Brazilian Semiarid region. **Anais da**

Academia Brasileira de Ciências. v. 91, p. e20170209, 2019.

ALVAREZ, V. M.; BAILLE, A.; MARTÍNEZ, J. M.; GONZÁLEZ-REAL, M. M. Efficiency of shading materials in reducing evaporation from free water surfaces. **Agricultural Water Management**, v. 84, n. 3, p. 229-239, 2006.

ALVAREZ, V. M.; GONZÁLEZ-REAL, M. M.; BAILLE, A.; & MARTÍNEZ, J. M. A novel approach for estimating the pan coefficient of irrigation water reservoirs: Application to South Eastern Spain. **Agricultural Water Management.** v. 92, n. 1-2), p. 29-40, 2007.

ASSOULINE, S. Estimation of lake hydrologic budget terms using the simultaneous solution of water, heat, and salt balances and a Kalman filtering approach- application to Lake Kinneret. **Water Resources Research.** v. 29, n. 9, p. 3041–3048, 1993.

ASSOULINE, S.; MAHRER, Y. Evaporation from Lake Kinneret. 1. eddy-correlation system measurements and energy budget estimates. **Water Resources Research.** v. 29, p. 901–910, 1993.

AYARS, J.; PHENE, C.; HUTMACHER, R.; DAVIS, K.; SCHONEMAN, R.; VAIL, S.; MEAD, R. Subsurface drip irrigation of row crops: A review of 15 years of research at the Water Management Research Laboratory. **Agricultural Water Management.** v. 42, p. 1–27, 1999.

BALDOCCHI, D.D., *et al.* The impact of expanding flooded land area on the annual evaporation of rice. **Agricultural and Forest Meteorology**, v. 223, p. 181–193, 2016.

BARNES, G. T. The potential for monolayers to reduce the evaporation of water from large water storages. **Agricultural Water Management.** v. 95, n. 4, p. 339-353, 2008.

BASTIAANSSEN, W. G. M. SEBAL-based sensible and latent heat fluxes in the irrigated Gediz Basin, Turkey. **Journal of Hydrology.** v. 229, n. 1–2, p. 87–100, 2000.

BASTIAANSSEN, W. G. M.; MENENTI, M.; FEDDES, R. A.; HOLTSLAG, A. A. M. A remote sensing surface energy balance algorithm for land (SEBAL). 1. Formulation. **Journal of Hydrology.** v. 212–213, p. 198–212, 1998.

BEER, T.; LI, J.; ALVERSON, K. **Global Change and Future Earth**: The Geoscience Perspective, Cambridge: Cambridge University Press, 2018.

BEVEN, K. A sensitivity analysis of the Penman-Monteith actual evapotranspiration estimates. **Journal of Hydrology.** v. 44, n. 3–4, p. 169–190, 1979.

BJØRNÆS, C. **A guide to representative concentration pathways**. Center for International Climate and Environmental Research. Available in: https://cicero.oslo.no/en/articles/a-guide-to-representative-concentration-pathways. Accessed in: 10 may 2022.

BLANKEN, P.D., *et al.* Eddy covariance measurements of evaporation from Great Slave Lake, Northwest Territories, Canada. **Water Resources Research.** v. 36, p. 1069–1077, 2000.

BOUCHET, R.J. Evapotranspiration réelle et potentielle, signification climatique. **International Association of Scientific Hydrology.** v. 62, p. 134–142, 1963.

BOU-FAKHREDDINE, B.; MOUGHARBEL, I.; FAYE, A.; POLLET, Y. Estimating daily evaporation from poorly-monitored lakes using limited meteorological data: A case study within Qaraoun dam - Lebanon. **Journal of Environmental Management**, v. 241, p. 502–513, 2019.

BREZNY, O.; MEHTA, I.; SHARMAS, R. K. Studies of evapotranspiration of some aquatic weeds. **Weed Sci.** v.21, n. 3, p. 197-204, 1973.

BRUTSAERT, W. **Hydrology**: An Introduction. Cambridge, Cambridge University Press, 2005.

BRUTSAERT, W.; PARLANGE, M. B. Hydrologic cycle explains the evaporation paradox, **Nature**, v. 396, n. 30, 1998.

BRUTSAERT, W. **Evaporation into the Atmosphere**. Dordrecht: Reidel, 1982.

BURN, D.H.; HESCH, N.M. Trends in evaporation for the Canadian Prairies. **Journal of Hydrology.** v. 336, n. 1-2, p. 61–73, 2007.

BURT, C. M.; MUTZIGER, A. J.; ALLEN, R. G.; HOWELL, T. A. Evaporation Research: Review and Interpretation. **Journal of Irrigation and Drainage Engineering**, v. 131, n. 1, 2005.

CAMPOS, J. N. B. **Dimensionamento de Reservatórios**. Fortaleza: Editora UFC. 1996

CAMPOS, N. J. B.: Modeling the Yield-Evaporation-Spill in the Reservoir Storage Process: The Regulation Triangle Diagram, **Water Resources Management.** v. 24, p. 3487–3511, 2010.

CHATTOPADHYAY, N. HULME, M.: Evaporation and potential evapotranspiration in India under conditions of recent and future climate change, **Agricultural and Forest Meteorology.** v. 87, p. 55–73, 1997.

CHEN, X. BUCHBERGER, S.G., 2018. Exploring the relationships between warm-season precipitation, potential evaporation, and “apparent” potential evaporation at site scale. **Hydrology and Earth System Sciences**, v. 22, p. 4535–4545, 2018.

CHOU, S.C. *et al.* Evaluation of the Eta Simulations Nested in Three Global Climate Models. **American Journal of Climate Change**. v. 3, p. 438–454, 2014b.

CHOU, S. C. *et al.* Assessment of Climate Change over South America under RCP 4.5 and 8.5 Downscaling Scenarios. **American Journal of Climate Change**, v. 3, n. 5, p. 512–527, 2014a.

CHYLEK, P. *et al.* Observed and model simulated 20th century Arctic temperature variability: Canadian earth system model CanESM2. **Atmos. Chem. Phys.** v. 11, p. 22893–22907, 2011.

COMPANHIA DE GESTÃO DE RECURSOS HÍDRICOS. **Portal Hidrológico do Ceará**. COGERH, 2020. Available in: http://www.hidro.ce.gov.br/. Accessed in: 22 dec 2020.

COGLEY, J.G. The albedo of water as a function of latitude. **Monthly Weather Review**, v.

107, p. 775–781, 1979.

CRAIG, I. P. Comparison of precise water depth measurements on agricultural storages with open water evaporation estimates. **Agricultural Water Management**, v. 85, n. 1–2, p. 193–200, 2006.

CRAIG, I.; GREEN, A.; SCOBIE, M.; SCHMIDT, E. **Controlling evaporation loss from water storages**. National Centre for Engineering in Agriculture. Publication 1000580/1, Toowoomba: USQ, 2005. Available in: http://www.ncea.org.au/. Accessed in: 10 may 2022.

CUI, X.; GUO, X.; WANG, Y.; WANG, X.; ZHU, W.; SHI, J.; LIN, C.; AND GAO, X.: Application of remote sensing to water environmental processes under a changing climate, **Journal of Hydrology.** v. 574, p. 892–902, 2019.

DALTON, J. Experimental essays on the constitution of mixed gases; on the force of steam or vapour from water and other liquids in different temperatures, both in a Torricellian vacuum and in air; on evaporation and on the expansion of gases by heat. **Memoirs of Manchester Literary and Philosophical Society**, v. 5, p. 535–602, 1802.

DARSHANA, D.; PANDEY, A.; PANDEY, R.P. Analysing Trends in reference evapotranspiration and weather variables in the Tons River basin in central India. **Stochastic Environmental Research and Risk Assessment**. v. 27, n. 6, p.1407–1421, 2013.

DE ARAÚJO, J. C.; DÖLL, P.; GÜNTNER, A.; KROL, M.; ABREU, C. B. R.; HAUSCHILD, M.; MENDIONDO, E. M. Water scarcity under scenarios for global climate change and regional development in semiarid northeastern Brazil. **Water International**, v. 29, n. 2, p. 209–220, 2004.

DE ARAÚJO, J. C.; GÜNTNER, A.; BRONSTERT, A. Loss of reservoir volume by sediment deposition and its impact on water availability in semiarid Brazil. **Hydrological Sciences Journal.** v. 51, n. 1, p. 157–170, 2016.

DE ARAÚJO, J. C.; LANDWEHR, T.; ALENCAR, P. H. L.; PAULINO, W. D. Water Management causes increment of reservoir silting and reduction of water yield in the semiarid State of Ceará, Brazil. **Journal of South American Earth Sciences.** v. 121, August, p. 104102, 2022.

DE ARAÚJO, J. C.; MAMEDE, G. L.; DE LIMA, B. P. Hydrological guidelines for reservoir operation to enhance water governance: Application to the Brazilian Semiarid region. **Water.** v. 10, n. 11, 2018.

DE ARAÚJO, J.C.; PIEDRA, J.I.G. Comparative hydrology: analysis of a semiarid and a humid tropical watershed. **Hydrological Processes.** v. 23, p. 1169–1178, 2009.

DE OLIVEIRA, V.A.; DE MELLO, C.R.; VIOLA, M.R.; SRINIVASAN, R., 2017. Assessment of climate change impacts on streamflow and hydropower potential in the headwater region of the Grande river basin, Southeastern Brazil. **International Journal of Climatology.** v. 37, p. 5005–5023, 2017.

DIBIKE, Y. Implications of future climate on water availability in the western Canadian river basins. **International Journal of Climatology**. v. 37, n. 7, p. 3247-3263, 2017.

DÍEZ-HERRERO, A.; GARROTE, J. Flood Risk Analysis and Assessment, Applications and Uncertainties: A Bibliometric Review. **Water**. v. 12, p. 1-24, 2020.

DJAMAN, K. *et al.* Evaluation of sixteen reference evapotranspiration methods under sahelian conditions in the Senegal River Valley. **Journal of Hydrology: Regional Studies**, v. 3, p. 139–159, 2015.

DUAN, Z. AND BASTIAANSSEN, W.G.M. A new empirical procedure for estimating intra-annual heat storage changes in lakes and reservoirs: review and analysis of 22 lakes. **Remote Sensing of Environment**, v. 156, p. 143–156, 2015.

DUETHMANN, D.; BLÖSCHL, G. Why has catchment evaporation increased in the past 40 years? A data-based study in Austria. **Hydrology and Earth System Sciences.** v.22, n.10, 2018.

DEUTSCHER VERBAND FÜR WASSERWIRTSCHAFT UND KULTURBAU. **Ermittlung der Verdunstung von Land und Wasserflächen**. DVWK Leaflet No. 238. 1996. Available in: https://de.dwa.de/de/regelwerk-news-volltext/berechnungsverfahren-der-landverdunstung-entwurf-merkblatt-dwa-m-504-2.html Accessed in: 22 dec 2021.

EDINGER, J. E.; DUTTWEILER, D. W.; GEYER, J. C. The response of water temperature to meteorological conditions. **Water Resources Research.** v. 4, p. 1137-1143, 1968.

EHSANI, N.; VÖRÖSMARTY, C.J.; FEKETE, B.M.; STAKHIV, E.Z. Reservoir operations under climate change: Storage capacity options to mitigate risk. **Journal of Hydrology.** v. 555, p. 435–446, 2017.

ELSAWWAF, M.; WILLEMS, P.; FEYEN, J. Assessment of the sensitivity and prediction uncertainty of evaporation models applied to Nasser Lake, Egypt. **Journal of Hydrology.** v. 395, p. 10–22, 2010.

FEITOSA, G. P.; DE ARAÚJO, J. C.; BARROS, M. U. G.: Different methods for measuring evaporation in a tropical reservoir: The case of the Gavião reservoir in the state of Ceará, **Rev. Caatinga**, v. 34, n. 2, p. 410–421, 2021.

FISEHA, B. M.; SETEGN, S. G.; MELESSE, A. M.; VOLPI, E.; AND FIORI, A.: Impact of climate change on the hydrology of Upper Tiber river basin using bias corrected regional climate model, **Water Resources Management.** v.28, p. 1327–1343, 2014.

FOWE, T.; KARAMBIRI, H.; PATUREL, J.E.; POUSSIN, J.C.; CECCHI, P. Water balance of small reservoirs in the Volta basin: A case study of Boura reservoir in Burkina Faso. **Agricultural Water Management.** v.152, p. 99–109, 2015.

FRIEDRICH, K., *et al.* Reservoir evaporation in the Western United States: current science, challenges, and future needs. **Bulletin of the American Meteorological Society**, v. 99, n. 1, p. 167–188, 2018.

FUENTES, I.; VAN OGTROP, F.; VERVOORT, R.W. Long-term surface water trends and relationship with open water evaporation losses in the Namoi catchment. Australia. **Journal of Hydrology**. v.584, p. 124714, 2020.

GAISER, T.; KROL, M.; FRISCHKORN, H; DE ARAÚJO, J.C. (eds.). **Global change and**

regional impacts. Berlin: Springer, 2003.

GALLEGO-ELVIRA, B.; BAILLE, A.; MARTIN-GORRIZ, B.; MAESTRE-VALERO, J. F.; & MARTÍNEZ-ALVAREZ, V. Energy balance and evaporation loss of an irrigation reservoir equipped with a suspended cover in a semiarid climate (south-eastern Spain). **Hydrological Processes.** v. 25, n. 11, p. 1694-1703, 2011.

GOKOOL, S.; JARMAIN, C.; RIDDELL, E.; SWEMMER, A.; LERM, R.; CHETTY, K.T. Quantifying riparian total evaporation along the Groot Letaba River: A comparison between infilled and spatially downscaled satellite derived total evaporation estimates. **Journal of Arid Environments.** v. 147, p. 114–124, 2017.

GRAHAM, L.; HAGEMANN, S.; JAUN, S.; BENISTON, M. On interpreting hydrological change from regional climate models. **Clim. Change** v. 81, p. 97–122, 2007.

GRANGER, R. J.; HEDSTROM, N. Modelling hourly rates of evaporation from small lakes. **Hydrology and Earth System Sciences**, v. 15, n. 1, p. 267–277, 2011.

GUO, Y., *et al.* Long-term changes in evaporation over Siling Co Lake on the Tibetan Plateau and its impact on recent rapid lake expansion. **Atmospheric Research**, v. 216, p. 141–150, 2019.

HAN, K. W., SHI, K. B.; & YAN, X. J. Evaporation loss and energy balance of agricultural reservoirs covered with counterweighted spheres in arid region. **Agricultural Water Management**, v. 238, p. 106227, 2020.

HELFER, F., *et al.* Artificial destratification for reducing reservoir water evaporation: is it effective? **Lakes & Reservoirs: Research and Management**, v. 23, p. 333–350, 2018.

HELFER, F.; LEMCKERT, C.; ZHANG, H. Impacts of climate change on temperature and evaporation from a large reservoir in Australia. **Journal of Hydrology.** v. 475, p. 365–378, 2012.

HOUNGUÈ, R.; LAWIN, A. E.; MOUMOUNI, S.; AFOUDA, A. A. Change in climate extremes and pan evaporation influencing factors over Ouémé Delta in Bénin. **Climate**, v. 7, n. 1, 2019.

HUANG, J.; MA, J.; GUAN, X.; LI, Y.; HE, Y. Progress in Semi-arid climate change studies in China. **Adv. Atmos. Sci**. v. 36, p. 922–937, 2019.

HUNTINGTON, T. G. Evidence for intensification of the global water cycle: review and synthesis, **Journal of Hydrology.** v. 319, p. 83–95, 2006.

INSTITUTO BRASILEIRO DE GEOGRAFIA E ESTATÍSTICA. **Censo Brasileiro de 2022**. Rio de Janeiro: IBGE, 2022. Available in: https://cidades.ibge.gov.br/brasil/ce/panorama. Accessed in:10 oct 2022

INSTITUTO NACIONAL DE METEOROLOGIA. **Normais Climatológicas do Brasil.** Brasília: INMET, 2019. Available in: http://www.inmet.gov.br/projetos/rede/pesquisa/inicio.php Accessed in: 16 dec 2022.

INTERGOVERNMENTAL PANEL ON CLIMATE CHANGE. **Contribution of Working**

Groups I, II and III to the Fifth Assessment Report of the Intergovernmental Panel on Climate Change. Geneva: IPCC, 2014. Available in: https://www.ipcc.ch/report/ar5/syr/. Accessed in: 22 dec 2020.

INSTITUTO DE PESQUISA E ESTRATÉGIA ECONÔMICA DO CEARÁ. **Ceará em Mapas**. Fortaleza: IPECE, 2015. Available in: http://www2.ipece.ce.gov.br/atlas/. Accessed in: 10 oct 2022.

ITIER, B.; BRUNET, Y. Recent developments and present trends in evaporation research: a partial survey. *In*: CAMP, C.R.; SADLER, E.J.; YODER, R.E. (org.). **Evapotranspiration and irrigation scheduling**. Texas: ASEA, 1996.

JANSEN, F. A.; TEULING, A. J. Evaporation from a large lowland reservoir-(dis)agreement between evaporation models from hourly to decadal timescales. **Hydrology and Earth System Sciences**, v. 24, n. 3, p. 1055–1072, 2020.

JENSEN, M.E. **Estimating evaporation from water surfaces**. 2010. Available in: https://coagmet.colostate.edu/ET_Workshop/ET_Jensen/ET_water_surf.pdf . Accessed in: 10 dec 2021.

JENSEN, M.E.; ALLEN, R.G. **Evaporation, Evapotranspiration, and Irrigation Water Requirements**. 2. ed. Reston: American Society of Civil Engineers, 2016.

JIA, X., *et al.* Impact of weather station fetch distance on reference evapotranspiration calculation. *In:* WORLD ENVIRONMENTAL AND WATER RESOURCES CONGRESS 2007, 2007, Tampa. **Anais [...]**. Tampa, 2007. p. 15-19.

JUNG, M.; *et al.* Recent decline in the global land evapotranspiration trend due to limited moisture supply, **Nature**, v. 467, p. 951–954, 2010.

KAMPF, S.K.; BURGES, T.J. Quantifying the water balance in a planar hillslope plot: effects of measurement errors on flow prediction. **Journal of Hydrology.** v. 380, p. 191–202, 2010.

KENDALL, M. G.; GIBBONS, J.D. **Rank Correlation Methods**. Oxford: Oxford University Press, 1990.

KENDALL, M.G. **Rank Correlation Measures**. London: Charles Griffin, 1975.

KENDON, E.J.; *et al.* Do convection-permitting regional climate models improve projections of future precipitation change? **Bull. Am. Meteorol. Soc.** v. 98, n. 1, p. 79–93, 2017.

KONAPALA, G.; MISHRA, A. K.; WADA, Y.; MANN, M. E. Climate change will affect global water availability through compounding changes in seasonal precipitation and evaporation. **Nature Communications**, v. 11, n. 3044, p. 1–10, 2020.

KROL, M.S.; BRONSTERT, A. Regional integrated modelling of climate change impacts on natural resources and resources usage in semi-arid Northeast Brazil. **Environmental Modelling & Software**. v. 22, p. 259-268, 2007.

KROL, M.S.; JAEGER, A.; BRONSTERT, A. Integrated modelling of climate change impacts in North- eastern Brazil. *In:* Gaiser T *et al.* (eds) **Global change and regional impacts: water availability and vulnerability of eco-systems and society in the semiarid**

Northeast of Brazil. Berlin: Springer, 2003.

KUNDZEWICZ, Z. W.; KRYSANOVA, V.; BENESTAD, R. E.; HOV, PINIEWSKI, M.; AND OTTO, I. M.: Uncertainty in climate change impacts on water resources, **Environ. Sci. Policy**, v. 79, p. 1–8, 2018.

LENSKY, N. G.; DVORKIN, Y.; LYAKHOVSKY, V. Water, salt, and energy balances of the Dead Sea. **Water Resources Research.** v. 41, p. 1–13, 2005.

LENSKY, N. G.; LENSKY, I. M.; PERETZ, A.; GERTMAN, I.; TANNY, J.; ASSOULINE, S. Diurnal course of evaporation from the Dead Sea in Summer: A Distinct Double Peak Induced by Solar Radiation and Night Sea Breeze. **Water Resources Research.** v. 54, n. 1, p. 150–160, 2018.

LENTERS, J. D.; KRATZ, T. K.; BOWSER, C. J. Effects of climate variability on lake evaporation: Results from a long-term energy budget study of Sparkling Lake, northern Wisconsin (USA). **Journal of Hydrology.** v. 308, p. 168–195, 2005.

LINACRE, E. T. Data-sparse estimation of lake evaporation, using a simplified Penman equation. **Agricultural and Forest Meteorology.** v. 64, p. 237–256, 1993.

LINACRE, E. T. Estimating US Class A pan evaporation from few climate data. **Water International.** v. 19, n. 1, p. 5-14, 1994.

LIRA, C.C.S.; MEDEIROS, P.H.A.; LIMA NETO, I.E. Modelling the impact of sediment management on the trophic state of a tropical reservoir with high water storage variations. **Anais da Academia Brasileira de Ciências.** v. 92, p. 1–18, 2020.

LIU, B.; XU, M.; HENDERSON, M.; GONG, W. A spatial analysis of pan evaporation trends in China, 1955–2000. **Journal of Geophysical Research: Atmospheres.** v. 109, n. D15, 2015.

LIU, H.; ZHANG, Y.; LIU, S.; JIANG, H.; SHENG, L.; WILLIAMS, Q. L. Eddy covariance measurements of surface energy budget and evaporation in a cool season over southern open water in Mississippi. **Journal of Geophysical Research.** v. 114, p. 1–13, 2009.

LIU, X.; YU, J.; WANG, P., ZHANG, Y.; DU, C. Lake evaporation in a hyper-arid environment, northwest of China – measurement and estimation. **Water**. v. 8, p. 1–21, 2016.

LOWE, L. D.; WEBB, J. A.; NATHAN, R. J.; ETCHELLS, T.; MALANO, H. M. Evaporation from water supply reservoirs: An assessment of uncertainty. **Journal of Hydrology.** v. 376, p. 261–274, 2009.

LYRA, A.; TAVARES, P.; CHOU, S. C.; SUEIRO, G.; DERECZYNSKI, C.; SONDERMANN, M.; SILVA, A.; MARENGO, J.; GIAROLLA, A.: Climate change projections over three metropolitan regions in Southeast Brazil using the non-hydrostatic Eta regional climate model at 5-km resolution, **Theor. Appl. Climatol.**, v.132, p. 663–682, 2018.

MADY, B.; LEHMANN, P.; OR, D. Evaporation suppression from small reservoirs using floating covers-field study and modeling. **Water Resources Research.** v. 57, p. 1–16, 2021.

MAESTRE-VALERO, J. F.; MARTÍNEZ-ALVAREZ, V.; GALLEGO-ELVIRA, B.;

PITTAWAY, P. Effects of a suspended shade cloth cover on water quality of an agricultural reservoir for irrigation. **Agricultural water management.** v. 100, n. 1, p. 70-75, 2011.

MAESTRE-VALERO, J.F.; MARTÍNEZ-ALVAREZ, V.; NICOLAS, E. Physical, chemical and microbiological effects of suspended shade cloth covers on stored water for irrigation. **Agricultural Water Management.** v. 118, p. 70–78, 2013.

MALVEIRA, V. T. C.; ARAÚJO, J. C. de; GÜNTNER, A. Hydrological Impact of a High-Density Reservoir Network in Semiarid Northeastern Brazil. **Journal of Hydrologic Engineering.** v. 17, n. 1, p. 109–117, 2012.

MAMASSIS, N.; PANAGOULIA, D.; AND NOVKOVIC, A. Sensitivity analysis of penman evaporation method. **Global NEST Journal**, v. 16, p. 628–639, 2014.

MAMEDE, G. L. *et al.* Modeling the Effect of Multiple Reservoirs on Water and Sediment Dynamics in a Semiarid Catchment in Brazil. **Journal of Hydrologic Engineering.** v. 23, n. 12, p. 05018020, 2018.

MAMEDE, G. L. *et al.* Overspill avalanching in a dense reservoir network. **Proceedings of the National Academy of Sciences.** v. 109, n. 19, p. 7191–7195, 2012.

MANN, H.B. Nonparametric tests against trend. **Econometrica.** v. 13, n. 3, 1945.

MARAUN, D. Bias correction, quantile mapping, and downscaling: Revisiting the inflation issue. **J Clim.** v.26, p. 2137–2143, 2013.

MARENGO, J. A. *et al.* Climatic characteristics of the 2010-2016 drought in the semiarid Northeast Brazil region. **Anais da Academia Brasileira de Ciências.** v. 90, p. 1973-1985, 2017.

MARENGO, J. A. *et al.* Drought in Northeast Brazil: A review of agricultural and policy adaptation options for food security, **Clim. Resil. Sustain.** v. 1, p.1–20, 2022.

MARENGO, J. A.; BERNASCONI, M. Regional differences in aridity/drought conditions over Northeast Brazil: present state and future projections**. Clim Change** v. 129, p. 103-115, 2015.

MARENGO, J.A. *et al.* Future change of temperature and precipitation extremes in South America as derived from the PRECIS regional climate modeling system. **Int J Climatol** v. 29, p. 2241–2255, 2009.

MARENGO, J.A., *et al.* Climatic characteristics of the 2010-2016 drought in the semiarid Northeast Brazil region. **Anais da Academia Brasileira de Ciências**, v. 90 (2 suppl 1), p. 1973–1985, 2018.

MARENGO, J.A., *et al.* Drought in Northeast Brazil: a review of agricultural and policy adaptation options for food security. **Climate Resilience and Sustainability**, v. 1, p. 1–20, 2022.

MARTÍNEZ ALVAREZ, V. *et al.* Regional assessment of evaporation from agricultural irrigation reservoirs in a semiarid climate. **Agricultural Water Management**, v. 95, p. 1056–1066, 2008.

MARTÍNEZ-GRANADOS, D. *et al.* The Economic Impact of Water Evaporation Losses from Water Reservoirs in the Segura Basin, SE Spain. **Water Resources Management**, v. 25, p. 3153–3175, 2011.

MAYS, L.W. **Water resources engineering**. 2. ed. New York: Wiley, 2011.

MCGLOIN, R.; MCGOWAN, H.; MCJANNET, D.; BURN, S. Modelling sub-daily latent heat fluxes from a small reservoir. **Journal of Hydrology.** v. 519, p. 2301–2311, 2014.

MCGOWAN, H.; STURMAN, A.; MACKELLAR, M.; WIEBE, A.; NEIL, D. Measurements of the local energy balance over a coral reef flat, Heron Island , southern Great Barrier Reef , Australia. **Journal of Geophysical Research.** v. 115, p. 1–12, 2010.

MCJANNET, D.; COOK, F. J.; BURN, S. Comparison of techniques for estimating evaporation from an irrigation water storage. **Water Resources Research.** v. 49, n. 3, p. 1415–1428, 2013.

MCMAHON, T. A.; FINLAYSON, B. L.; PEEL, M. C. Historical developments of models for estimating evaporation using standard meteorological data. **Wires Water.** v. 3, n. 6, p. 788–818, 2016.

MCMAHON, T. A.; MEIN, R. G. **River and Reservoir Yield**. Littleton: Water Resources Publications, 1986.

MCMAHON, T. A.; PEEL, M. C.; LOWE, L D.; SRIKANTHAN, R.; MCVICAR, T. R. Estimating actual, potential, reference crop and pan evaporation using standard meteorological data: a pragmatic synthesis. **Hydrology and Earth System Sciences.** v. 17, p. 1331–1363, 2013.

MCMAHON, T.A.; PEEL, M.C.; LOWE, L.D.; SRIKANTHAN, R.; MCVICAR, T.R. Estimating actual, potential, reference crop and pan evaporation using standard meteorological data: a pragmatic synthesis. **Hydrology and Earth System Sciences.** v. 17, p. 1331–1363, 2013.

MEDEIROS, P. H. A. DE ARAÚJO, J. C. Temporal variability of rainfall in a semiarid environment in Brazil and its effect on sediment transport processes, **Journal of Soils and Sediments.** v. 14, n. 7, p. 1216–1223, 2014.

MEDEIROS, P. H. A.; SIVAPALAN, M. From hard-path to soft-path solutions: slow-fast dynamics of human adaptation to droughts in a water scarce environment, **Hydrological Sciences Journal**. v. 65, n. 11, p. 1803-1814, 2020.

MESINGER, F. *et al.* An upgraded version of the Eta model. **Meteorog Atmos Phys** v. 116, p. 63-79, 2012.

MESQUITA, J. B. de F.; LIMA NETO, I. E.; RAABE, A.; DE ARAÚJO, J. C. The influence of hydroclimatic conditions and water quality on evaporation rates of a tropical lake. **Journal of Hydrology.** v. 590, June, p. 125456, 2020.

METZGER, J.; *et al.* Dead Sea evaporation by eddy covariance measurements vs. aerodynamic, energy budget, Priestley-Taylor, and Penman estimates. **Hydrology and Earth System Sciences**, v. 22, p. 1135–1155, 2018.

MINVILLE, M.; BRISSETTE, F.; LECONTE, R. Impacts and uncertainty of climate change on water resource management of the Peribonka River System (Canada). **J Water Resour Plan Manag**, v. 136, p. 376–385, 2010.

MIRALLES, D.G.; *et al.* El Niño–La Niña cycle and recent trends in continental evaporation. **Nature Climate Change.** v. 4, n. 2, p. 122–126, 2014.

MIRANDA RODRIGUES, C.; *et al.* Reservoir evaporation in a Mediterranean climate: comparing direct methods in Alqueva Reservoir, Portugal. **Hydrology and Earth System Sciences.** v. 24, p. 5973–5984, 2020.

MOAZENZADEH, R.; *et al.* Coupling a firefly algorithm with support vector regression to predict evaporation in northern Iran. **Engineering Applications of Computational Fluid Mechanics**, v. 12, n. 1, p. 584–597, 2018.

MONTEITH, J.L.; UNSWORTH, M.H. **Principles of Environmental Physics**. London: Arnold, 1990.

MOONEN, A. C.; ERCOLI, L.; MARIOTTI, M.; ANDMASONI, A. Climate change in Italy indicated by agrometeorological indices over 122 years. **Agricultural and Forest Meteorology.** v. 111, n. 1, p. 13-27, 2002.

MOZNY, M.; *et al.* Past (1971–2018) and future (2021–2100) pan evaporation rates in the Czech Republic. **Journal of Hydrology.** v. 590, p. 125390, 2020.

NAVARRO-RACINES, C.; TARAPUES, J.; THORNTON, P.; JARVIS, A.; RAMIREZ-VILLEGAS, J. High-resolution and bias-corrected CMIP5 projections for climate change impact assessments. **Scientific Data.** v. 7, n. 1, p. 1–14, 2020.

OKI, T.; KANAE, S. Global Hydrological Cycles and World Water Resources, **Science.** v. 313, p. 1068–1072, 2006.

OLIVEIRA, P. T.; SANTOS E SILVA, C. M.; AND LIMA, K. C. Climatology and trend analysis of extreme precipitation in subregions of Northeast Brazil, **Theor. Appl. Climatol.** v. 130, p. 77–90, 2017.

OTIS, C.H. The Transpiration of Emersed Water Plants: Its Measurement and Its Relationships. **Botanical Gazette.** v. 58, p. 457 – 494, 1914.

PATEL, J.N.; MAJMUNDAR, B.P. Development of evaporation estimation methods for a reservoir in Gujarat, India. **J. Am. Water Works Assoc.** v. 108, p. E489–E500, 2016

PENMAN, H. L. Natural evaporation from open water, bare soil and grass. **Proceedings of the Royal Society**, v. 193, p. 120–145, 1948.

PENMAN, H.L. Evaporation: an introductory survey. **Netherlands Journal of Agriculture Science**, v. 4, p. 9–29, 1956.

PETER, S. J.; DE ARAÚJO, J. C.; ARAÚJO, N. A. M.; JÜRGEN, H. Flood avalanches in a semiarid basin with a dense reservoir network. **Journal of Hydrology.** v. 512, p. 408–420, 2014.

QIN, M.; ZHANG, Y.; WAN, S.; YUE, Y.; CHENG, Y.; AND ZHANG, B.: Impact of climate change on “evaporation paradox” in province of Jiangsu in southeastern China, **PLoS One**, v. 16, p. 1–26, 2021.

RAABE, A.; HOLSTEIN, P.; DE ARAÚJO, J. C. Verwendung eines akustischen Verfahrens zur Messung der Verdunstung freier Wasserflächen. *In*: DAGA, 2020, Hannover. **Anais [...].** Hannover, 2020.

RAABE, A.; HOLSTEIN, P.; RODRIGUES, G.P.; DE ARAÚJO, J.C. Direkte Messung des Tagesgangs der Verdunstung einer freien Wasserfläche. *In*: XI METTOOLS, 9., 2021, Hamburg. **Anais [...]**. Hannover, 2021.

RICHTER, D. Vergleichende Betrachtung verschiedener Methoden zur Bestimmung der Verdunstung von freien Wasserflächen. **Zeitschr. F. Meteorol, Bd**. v. 255, n. 12, 1975.

ROCHA, T. X. de S. **Uso do sensoriamento remoto no mapeamento de macrófitas aquáticas em um reservatório do semiárido.** Dissertação (Mestrado em Engenharia Agrícola) – Centro de Ciências Agrárias, Universidade Federal do Ceará, Fortaleza, 2016.

RODERICK, M.L.; FARQUHAR, G.D. Changes in Australian pan evaporation from 1970 to 2002. **International Journal of Climatology** v. 24, n. 9, p. 1077–1090, 2004.

RODRIGUES, Í. S. *et al.* Trends of evaporation in Brazilian tropical reservoirs using remote sensing. **Journal of Hydrology.** v. 598, May, 2021a.

RODRIGUES, Í. S. *et al.* Evaporation in Brazilian dryland reservoirs: Spatial variability and impact of riparian vegetation. **Science of the Total Environment**, v. 797, p. 149059, 2021b.

RODRIGUES, Í.S.; RAMALHO, G.L.B.; MEDEIROS, P.H.A. Potential of floating photovoltaic plant in a tropical reservoir in Brazil. **Journal of Environmental Planning and Management.** v. 63, n. 13, p. 2334–2356, 2020.

ROSENBERRY, D. O.; WINTER, T.C.; BUSO, D. C.; LIKENS, G. E. Comparison of 15 evaporation methods applied to a small mountain lake in the northeastern USA. **Journal of Hydrology.** v. 340, n. 3–4, p. 149–166, 2007.

ROSENBERRY, D.O.; STURROCK, A.M.; AND WINTER, T.C. Evaluation of the energy budget method of determining evaporation at Williams Lake, Minnesota, using alternative instrumentation and study approaches. **Water Resources Research.** v. 29, p. 2473–2483, 1993.

ROSENZWEIG, C. *et al.* Assessment of observed changes and responses in natural and managed systems. *In*: M.L. PARRY, *et al.* (ed.) **Climate change 2007**: impacts, adaptation and vulnerability. Contribution of Working Group II to the Fourth Assessment Report of the Intergovernmental Panel on Climate Change. Cambridge: Cambridge University Press, 2007.

SAHU, A.; YADAV, N.; AND SUDHAKAR, K. Floating photovoltaic power plant: a review. **Renewable and Sustainable Energy Reviews** v. 66, p. 815–824, 2016.

SAMBASIVA RAO, A. Evapotranspiration rates of Eichhornia crassipes (Mart.) Solms, Salvinia molesta d.s. Mitchell and Nymphaea lotus (L.) Willd. Linn. in a humid tropical climate. **Aquatic Botany.** v. 30, n. 3, p. 215-222, 1988.

SENE, K. J.; GASH, J. H. C.; MCNEIL, D. D. Evaporation from a tropical lake: comparison of theory with direct measurements. **Journal of Hydrology.** v. 127, p. 193–217, 1991.

SHIRSATH, P.B.; SINGH, A.K. A comparative study of daily pan evaporation estimation using ANN, regression and climate-based models. **Water Resources Management.** v.24, p. 1571–1581, 2010.

SHUTTLEWORTH, W. J. *et al.* An integrated micrometeorological system for evaporation measurement. **Agricultural and Forest Meteorology**, v. 43, n. 3–4, p. 295–317, 1988.

SIVAPALAN, M.; SAVENIJE, H.H.G.; BLÖSCHL, G. Socio-hydrology: a new science of people and water. **Hydrological Processes**. v. 26, p. 1270-1276, 2012.

SNYDER, R.; BOYD, C. Evapotranspiration by Eichhornia crassipes (Mart.) Solms and Typha latifolia L. **Aquatic Botany**. v. 27, p. 217–227, 1987.

SOLOMON, S.; QIN, D.; MANNING, M. (org.). **Contribution of Working Group I to the Fourth Assessment Report of the Intergovernmental Panel on Climate Change**. Cambridge: Cambridge University Press, 2007.

SU, Z. The Surface Energy Balance System (SEBS) for estimation of turbulent heat fluxes. **Hydrology and Earth System Sciences**, v. 6, n. 1, p. 85–99, 2002.

SWINBANK, W. C. The measurement of vertical transfer of heat and water vapor by eddies in the lower atmosphere. **Journal of Meteorology**, v. 8, n. 3, p. 135–145, 1951.

TAN, S.B.K.; SHUY, E.B.; AND CHUA, L.H.C. Modelling hourly and daily open-water evaporation rates in areas with an equatorial climate**. Hydrological Processes.** v. 21, p. 486–499, 2007.

TANNY, J.; COHEN, S.; ASSOULINE, S.; LANGE, F.; GRAVA, A.; BERGER, D.; TELTCH, B.; PARLANGE, M. B. Evaporation from a small water reservoir: Direct measurements and estimates. **Journal of Hydrology.** v. 351, n. 1–2, p. 218–229, 2008.

TANNY, J.; COHEN, S.; BERGER, D.; TELTCH, B.; MEKHMANDAROV, Y.; BAHAR, M.; KATUL, G. G.; ASSOULINE, S. Evaporation from a reservoir with fluctuating water level: Correcting for limited fetch. **Journal of Hydrology.** v. 404, n. 3–4, p. 146–156, 2011.

TEUTSCHBEIN, C.; SEIBERT, J. Bias correction of regional climate model simulations for hydrological climate-change impact studies: Review and evaluation of different methods. **Journal of Hydrology.** v. 456–457, p. 12–29, 2012.

TIAN, W. *et al.* Estimation of global reservoir evaporation losses. **Journal of Hydrology.** v. 607, November, 2022.

TIAN, W. *et al.* Estimation of reservoir evaporation losses for China. **Journal of Hydrology.** v. 596, p. 126142, 2021.

TRENBERTH, K. E.; DAI, A.; VAN DER SCHRIER, G.; JONES, P. D.; BARICHIVICH, J.; BRIFFA, K. R.; AND SHEFFIELD, J.: Global Warming and Changes in Drought, **Nat. Clim. Change**, v. 4, p. 17–22, 2014.

VALIANTZAS, J. D. Simplified forms for the standardized FAO-56 Penman-Monteith reference evapotranspiration using limited weather data. **Journal of Hydrology.** v. 505, p. 13–23, 2013.

VELLAME, L.M.; *et al.* Method to assess evapotranspiration based on simple measurements: development and application to the brazilian semiarid Caatinga biome. **Hydrological Processes.** Unpublished results.

VIMAL, S.; SINGH, V. P. Rediscovering Robert E. Horton's lake evaporation formulae: New directions for evaporation physics. **Hydrology and Earth System Sciences**, v. 26, n. 2, p. 445–467, 2022.

WANG, W.; XIAO, W.; CAO, C.; GAO, Z.; HU, Z.; LIU, S.; SHEN, S.; WANG, L.; XIAO, Q.; XU, J.; YANG, D.; LEE, X.. Temporal and spatial variations in radiation and energy balance across a large freshwater lake in China. **Journal of Hydrology.** v.511, p. 811–824, 2014.

WATANABE M, *et al.* Improved climate simulation by MIROC5: mean states, variability, and climate sensitivity. **J. Clim.** v. 23, n. 23, p. 6312–6335, 2010.

WEBER, E. **Mapping floating and emergent macrophytes on reservoirs in Ceará (BR) by using optical time-series satellite data**. 2020. Dissertação (Mestrado em Environmental Geography and Management) – Faculdade de Matemática e Ciências Naturais, Universidade de Kiel, Alemanha.

WEERT, R.V.D.; KAMERLING, G. Evapotranspiration of water hyacinth (Eichhornia crassipes). **Journal of Hydrology**. v. 22, n. 38, p. 201–212, 1974.

WORLD METEOROLOGICAL ORGANIZATION. **Guide to meteorological instruments and methods of observation**. Geneva: WMO-No. 8, 2018.

WURBS, R. A.; AYALA, R. A. Reservoir evaporation in Texas, USA. **Journal of Hydrology.** v. 510, p. 1–9, 2014.

XU, C.Y.; SINGH, V. P. Evaluation and generalization of temperature-based methods for calculating evaporation. **Hydrological Processes.** v. 14, p. 339–349, 2000.

YASEEN, Z.M. *et al.* Prediction of evaporation in arid and semi-arid regions: a comparative study using different machine learning models. **Engineering Applications of Computational Fluid Mechanics.** v. 14, p. 70–89, 2020.

YE, N. *et al.* A bibliometric analysis of corporate social responsibility in sustainable development. **Journal of Cleaner Production.** v. 272, p. 122679, 2020.

ZARFL, C. *et al.* Klement. A global boom in hydropower dam construction. **Aquatic Sciences**, v. 77, n. 1, p. 161–170, 2015.

ZHANG, H.; GORELICK, S. M.; ZIMBA, P. V.; ZHANG, X. A remote sensing method for estimating regional reservoir area and evaporative loss. **Journal of Hydrology.** v. 555, p. 213–227, 2017.

ZHANG, S. *et al.* Bathymetric survey of water reservoirs in northeastern Brazil based on

TanDEM-X satellite data. **Science of the Total Environment** v. 571, p. 575–593, 2016.

ZHANG, S. Mapping regional surface water volume variation in reservoirs in northeastern Brazil during 2009–2017 using high-resolution satellite images, **Science of the Total Environment.** v. 789, p. 147711, 2021.

ZHAO, G. Evaporative water loss of 1.42 million global lakes. **Nature Communications**, v. 13, n. 1, p. 1–10, 2022.

ZHAO, G.; GAO, H. Estimating reservoir evaporation losses for the United States: Fusing remote sensing and modeling approaches, **Remote Sensing of Environment.** v. 226, p. 109-124, 2019.

ZUO, D. Simulating spatiotemporal variability of blue and green water resources availability with uncertainty analysis. **Hydrological Processes.** v. 29, p. 1942–1955, 2015.

APPENDIX A - LIST OF PUBLICATIONS

Conference papers

- RAABE, A.; HOLSTEIN, P.; **RODRIGUES, G.P.**; de ARAÚJO, J.C. Direkte Messung des Tagesgangs der Verdunstung einer freien Wasserfläche. **XI METTOOLS**, Hamburg 2021.
- **RODRIGUES, G.P.**; RAABE, A.; VELLAME, L.M.; de ARAÚJO, J.C.; HOLSTEIN, P. Uncertainty assessment of open water evaporation measurements: case study in a tropical reservoir in Brazil – **DACH**, Leipzig https://doi.org/10.5194/dach2022-45, 2022.
- **RODRIGUES, G. P.**; BROSINSKY, A.; RODRIGUES, Í. S.; MAMEDE, G.L.; de ARAÚJO, J. C. Possíveis impactos das mudanças climáticas na evaporação de açudes: o caso da Região Metropolitana de Fortaleza, Brasil *In*: **VI Simpósio Brasileiro de Recursos Naturais do Semiárido – SBRNS**, 2023, Fortaleza. Submitted on: 11 Sep 2023.

Paper published in a peer reviewed journal

- **RODRIGUES, G. P.**; RODRIGUES, Í. S.; RAABE, A.; HOLSTEIN, P.; DE ARAÚJO, J. C. Direct measurement of open-water evaporation: a newly developed sensor applied to a Brazilian tropical reservoir. **Hydrological Sciences Journals.** v. 68, n. 3, p. 1–16. Taylor & Francis. https://doi.org/10.1080/02626667.2022.2157278, 2023.

Paper accepted to a peer reviewed journal

- **RODRIGUES, G. P.**; BROSINSKY, A.; RODRIGUES, Í. S.; MAMEDE, G. L.; DE ARAÚJO, J. C.: Climate-change impact on reservoir evaporation and water availability in a tropical sub-humid region, north-eastern Brazil, **Hydrology and Earth System Sciences - Discussions.** [preprint], https://doi.org/10.5194/hess-2023-189, in review, 2023.

APPENDIX B - AQUASEBS OVERVIEW

The Surface Energy Balance of Fresh and Saline Waters (AquaSEBS, as in Abdelrady *et al.*; 2016) is an adaptation of the SEBS model (Su, 2002) to estimate evaporation in open water. It consists of a set of tools to determine physical water surface parameters (such as albedo, emissivity, temperature etc.) from spectral reflectance and radiance. It requires three sets of data as input: (1) remote-sensing data including emissivity, surface albedo and water surface temperature; (2) meteorological data, including air pressure, air temperature, relative humidity and wind speed at a reference height; and (3) radiative forcing parameters, such as downward shortwave and long-wave radiations. The algorithm was validated in several water bodies at different environmental conditions (ABDELRADY *et al.*; 2016; LOSGEDARAGH and RAHIMZADEGAN, 2018) including Brazilian tropical reservoirs (RODRIGUES *et al.*; 2021).

AquaSEBS uses the energy balance to calculate the instantaneous latent heat flux of evaporation (Equation 1), thus, evaporation is calculated for each pixel of the image.

$$\lambda E_{inst} = R_n - G_{0W} - H \quad \text{(S1)}$$

where λE_{inst} is latent heat flux of evaporation at imaging time (W m^{-2}), R_n is net radiation flux at the surface (W m^{-2}), G_{0W} is the water flux heat (W m^{-2}), and H the sensible heat flux to air.

Afterwards, atmospheric transmissivity is obtained, which is defined as the fraction of incident radiation that is transmitted by the atmosphere and which represents the effects of absorption and reflection occurring within the atmosphere. This effect occurs to incoming radiation and to outgoing radiation and is, thus, squared in Equation 2. The τ_{sw} includes transmissivity of both direct solar beam radiation and diffuse (scattered) radiation to the surface. We calculate τ_{sw} using an elevation-based relationship from Allen *et al.* (2002).

$$\tau_{sw} = 0.75 + 2 \cdot 10^{-5} \cdot DEM \quad \text{(S2)}$$

Where DEM is the Digital Elevation Model file. The albedo at the top of the atmosphere (unadjusted for atmospheric transmissivity) was computed through linear combination of the monochromatic reflectance (ρ) of the reflective bands (from 2 to 7, excluding band 6) according to Liang (2000) for MODIS products. It is necessary to apply radiometric corrections on images, and image bands are converted to radiance and reflectance according to their wavelengths, as

follows:

$$\alpha = 0.160\rho_1 + 0.291\rho_2 + 0.243\rho_3 + 0.116\rho_4 + 0.112\rho_5 + 0.081\rho_7 - 0.0015 \quad \text{(S3)}$$

Da Silva *et al.* (2016) according to the methodology proposed by Chander & Markham (2003), found the values for Landsat 8 and present on the following equation:

$$\alpha = 0.3_{\rho 2} + 0.277_{\rho 3} + 0.233_{\rho 4} + 0.143_{\rho 5} + 0.036_{\rho 6} + 0.012_{\rho 7} \quad \text{(S3.1)}$$

The indexes in each ρ stand for the respective reflectance band. Incoming shortwave radiation (W m^{-2}) is calculated as:

$$R_{s\downarrow} = G_{sc} \cdot \cos(90° - \theta) \cdot d_r \cdot \tau_{sw} \quad \text{(S4)}$$

G_{SC} is the solar constant (1367 W m^{-2}), θ the sun elevation angle and d_r is the inverse squared relative distance between sun and earth, all in conformity with Allen *et al.* (1998). Incoming longwave radiation is the downward thermal radiation flux from the atmosphere (W m^{-2}). It is computed by means of the Stefan-Boltzmann equation:

$$R_{L\downarrow} = \varepsilon_a \cdot \sigma \cdot T_a^4 \quad \text{(S5)}$$

Where T_a is the near surface air temperature (monthly average, in K), σ is the Stefan-Boltzmann constant (5.67×10^{-8} W m^{-2} K^{-4}), and ε_a is the atmospheric emissivity (dimensionless). The following empirical equation by Bastiaanssen (1995) is used to assess ε_a:

$$\varepsilon_a = 0.85 \cdot (-\ln \tau_{sw})^{0.09} \quad \text{(S6)}$$

Water heat flux can be described as the imbalance between solar radiation, thermal radiation, sensible heat and latent heat fluxes. Remote sensing observations only obtain the skin temperature of the water; consequently, the Equilibrium Temperature Model (ETM) was used. The ETM model (AHMAD; SULTAN, 1994; EDINGER *et al.*, 1968) integrates water surface temperature (T_S) and equilibrium temperature (T_e) through the thermal exchange coefficient (β, which represents the sum of temperature-dependent heat exchange processes including sensible, evaporative and back radiative fluxes) to estimate the water heat flux (G_w). In order to derive

water heat flux, the following equations (ABDELRADY *et al.*, 2016) should be applied:

$$G_w = \beta\,(T_e - T_S) \tag{S7}$$

$$T_e = T_D + \frac{R_{L\downarrow}}{\beta} \tag{S8}$$

$$\beta = 4.5 + 0.05T_S + (\eta + 0.47)3.3u \tag{S9}$$

$$\eta = 0.35 + 0.015T_S + 0.0012\,(T_n)^2 \tag{S10}$$

$$T_n = 0.5\,(T_S - T_D) \tag{S11}$$

where T_e is equilibrium temperature (°C), T_D the dew temperature (°C), T_n is the net rate of heat exchange, $R_{S\downarrow}$ the incoming shortwave, u is wind speed at 2m height (m s^{-1}), η represents the predicted percentage of heat loss through the surface[4]. Thus, equation S11 calculates the net rate of heat exchange as half of the difference between the surface temperature and the dew temperature.

The equation to calculate net radiation is given by:

$$R_n = (1 - \alpha)\,R_{S\downarrow} + \varepsilon \cdot R_{L\downarrow} - \varepsilon \cdot \sigma \cdot T_S^4 \tag{S12}$$

According to Su (2002), the sensible heat flux at the wet-limit is obtained as follows:

$$H_{wet} = \frac{\left((R_n - G_{0w}) - \frac{\rho_a C_p}{r_{ew}} \cdot \frac{e_s - e}{\gamma}\right)}{\left(1+\frac{\Delta}{\gamma}\right)} \tag{S13}$$

The term $e_s - e$ represents the vapour pressure deficit, C_p is the specific heat capacity of air (1004 J Kg^{-1} $°C^{-1}$), ρa the specific mass of air (1.184 Kg m^{-3}), γ is the psychrometric parameter (hPa $°C^{-1}$), Δ is the rate of change of saturation vapour pressure with temperature (hPa $°C^{-1}$), while r_{ew} is external resistance and uses the variables wind friction and sensible heat flux.

Remote sensing images can be used to provide evaporation maps with high spatial resolution during overpass, but they are temporarily limited to a definite time during the day. A daily stable term such as the evaporative fraction (EF) can be used together with satellite images

[4] In Equation S9, η represents the predicted percentage of heat loss through the surface relative to the maximum possible heat loss. This equation is known as the "Gagge formula", and it is used to estimate the percentage of heat loss through the surface based on the mean surface temperature (T_S) and the net rate of heat exchange (T_n). Thus, η does not directly represent the mean surface temperature. Instead, it's a parameter that quantifies the efficiency of heat loss through the skin under specific thermal conditions.

to upscale latent heat and the evaporation rate from instantaneous to daily estimation (Allen *et al.*; 2002; Abdelrady *et al.*; 2016). Evaporative fraction is the ratio between latent heat and available energy at the water surface, as follows:

$$EF = \frac{\lambda E}{(R_n - G_w)} \tag{S14}$$

Latent heat is the energy needed for evaporation (equation S1, $\lambda E = R_n - G_{0w} - H_{wet}$). SEBS estimates the total energy used for evaporation in a day-based evaporative fraction term using Equation (Su, 2002). First, latent heat is converted to water depth in (mm) per day, then daily potential evaporation can be calculated as water depth utilising the following equation:

$$E_{daily=} \frac{86400 \cdot EF\,(R_n - G_w)}{\lambda E_{daily}} \tag{S15}$$

E_{daily} in equation S15 is given in water depth (mm) for each pixel in the image.

APPENDIX C - BIAS CORRECTION OF ETA-MIROC5 OUTPUTS USING LS METHOD

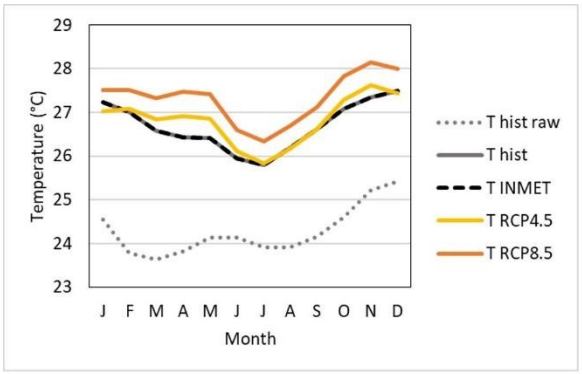

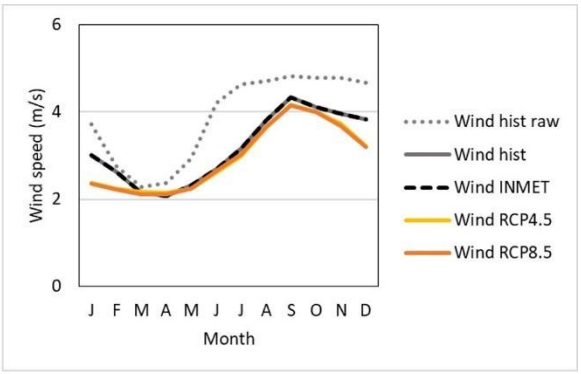

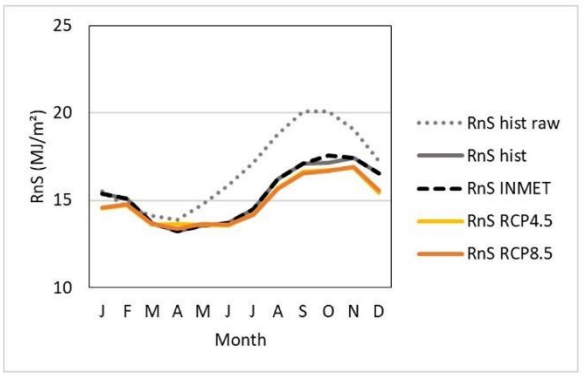

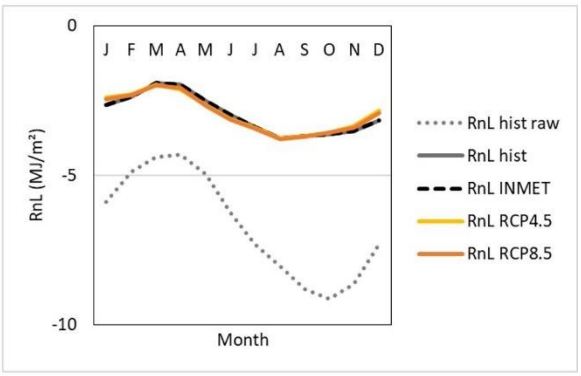

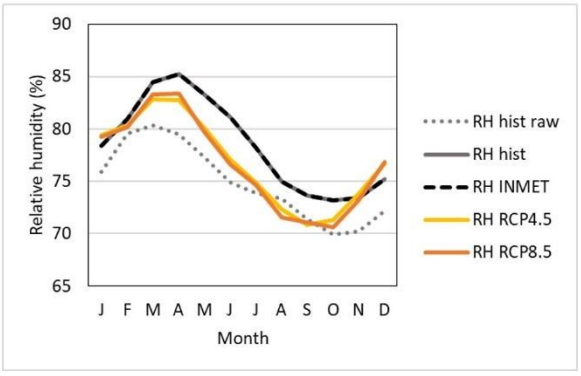

APPENDIX D - BIAS CORRECTION OF ETA-CANESM2 OUTPUTS APPLYING LS METHOD